Doctoral theses at NTNU, 2018:357

Chhatra Bahadur Basnet

Applicability of Unlined/ Shotcrete Lined Pressure Tunnels for Hydropower Projects in the Himalaya

Doctoral thesis

Chhatra Bahadur Basnet

ISBN 978-82-326-3502-3 (printed ver.)
ISBN 978-82-326-3503-0 (electronic ver.)
ISSN 1503-8181

NTNU
Norwegian University of
Science and Technology

NTNU

Norwegian University of Science and Technology
Thesis for the Degree of
Philosophiae Doctor
Faculty of Engineering
Department of Geoscience and Petroleum

Doctoral theses at NTNU, 2018:357

NTNU
Norwegian University of
Science and Technology

Chhatra Bahadur Basnet

Applicability of Unlined/Shotcrete Lined Pressure Tunnels for Hydropower Projects in the Himalaya

Thesis for the Degree of Philosophiae Doctor

Trondheim, November 2018

Norwegian University of Science and Technology
Faculty of Engineering
Department of Geoscience and Petroleum

NTNU
Norwegian University of
Science and Technology

NTNU
Norwegian University of Science and Technology

Thesis for the Degree of Philosophiae Doctor

Faculty of Engineering
Department of Geoscience and Petroleum

ISBN 978-82-326-3502-3 (printed ver.)
ISBN 978-82-326-3503-0 (electronic ver.)
ISSN 1503-8181

Doctoral theses at NTNU, 2018:357

Printed by NTNU Grafisk senter

Preface

A research project has been accomplished during the period from August 2014 – August 2018 at the Department of Geoscience and Petroleum, Faculty of Engineering of the Norwegian University of Science and Technology (NTNU), Norway. The project was funded by the Faculty of Engineering of NTNU and Norwegian Hydropower Center (NVKS). The project was developed to study the possibility of implementing the unlined pressure tunnel concept developed in Norway to the Himalayan region. This PhD thesis is written to present the outcome of the research project where NTNU, NVKS and Nepal Electricity Authority (NEA) have contributed both financially and by giving access to field data and information. The thesis presents a brief summary of the main outcomes together with a collection of research articles written during the project period.

Acknowledgements

I am grateful from the bottom of my heart to my supervisor Associate Professor Dr. Krishna Kanta Panthi for his continuous motivation, guidance, vision and support towards accomplishment of this PhD study. His vast knowledge and experience in the field of rock engineering and tunneling have been crucial for the output of my research work. His ability to solve the particular task taught me on how to critically think and solve the problem.

I am also thankful to the Department of Geoscience and Petroleum, Faculty of Engineering (IV), Norwegian University of Science and Technology (NTNU) for the continuous support during my PhD project. I would also like to thank Faculty of Engineering (IV), Norwegian Hydropower Centre (NVKS) and Nepal Electricity Authority (NEA) for their financial and field support during the PhD research. I am also grateful to the project operation team of the Modi Khola and Chilime Hydroelectric Projects in Nepal for their support during field test and data collection. I am grateful to Mr. Prakash Karki for his logistic support during field test at Chilime Project. Similarly, I am also grateful to the project management team and other staffs of the Upper Tamakoshi Hydroelectric Project (under construction) in Nepal for their support during field work and data collection. Especial thanks goes to the Deputy Project Chief Mr. Pradeep Thike, Senior Geologist Mr. Babu Krishna Bhandari and Geologist Mr. Sanjeep Sapkota. I am also thankful to the Norwegian Hydropower Industry for access to data and information on the Norwegian cases. I am grateful to Prof. Einar Broch for providing the valuable data and information regarding the Norwegian hydropower projects.

I would also like to thank all my friends, professors and other staffs of the NTNU and SINTEF who have directly or indirectly helped me to execute the assigned work. I am thankful to Mario Morales for shearing the office room and having useful discussions. Especial thanks goes to Ms. Hege Brende for continuous support I have received from NVKS and Mr. Gunnar Vistnes for his support in the Lab. I am grateful to Dr. Pawan Kumar Shrestha for his valuable input in numerical modeling in the beginning of the research work. I would also like to thank Mr. Bibek Neupane for the valuable conversations and discussions about the research work.

I would further like to extend my especial thanks to Er. Mani Raj Dahal for letting me to come to Norway for this PhD research. I would also like to thank my friends from IDEA, Nepal for their wishes and supports towards the success of my research work. I would also like to extend my gratitude to all Norwegian people for welcoming me to conduct the research work in a world-class research environment. I would also like to thank all Nepalese friends and families who are in Trondheim, Norway, without them I would be homeless. I am especially indebted to Laxmi bhauju, Kriti and Kritagya for being with us (me and my family) in every ups and downs of our stay in Norway.

Finally; I would like to express my gratitude to my parents, sisters, brothers and other family members. Especially, I would like to express love towards my wife (Sarbada) and two little princes (Sambodhi and Samyami) and I am very much thankful to them for inspiring me every moment to conduct this research work. I feel very sorry for not being with my father at the entire time when he was sick and waiting for the death. Likewise, I feel very regret for not being able to take care of my mother in the absence of my father. They sacrificed a lot for my research work and I would like to dedicate this work to both of them. Finally, I would like to extent my gratitude to all the masters (GURUs) of my life and the whole existence and non-existence.

Abstract

Nowadays, unlined or shotcrete lined pressure tunnels and shafts are used in hydropower projects worldwide. The prime requirements for these tunnels and shafts are that they should be economically attractive and should be able to operate without any significant problems in the long run. The concepts and design principles behind these conduits developed from the Norwegian planning, design, construction and operational experiences have been crucial for their successful implementation. However, by virtue of the different topographical, geological and tectonic environment of the Himalaya than that of the Scandinavia, the implementation of unlined pressure tunnels in the Himalaya has been emerging as a challenging issue. As a matter of fact, it was realized that a clear gap exists between the success of the unlined pressure tunnel concept in Norway and the challenge of its implementation in the Himalaya. To fulfill this gap, this PhD research project was formulated to study the possibility of implementing the unlined or shotcrete lined pressure tunnels in the Himalaya.

First of all, the economical attractiveness of the shotcrete lined pressure tunnel of the Himalayan hydropower projects was evaluated. Since the tunnel roughness is one of the decisive parameters for cost effectiveness, a methodology was developed to estimate the roughness of shotcrete lined tunnel based on the study of two tunnel cases from Nepal Himalaya. The tunnel cases were taken from Modi Khola Hydroelectric Project (MKHP) and Chilime Hydroelectric Project (CHP). It was found that the shotcrete lined tunnels are one of the economically attractive solutions in the waterway system of hydropower projects. In addition, the roughness of shotcrete lined tunnel of Upper Tamakoshi Hydroelectric Project (UTHP), which is also located in Nepal and is under construction, was predicted by using the developed methodology. More importantly, the shotcrete lined tunnels in all cases were provided with the concrete lining in the invert.

The PhD work further reviewed the Norwegian design principles for unlined pressure tunnel and their applicability in different topographical, geological and tectonic environments. In doing so, ten Norwegian hydropower projects including both failure and successful cases of unlined pressure shafts and tunnels were studied in detail. The review process revealed that the hydrostatic head gives water pressure to the rock mass surrounding the tunnel periphery. In an unlined tunnel, the confining pressure from the rock mass should be able to counteract the water pressure for the safety of unlined tunnel against hydraulic jacking. The attempt of

all design criteria is then to define the confining pressure as accurate as possible. The Norwegian confinement criteria use both vertical and lateral rock covers to estimate the confining pressure. On the other hand, the magnitude of minimum principal stress in the rock mass is considered as a limiting confining pressure to counteract the water pressure. This criterion came out as a stress criterion and is the state-of-the-are design principle for unlined pressure shaft and tunnel. However, some discrepancies were noticed between the confining pressures given by these different criteria.

The Norwegian design concepts and criteria were then applied to the UTHP. The fact is that the pressure tunnel of the UTHP was designed as a shotcrete lined tunnel with concrete lining in the invert. This tunnel is different from the one which is normally fully unlined in Norwegian Hydropower projects. However, same design criteria as for the unlined pressure tunnel were used in the shotcrete lined pressure tunnel as well by virtue of the permeable nature of shotcrete lining. The extensive assessments carried at the UTHP concluded that the good quality rock mass with tight joints is suitable for unlined or shotcrete lined tunnel provided that the stress requirement is fulfilled. However, the presence of weakness zones, local shear bands, unfavorable jointing, and destressed area makes the use of unlined or shotcrete lined tunnel more challenging. Even though the Norwegian confinement criteria show headrace tunnel alignment is safe for unlined tunnel concept at the UTHP, the detailed rock engineering assessment, stress state analysis, fluid flow and leakage analyses indicates that some critical locations along the headrace tunnel alignment are vulnerable for the unlined or shotcrete lined tunnel concept. More importantly, the weakness zone considerably attenuates the in-situ stress state. In addition, the open joints and the joints filled with silt and clay having low stiffness are vulnerable for hydraulic jacking and water leakages even the stress conditions are fulfilled. Considering these facts, this thesis finally argues that there is a need for the modification of the Norwegian confinement criteria in order to successfully apply in the Himalayan rock mass conditions. This is mainly due to the presence of complex topography, geology and tectonic environment of this region.

Thesis structure

Part I

Summary

Part II

Main publications

Table of Contents

Part I

Summary

1 Introduction

1.1 Background

Waterway tunnels represent the most significant source of construction cost for hydropower projects, especially for run-of-the-river plants. Reducing and optimizing the cost of waterway systems is therefore a major issue to make hydropower projects financially attractive. One of the possible solutions is to use unlined or shotcrete lined pressure tunnel / shaft or combination of both for the waterway system if the rock mass and applied shotcrete and/or systematic bolting guarantee long-term stability and safety (Panthi, 2015; Basnet and Panthi, 2018a). Fig. 1 shows a typical layout of an underground hydropower scheme with the possible locations of unlined / shotcrete lined pressure shaft and tunnel in the waterway system. Around the globe, Norwegian hydropower projects are the best examples to apply the unlined high pressure shafts and tunnels successfully in the waterway system (Palmstrom and Broch, 2017).

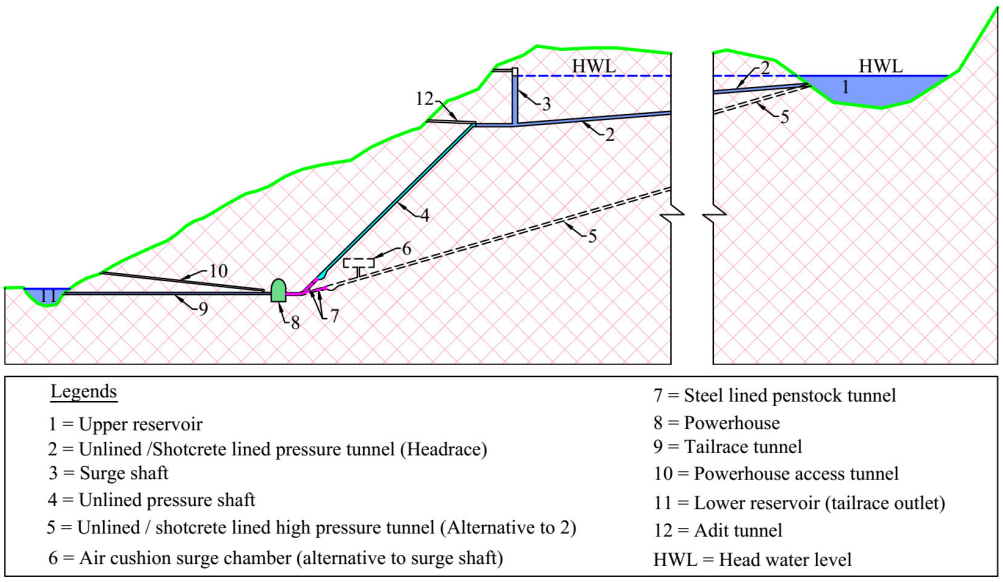

Fig. 1. A typical layout of underground hydropower scheme with unlined pressure shaft and tunnel

Norway has built more than 200 underground powerhouses and 4200 km-long hydropower tunnels in the past 100 years (Broch, 2013). In Norway, it is estimated that over 95% of total length of shafts and tunnels of Norwegian hydropower schemes are left unlined (Johansen, 1984; Panthi, 2014). The earliest attempt to apply such concept in Norway was in

Herlandsfoss project in 1919 (Vogt, 1922), and up to now, more than 4000 km-long unlined pressure shafts and tunnels with maximum static water head of 1047 m have been in successful operation. It is believed that favorable topographical, geological and tectonic environment of the Scandinavian landscape has favored the use of unlined pressure tunnel concept in Norway (Selmer-Olsen, 1969). Owing to this fact, it is very logical to say that Norwegian planning, design, construction and operational experiences in unlined pressure tunnels and shafts are essentially the backbones while implementing such tunnels and shafts in different topographical, geological and tectonic environment. From the experiences, it has been concluded that the basic criteria for the applicability of unlined or shotcrete lined pressure shafts and tunnels are cost effectiveness, tunnel stability, safety against hydraulic jacking and water leakage (Broch, 1982; Brekke and Ripley, 1987; Benson, 1989). However, the principle of using unlined high pressure tunnels and shafts depends greatly on the topography, geology and tectonic environment at the area of tunnel location.

Apart from Norway, there have been some attempts in Nepal Himalaya to use shotcrete lined pressure tunnel in the headrace system of the hydropower waterways. As an earliest attempt in 2000, Khimti I Hydropower Project (KHP) used a low pressure shotcrete lined tunnel with a maximum water head of about 40 m at its headrace tunnel system (Panthi, 2006; Panthi and Nilsen (2007); Panthi and Nilsen, 2010). The KHP has been in successful operation after the rock mass around tunnel was sealed at the locations where unacceptable water leakage occurred during test water filling. Similarly, the shotcrete lined tunnels in Modi Khola Hydroelectric Project (MKHP) with maximum water head of about 30 m and in Chilime Hydroelectric Project (CHP) with maximum water head of about 20 m have been in successful operation since the start of commercial operation of the project in 2000 and 2003, respectively. On the other hand, a shotcrete lined pressure tunnel with maximum water head of about 115 m in Upper Tamakoshi Hydroelectric Project (UTHP) is under construction since 2011.

The topographical, geological and tectonic environment of the Scandinavia and the Himalaya are quite different (Panthi, 2014). The experience of planning, design and construction of the pressure tunnel in the UTHP indicates that the prevailing environment of the Himalaya is making the use of unlined or shotcrete lined tunnel a challenging issue. Regarding the tectonics of Himalaya, the Indian and the Asian plates in the Himalaya region have been continuously converging to each other for more than 70 million Years (Rowley, 1996). Tectonically, it is a very active region and this region witnessed large, moderate and small

scale earthquakes in large numbers. The magnitude of major tectonic principal stress in the Himalayan region has been influenced by the compressional tectonic deformation and active reverse faulting mechanism (Panthi, 2006). Periodic earthquakes that occur in this region releasing the stress accumulated and de-stressing the rock mass. Hence, the tectonic stress magnitude greatly depends on the geological and tectonic environment of a particular area (Panthi, 2014). From the above facts, it can be concluded that the Himalayan rock mass are weathered and fractured along the topographic slopes and valleys leading to deep weathering and are distressed due to stress release. As a result, the topography at the Himalaya is complex in nature. Hence, topography, geology and tectonics of this region are challenging for the applicability of unlined or shotcrete lined pressure tunnel. But, at the same time it is believed that today's tunneling technology and possibility of advanced research activities will certainly fulfill the gap between the current state of the art principle and its applicability in such challenging area. This PhD work is intended to fulfill part of this gap.

1.2 Research question

The research question of this PhD study is particularly formulated with three broad queries:

"Is it possible to use unlined or shotcrete lined pressure tunnels in the Himalaya? Is it possible to apply Norwegian design principles for unlined pressure tunnels and shafts in the Himalaya? What improvements are needed to implement the Norwegian concept in the Himalaya?"

1.3 Scope of the research

In order to fulfill the research objectives, the rock engineering assessment, stress state analysis and fluid flow analysis were carried out. For that, data collection, field mapping, laboratory testing of rock samples and numerical analysis were executed extensively. More importantly, the measured stress data were collected based on the availability. The topography, the rock mass and the rock stress conditions of both the Scandinavia and the Himalaya were studied in detail. In doing so, the major hydropower projects having unlined / shotcrete lined pressure tunnel were chosen as case studies from Norway and Nepal.

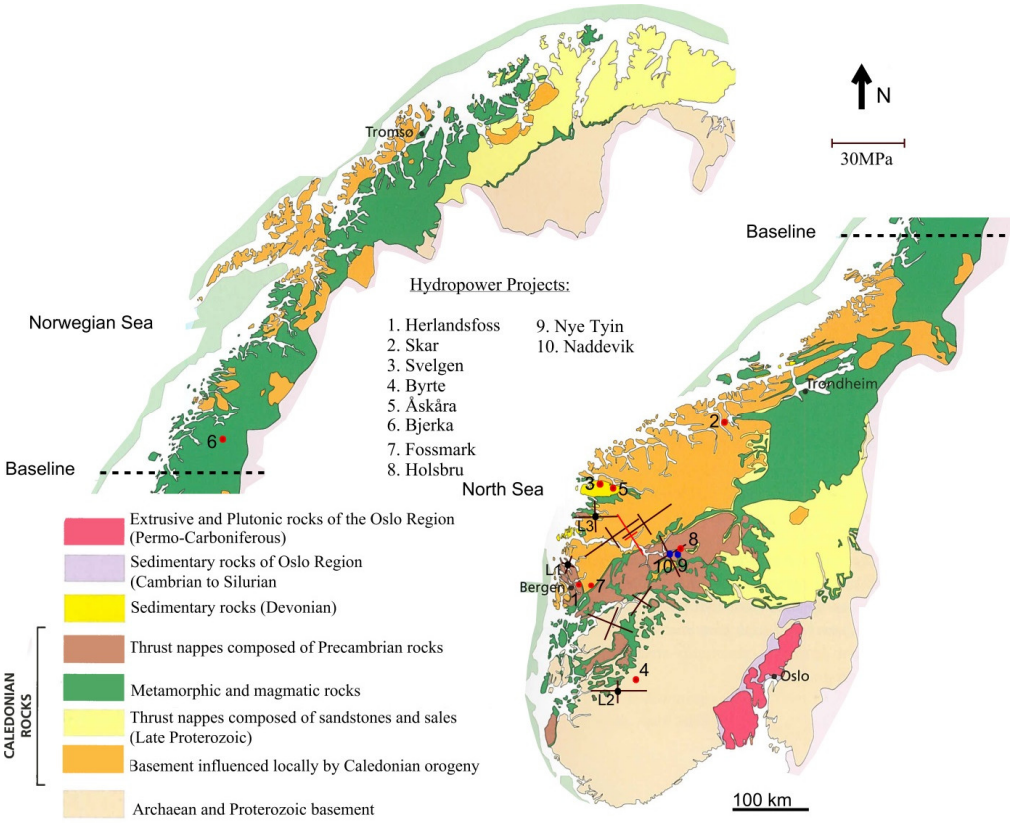

Fig. 2. Location of the hydropower projects in the geological map of Norway with direction and magnitude of horizontal rock stresses superimposed (Basnet and Panthi, 2018b, Map source: Geological Survey of Norway, NGU)

Particularly, Norwegian cases were studied to explain the principle philosophy behind the concept of unlined high pressure tunnels and shafts. The concept was verified by using numerical analysis for some of the selected tunnel cases. All selected project cases from Norway are shown in Fig. 2. These projects represent gradual development in the application of unlined high pressure tunnels in Norway. The adopted design principles for these unlined pressure tunnels and shafts were reviewed and assessments were carried out on the required geological condition and geo-tectonic environment for developing design criteria.

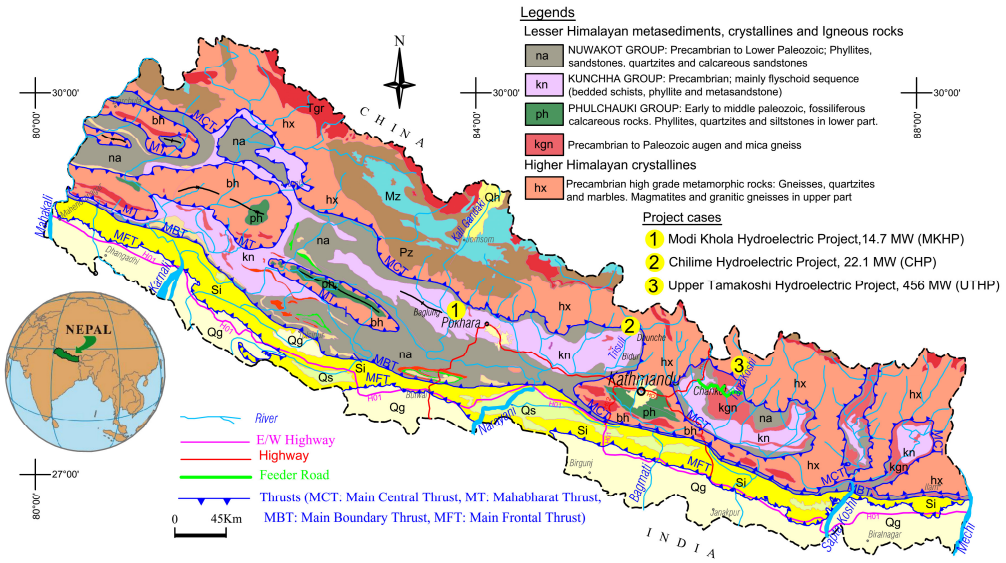

Fig. 3. Locations of hydropower projects in the Geological Map of Nepal Himalaya (Basnet and Panthi, 2018a; Panthi and Basnet, 2017; and Geological Map source: DGM, 1994)

In order to apply the unlined / shotcrete lined pressure tunnel concept in the Himalaya, three project cases were selected from Nepal as shown in Fig. 3. The projects are; Chilime Hydroelectric Project (CHP), Modi Khola Hydroelectric Project (MKHP) and Upper Tapakoshi Hydroelectric Project (UTHP). Among them, CHP and MKHP were used to evaluate the roughness of shotcrete lined tunnel whereas detailed assessments were carried out for UTHP to apply and modify the existing design principles.

2 Unlined or shotcrete lined pressure tunnel

The use of unlined or shotcrete lined pressure tunnel entirely depends on the theory behind the concept and its applicability to different topographic, geological and tectonic environment. The hydraulics of unlined or shotcrete lined tunnel determines its cost effectiveness compared to the other types of tunnels such as; concrete or steel lined tunnels. On the other hand, the design criteria for the unlined or shotcrete lined tunnels should be defined in order to safely locate the tunnels at favorable ground conditions. In addition, both short and long term stability should be ascertained for safe operation of the tunnel.

2.1 Basic theory review

2.1.1 Unlined or shotcrete lined tunnel hydraulics

While transferring water from upper reservoir / intake to the surge shaft (SS), a part of the energy is lost due to both friction of the tunnel and obstruction of other local components such as; intake, trashrack, gates, bends, exit etc. The lost part of the energy is termed as head loss in the hydropower scheme. It is very logical to say that higher headloss causes more energy to be lost which would have been used to generate more electricity instead. This indicates that more revenue will be lost with higher headloss. Since the local components must be essentially built irrespective of the type of tunnel, friction loss is the most influential parameter that determines the extent of the headloss for optimization purpose.

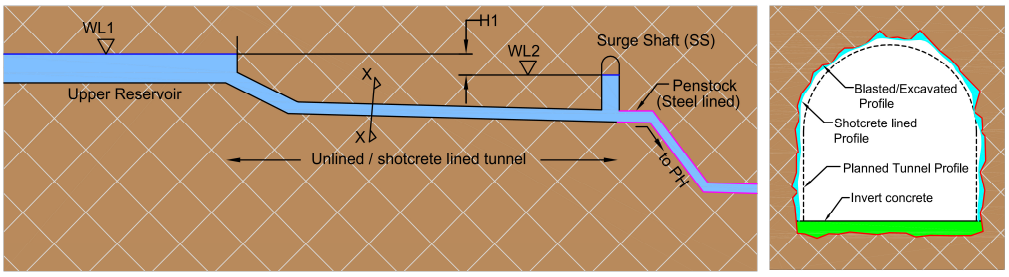

Fig. 4. Location of unlined / shotcrete lined tunnel (left) and its enlarged section @ X-X (right)

In Fig. 4 (left), H_1 is the total headloss incurred while transferring the water from the intake to the SS. In other words, the total headloss is the vertical height difference between the water level at the upper reservoir (WL1) and water level at the SS (WL2). Here, the total headloss is

sum of the friction loss (H_f) and the singular losses (H_s). The friction loss (H_f) in an unlined or shotcrete lined tunnel can be expressed by Eq. 1 (Solvik, 1984);

$$H_f = \frac{l\, v^2}{M^2 R_h^{4/3}} \quad (1)$$

Where, l is length of tunnel, v is flow velocity, M is the Manning's roughness coefficient (hydraulic roughness) and R_h is the hydraulic radius. The flow velocity is the ratio between water discharge (Q) and cross sectional area of tunnel (A) and hydraulic radius is the ratio between the area and the perimeter (P) of the tunnel. Here, smaller M-value represents higher roughness. Usually, as shown in Fig. 4 (right), the shotcrete lined tunnel is provided with concrete lining in the invert. The frictional headloss along the shotcrete lined tunnel can be calculated once the resulting Manning's roughness coefficient of shotcrete lined tunnel with invert concrete lining (M_R) is estimated. Where, the Manning's roughness coefficient entirely depends on the physical roughness of the tunnel periphery. It is hence important to define the physical roughness of the tunnel first and then convert it to hydraulic roughness (Manning's roughness coefficient in this case) in order to define the hydraulics of unlined or shotcrete lined tunnel.

2.1.2 Design criteria

Once the unlined or shotcrete lined tunnel is found economically attractive option, the tunnel should be located in the favorable ground with the help of developed design criteria so that both structural and functional safety is assured. In an unlined pressure tunnel /shaft of a hydropower scheme, water gives pressure to the rock mass around the tunnel periphery equal to the pressure given by vertical water column measured from 'head water level' (HWL) to the point of consideration. This pressure is further termed as water pressure (P_w) and is illustrated in Fig. 5. According to Brekke and Ripley (1987), it is common to use static water head in the design of unlined tunnel. Therefore the dynamic pressure is not considered in the present study. Furthermore, it is obvious to argue here that the water pressure should be resisted by some counter pressure to avoid failure of rock mass around the tunnel. Based on this hypothesis, several design concepts came in practice in the history of unlined pressure tunnel (Palmstrom and Broch, 2017). However, a common requirement for all criteria is that the rock mass around the tunnel should be safe against hydraulic jacking (Basnet and Panthi, 2018c). Two fundamental aspects were considered while defining different design criteria for unlined tunnel; i.e. the topography (overburden) and the in-situ stress state. It is hence

practical to mention a brief history of the development of design criteria for unlined tunnel for better understanding of the concepts and their applicability to the variety of topographical and stress conditions.

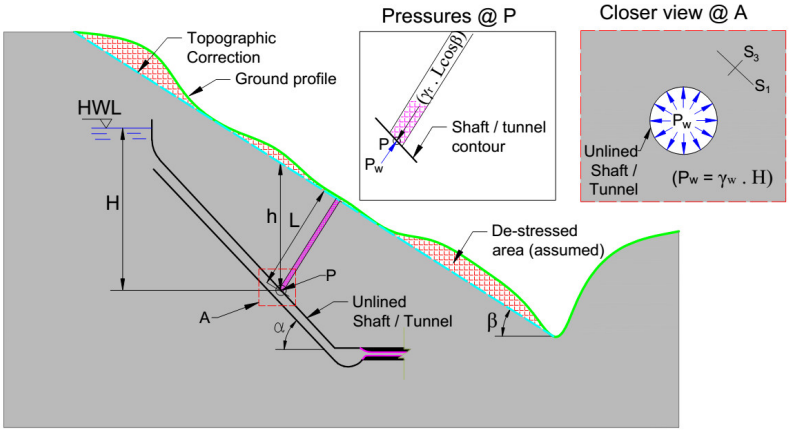

Fig. 5. Different parameters used in different design criteria for unlined shaft / tunnel (Note: S1 is major principal stress, S3 is minor principal stress and HWL is head water level) (Basnet and Panthi, 2018d)

Norwegian confinement criteria

After a failure occurred at Byrte project in Norway in 1968, a criterion for unlined tunnel came in practice with a concept that the ground pressure given by vertical rock cover is sufficient to resist the water pressure so that hydraulic jacking is avoided (Selmer-Olsen, 1969). Mathematically, the criterion is expressed by Eq. 1.

$$h > \frac{P_w}{\gamma_r \times \cos\alpha} \tag{2}$$

Where, h is the vertical rock cover above tunnel alignment, H is the hydrostatic head acting in the tunnel, γ_w is the unit weight of water, γ_r is the specific unit weight of the rock, and α is the inclination of shaft / tunnel with respect to horizontal plane (Fig. 5). The criterion represented by Eq. 2 was governed by the principle that the vertical load of rock mass is well enough to counteract the water pressure. This condition is applicable at relatively flat ground where the horizontal stress is significantly contributed by the tectonic stress. However, the ground is not always flat; rather it is characterized by typical slope topography in the areas where hydropower plants are located. This condition imposed more challenges in reality when a failure occurred in an unlined pressure tunnel at Askara project in Norway in 1970 where the

tunnel was initially designed by using the criteria defined by Eq. 2 (Bergh-Christensen, 1975). This failure demanded the Norwegian design engineers to modify the criterion. The criterion was then modified by incorporating the slope topography to calculate the resisting ground pressure against water pressure. The criterion is mathematically expressed by Eq. 3.

$$\mathrm{L}\cos\beta > \frac{\mathrm{P_w}}{\gamma_\mathrm{r}} \tag{3}$$

Where, L is shortest distance from the ground profile to the tunnel location and β represents the angle of valley side slope with respect to horizontal plane. Both the criteria represented by Eq. 2 and Eq. 3 are commonly known as Norwegian criteria for confinement (Selmer-Olsen, 1969; Bergh-Christensen and Dannevig, 1971; Broch, 1982; Panthi, 2014; Palmstrom and Broch, 2017). In addition to these criteria, a concept came in 1984 that a topographic correction in an undulated ground surface is required to refine the geometrical parameters as shown in Fig. 5 (Broch, 1984). The concept was based on the principal that the rock mass outside of the correction line is supposed to have negligible contribution to the confinement (de-stressed area indicated in Fig. 5).

Furthermore, in a complex topography having slopes in multiple directions, the different slopes have different vertical rock covers, lateral rock covers and valley slope angles for a selected location of unlined pressure tunnel. Hence, Basnet and Panthi (2018d) suggests that there is a necessity to define the representative geometrical parameters required for the confinement criteria in multiple valley slopes. In topography with slopes in different directions, representative values of both vertical rock cover and the term '*Lcosβ*' should be minimum of all possible values. Mathematically, both terms can be represented by Eq. 4 and Eq. 5, respectively.

$$\mathrm{h} = \min(\mathrm{h_i})_{\mathrm{i=1}}^{\mathrm{n}} \tag{4}$$

$$L\cos\beta = min(L_i\cos\beta_i)_{i=1}^{n} \tag{5}$$

In the equations, n is the total number of slopes in different directions. The critical geometrical parameters required for Eq. 2 and Eq. 3 should be estimated by using Eq. 4 and Eq. 5 respectively, in a complex topography. In doing so, the topographic correction should be applied for each slope.

Stress criterion

It is further highlighted that the criterion defined by Eq. 3 was not adequate in some Norwegian projects and one more criterion was evolved with the concept of minimum principal stress after 1970s. The criterion is that the in-situ minimum principal stress (S_3) should always be greater than the water pressure inside tunnel in order to ensure the safety against hydraulic jacking (Selmer-Olsen, 1974; Broch, 1982; Basnet and Panthi, 2018c). The criterion is the state-of-the-art in the design of unlined pressure tunnel and shaft and is represented by Eq. 6.

$$S_3 > P_w \tag{6}$$

It is further highlighted here that the shotcrete lined tunnels act principally very similar to the unlined tunnels in high water pressure. This is due to the fact that 'shotcrete' is a permeable material and almost equal water pressure will act on the rock mass as that on the shotcrete lining (Brekke and Ripely, 1987). Hence, same design criteria as that of the unlined pressure tunnel is recommended to be used for shotcrete lined pressure tunnel as well.

2.1.3 Fluid flow and leakage

It is well known fact that the rock mass composed of both intact rock and discontinuities. Apart from some high-porosity rocks such as young sandstones and certain volcanic rocks, most of the intact rocks have usually very little porosity that means the permeability of the intact rock is very low (Nilsen and Thidemann, 1993). The fluid flow characteristic in most of the rock mass is then governed by the permeability of joints and other discontinuities rather than the permeability of the intact rocks. In an unlined or shotcrete lined pressure tunnel, water comes in contact with rock mass at a certain pressure and the rock mass behaves differently when exposed to the water pressure. The interaction between the water pressure and the rock mass is therefore an important issue to be understood. Since the rock mass has joints, the fluid flow is governed by the conductivity of the joints. For simplicity, if the joint surface is assumed to be planner, the flow may be idealized by means of the parallel plate model (Louis, 1969) and the flow rate per unit width can be represented by Eq. 7.

$$q = -k_j \times a^3 \times \frac{\Delta P}{l} \tag{7}$$

Where, a is the joint hydraulic aperture, k_j is a permeability factor of the joint. ΔP is the fluid pressure drop when the fluid flows between two adjacent joints and l is the spacing of joint or

the length of flow path between two successive flow domains. The concept of flow domain is used in the UDEC model to analyze the fluid flow through joints (ITASCA, 2018). It is now clear that the flow is governed by the pressure differential between adjacent domains where the joint hydraulic aperture has an important role. Once the fluid flow analysis is performed, the possibility of hydraulic jacking and water leakage through the joints can be assessed.

Furthermore, the water leakage from an unlined or shotcrete lined tunnel can be estimated quantitatively with the jointing information along the tunnel. An empirical solution is proposed by Panthi (2006) to estimate the specific leakage (q_t in l/min/m) from the tunnel (Eq. 8).

$$q_t = f_a \times H \times \frac{J_n \times J_r}{J_a} \tag{8}$$

Where, f_a is a joint permeability factor with unit l/min/m^2. This factor is related to the permeability condition of joint sets and expresses conductivity of joint sets, i.e. joint spacing, aperture, roughness infilling conditions etc. H is the static water head (Fig. 5), J_n is joint set number, J_r is joint roughness number and J_a joint alteration number. H, J_n and J_r tend to increase the leakage while the J_a tends to decrease the leakage.

2.2 Applicability issue

Apart from the developed theories, many other important issues need to be addressed while applying the unlined / shotcrete lined pressure tunnel in hydropower project at different topographical, geological and tectonic environment. Some of the important issues are highlighted further in this chapter. The first and foremost condition for unlined pressure conduits is that the rock is impervious, durable and suitable for tunneling (Palmstrom, 1987). It is hence hazardous to place unlined shaft in porous rocks like certain lavas and young sandstones and very blocky and seamy rocks (Nilsen and Thidemann, 1993). In addition, karst phenomenon in limestone and marble is a very challenging issue.

2.2.1 Cost effectiveness

Cost effectiveness is ascertained comparing the cost requirement for different alternative supports in the tunnel. In this regard, the unlined / shotcrete lined tunnels can be compared with the concrete lined tunnel or steel lined tunnel. To achieve same headloss, different linings require different cross-sectional area depending upon the roughness of tunnel meaning that rougher tunnel require bigger tunnel size compared to smother tunnel. For the comparison

purpose, let us consider two different tunnels such as; shotcrete lined tunnel with invert concrete lining and concrete lined tunnel. Since the frictional loss depends on both cross sectional area and the roughness, shotcrete lined tunnel needs larger cross-sectional area compared to concrete lined tunnel for the same headloss. On the contrary, the smoothness achieved with concrete lining demands considerable additional cost. Hence, the tradeoff between the roughness and the cross sectional area of different tunnel types determines the cost effectiveness.

2.2.2 Stability of tunnel

In tunneling, a general requirement is that the tunnel should be stable from both short and long term perspective. There are mainly two types of instabilities in the tunnel. First, structurally controlled gravity driven instability in low in-situ stress environment (Martin et al., 1999) and second, instability caused by stresses in intermediate and high in-situ stress environment (Panthi, 2006 and Panthi, 2012). The first type of instability is experienced as wedge failure and unravelling of blocks from the excavation surface whereas the second is experienced as rock spalling / burst and tunnel squeezing. These instabilities are usually experienced both during excavation and operation of the tunnel. Since the design criteria for unlined pressure tunnel don't directly account these instabilities in the analysis, the stability analysis of the tunnel should be carried out separately. The point here is that the stability of tunnel should be ascertained before applying any design criteria for unlined pressure tunnel.

2.2.3 Jointing and faults/weakness zones

Even though the design criteria are fulfilled, experience shows that the presence of unfavorable joints and faults / weakness zones may hinder the safety of unlined tunnel. The joints which are striking parallel to valley and steeply dipping are vulnerable to hydraulic jacking because of the development of cleft-water pressure. The consequence in such cases would be the deformation of rock mass resulting rock slides at the surface and water leakage through the joints (Broch, 1982). On the other hand, the joints which are dipping towards the valley slope provide leakage paths to drain out the ground water reducing the ground water table. Besides, the presence of faults / weakness zones in the rock mass at the area of unlined tunnel water pressure imposes more challenges. The destressing caused by faults / weakness zones increase the risk of hydraulic jacking. In such cases, the tunnel should be located beyond the influence of the weakness zone if possible. If not, an attempt should always be tried to align the tunnel alignment perpendicular to the zone so that the extent of influence of

the zone along the tunnel alignment is made as short as possible. In conclusion, a careful mapping of all types of influential discontinuities should be carried out during planning, design and construction of the unlined pressure tunnel.

2.2.4 Water inflow and Leakage

In hydropower projects, water leakage is undesirable phenomenon since it causes the loss of revenue. However, it is very difficult to achieve no leakage condition in an unlined or shotcrete lined pressure tunnel. Despite, an attempt should always be tired to minimize the leakage. An initial attempt is to register the tunnel inflow locations during tunneling. The inflow locations are potential leakage locations during the operation of the unlined or shotcrete lined pressure tunnel. More importantly, water leakage occurs though pre-existing open joints and fractures in jointed rock mass, hydraulically jacked joints and weakness zones. These discontinuities in the rock mass have to be sealed to minimize leakage.

2.2.5 Construction issues

Construction easiness, cost saving, reduction of construction time, very limited support requirement etc. are the main attractions of unlined / shotcrete lined pressure tunnels. However, tunneling activities should be carried out using advance technology by experienced tunneling crews. One of the general requirements is that smooth contour blasting may be necessary to make the tunnel surface relatively smooth to reduce the roughness of the tunnel surface. Furthermore, adits at the very difficult steep topography can be avoided with the use of unlined high pressure tunnel provided that the surging facility is fulfilled. One of the surging facilities in such situation is the use of unlined air cushion surge chamber. In Norway, ten hydropower projects are provided with air cushion surge chambers. However, air tightness of the rock mass is main issue in the air cushion chamber which could be a challenging task in the Himalayan rock mass conditions. It is further highlighted that after the tunnel is excavated, the potential leakage zones such as; open joints and fractures should be sealed by means of grouting, using a pressure slightly higher than static water pressure in the tunnel (Buen and Palmstrom, 1982). In Khimti project in Nepal (KHP), both pre-grouting and post-grouting techniques were applied to seal the water leakage (Panthi, 2006; Panthi and Nilsen, 2010). However, it was realized that pre-grouting is a better solution for that particular case.

2.2.6 Filling and dewatering of tunnel

A slow and controlled first filling-up of the unlined or shotcrete lined pressure tunnel and shaft is always recommended to avoid rapid change is pore pressure which may reduce the possible deformations of rock mass caused by local stress anomalies (Buen and Palmstrom, 1982; Palmstrom, 1987 and Palmstrom and Broch, 2017). This will also help to detect any unforeseen leakage so that an appropriate action can be taken in time. In this respect, a standard procedure for filling-up of the tunnel has to be strictly followed. A typical filling-up rate is limited to about 10 m per hour (Buen and Palmstrom, 1982). A normal procedure is that the unlined tunnel or shaft is filled in steps or intervals of 10 to 30 hours. During these intervals, the water level in the shaft should be continuously and accurately monitored. Possible big leakages may thus be detected and the tunnel system can be emptied before any extensive damage is created. On the other hand, Palmstrom and Broch (2017) emphasized that dewatering should be carried out within a month of operation of the power plant without any delay. This is the most critical step to be followed in order to detect the potential stability problems caused by abrupt change in pore pressure in the rock mass. Furthermore, it is recommended that the dewatering should be carried out after approximately one year of operation and after two to five years afterwards. However, if the monitoring of water level indicates even a small stability problems, dewatering should be carried out irrespective of the pre-determined schedule to prevent the problems developing further.

2.2.7 Long term stability

Change in rock mass properties due to the change in pore pressure during operation could cause instability in the initially stable tunnel. Particularly, change in long term behavior of some rocks, minerals and infillings such as; swelling clay, dissoluble minerals, karstic limestone, calcite coatings or fillings in the discontinuities would accelerate the instability problems (Brekke and Ripley, 1987). Block falls and erosion during operation are most common problems in the tunnel. Another important long term issue particularly in the Himalaya could be the impact of dynamic activities. Large seismic events instigate the change in stress state and differential movements at faults and weakness zones (Panthi and Basnet, 2018; Shen et al. 2014). The dynamic activity may also initiate and propagate water flow in the rock mass.

3 Methodology

As has been explained earlier, the use of unlined / shotcrete lined pressure tunnel greatly depends on the cost effectiveness and safety against hydraulic jacking and water leakage. To address these issues, two parallel assessments were carried out in this research work. Fig. 6 shows a generalized flow chart showing the stepwise methodology for the execution of this research work. Since this thesis is the collection of main publications, altogether seven different papers were written covering different issues which are important to demonstrate the applicability of unlined / shotcrete lined tunnel in the Himalaya (Fig. 6).

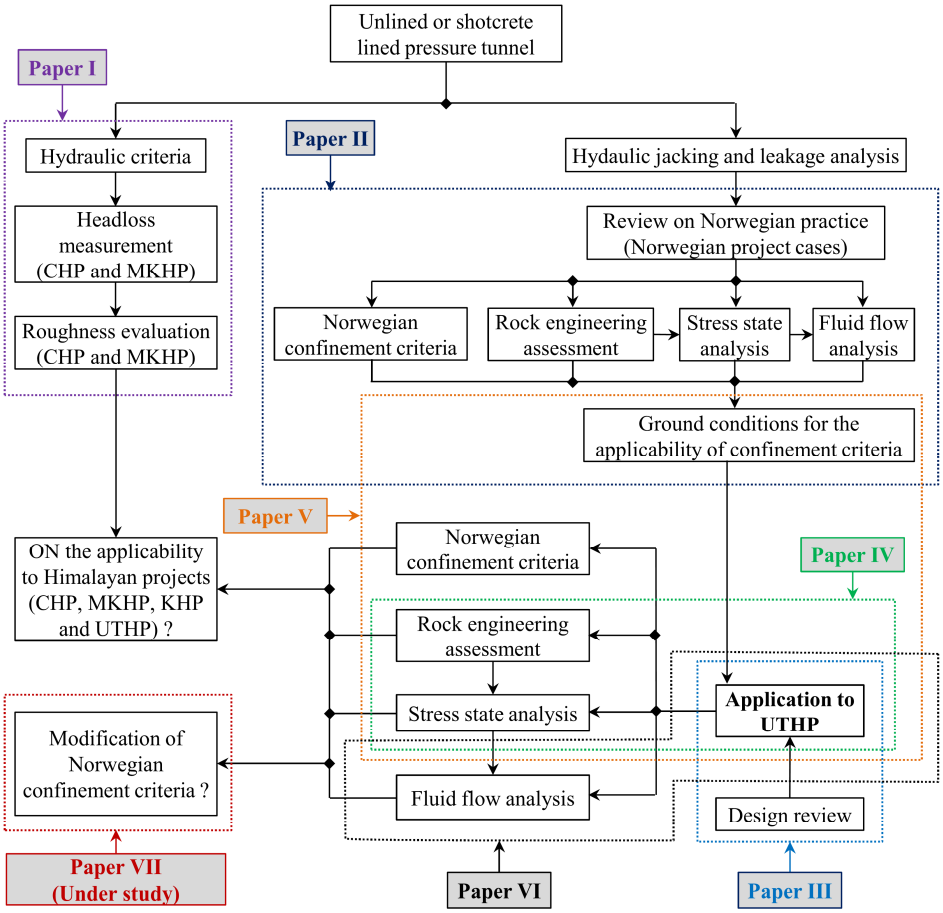

Fig. 6. Flow chart showing the methodology of the research work and formulation of main papers

The research work started with the assessment related to the hydraulic criteria of unlined or shotcrete lined tunnel. The hydraulics of unlined or shotcrete lined tunnel was defined with

the help of existing theory. The roughness of tunnel was found to be a most important parameter in this regard. Head loss was measured in two tunnel cases from the Nepal Himalaya (i.e. CHP and MKHP), which was used as observational data in the analyses. The analyses results and methodology of roughness estimation for shotcrete lined tunnel were published as outcomes in Paper I. Most importantly, the cost effectiveness of the shotcrete lined pressure tunnel was evaluated.

At the same time, the review of Norwegian design practices for unlined pressure tunnels and shafts was continued in parallel (Fig. 6). Both failure and successful cases of unlined pressure shaft and tunnels were taken as case studies. The cases were studied by using Norwegian confinement criteria, rock engineering assessment, stress state analysis and fluid flow analysis. In doing so, information regarding topography, geology, mechanical properties of rocks and stress measurements was gathered from respective sources such as; both published and unpublished reports and articles. In addition, field mapping at some crucial projects and laboratory testing were also executed. More importantly, the stress state and fluid flow analysis were carried out using numerical models called FLAC^{3D} and UDEC, respectively. Both models are developed by ITASCA (ITASCA, 2018). Covering all the information and analyses related to the Norwegian project cases, Paper II was written.

Regarding the assessment of the project cases from Himalaya, the UTHP was taken as a case study. The design of the shotcrete lined pressure tunnel of the UTHP was reviewed and published as Paper III (Fig. 6). The geology and tectonics of the Himalaya in general and of the project area in particular were highlighted. In addition, the most important design issues related to shotcrete lined pressure tunnel of the UTHP were also identified. Once the geo-tectonic environment of the project area was understood, a stress state analysis was carried out using FLAC^{3D} model to estimate the magnitude of in-situ minimum principal stress and Paper IV was written. In addition to the state stress analysis, the shotcrete lined tunnel was analyzed with the confinement criteria, the rock engineering assessment and the outcome of Paper II. Paper V was then written covering the detailed assessments executed for the newly shifted headrace tunnel alignment. Furthermore, the fluid flow analysis was carried out using UDEC model in order to assess the possibility of hydraulic jacking and water leakage and Paper VI was written.

With the help of the outcome of Paper V, it was concluded that the unlined or shotcrete lined pressure tunnels are feasible options in the waterway system of the hydropower project in the

Himalaya with a condition that the tunnels are located in favorable ground conditions. Furthermore, the assessment in this research work (Papers II-VI) concluded that the prevailing design criteria for confinement have to be modified in order to fit into the Himalayan topographical and geo-tectonic conditions. The studies for the modification of Norwegian confinement criteria will be continued in the future with more cases applying this concept are built. A preliminary adjustment in the criterion is presented in Paper VII.

4 Results and discussions

This thesis is mainly a collection of the main manuscript publications. There are altogether seven main papers which were written to fulfill the objective of this research work. The full version of the papers is presented in Part II of this thesis. The synopsis of the outcome of the papers and some supplementary results are summarized in the following. The limitations of the research work are also highlighted.

4.1 Summary of main publications

4.1.1 Paper I

Basnet, C.B. *and Panthi, K.K., 2018a. Roughness evaluation in shotcrete-lined water tunnels with invert concrete based on cases from Nepal. Journal of Rock Mechanics and Geotechnical Engineering; 10(1): pp. 42-59.*

Tunnel hydraulics and cost effectiveness

This paper proposes a relationship between tunnel over break thickness (t_m) and physical roughness of shotcrete lining (ε_{sc}) in walls and crown of the tunnel based on the tunnel cases from the CHP (Eq. 9). Since the shotcrete lined tunnel had concrete lining in the invert, the resulting physical roughness of the whole tunnel periphery (ε_R) was calculated by weighted average of the respective roughness with respect to the perimeter (Eq. 10). In Eq. 10, the physical roughness of the concrete lining in the invert is denoted by ε_c. In addition, the relationship between physical roughness and Manning's roughness coefficient proposed by Colebrook (1958) and Solvik (1984) has been modified and a new relationship is proposed (Eq. 11).

$$\varepsilon_{sc} = \frac{1}{1.7} {t_m}^{1/1.3} \tag{9}$$

$$\varepsilon_R = \frac{\varepsilon_{sc} p_{min} + \varepsilon_c W_{min}}{p_{min} + W_{min}} \tag{10}$$

$$M_R = \frac{24}{{\varepsilon_R}^{1/5}} \tag{11}$$

Where, P_{min} is the perimeter of walls and crown of the tunnel and W_{min} is width of the tunnel. For the prediction of the roughness before the tunnel is excavated, the geometrical parameters are calculated from the designed tunnel profile.

Furthermore, the cost effectiveness of the shotcrete lined tunnel with invert concrete lining has also been evaluated in this article. It has been concluded that the shotcrete lined tunnel with invert concrete lining are economically more attractive than the fully concrete lined tunnel as far as hydraulic criteria is concerned.

4.1.2 Paper II

Basnet, C.B. *and Panthi, K.K., 2018b. Analysis of unlined pressure shafts and tunnels of selected Norwegian hydropower projects. Journal of Rock Mechanics and Geotechnical Engineering; 10(3): pp.1-27.*

Review of Norwegian practice in unlined pressure tunnels and shafts

This paper reviews some of the first attempts of the use of unlined pressure shaft and tunnel concepts in Norway. More specifically, the major failure cases and two successful cases of significance are considered as reference cases for the detail study. The Norwegian criteria for unlined pressure tunnel and shaft are applied to the cases and the triggering factors for failure are identified. In addition, detailed engineering geology of failure cases is evaluated and also common geological features that could have aggravated the failure are assessed. The magnitude of minimum principal stress is investigated and quantified along unlined pressure shaft and tunnel alignment of six selected project cases by using three-dimensional numerical model. Furthermore, conditions of failure through pre-existing open joints by hydraulic jacking and leakage are assessed by using two-dimensional fluid flow analysis. As an outcome of all executed analyses and assessments, both favorable and unfavorable ground conditions required for the applicability of Norwegian confinement criteria in locating the unlined pressure shafts and tunnels at different geo-tectonic environments are highlighted. More importantly, the adverse impact of unfavorably oriented joints, presence of weakness zones in the rock mass, nearby fault zones, and three-dimensional complex geometry etc. in an unlined pressure tunnel and shaft is recognized and verified by the analyses.

4.1.3 Paper III

Panthi, K.K. and ***Basnet, C.B.,*** *2017. Design review of the headrace system for the Upper Tamakoshi project, Nepal. The International Journal on Hydropower and Dams; Vol. 24, Issue 1, pp. 60-67.*

Design review of pressure tunnel in the UTHP

The paper highlights and reviews both old and modified designs of the headrace tunnel of the UTHP and reasons for design modification requirement had been discussed. In addition, evaluation had been made on engineering geological characteristics of the rock mass and in-situ stress state prevailing of the project area. Finally, the issues related to the design of shotcrete lined pressure tunnel of the UTHP are discussed in detail.

4.1.4 Paper IV

Basnet, C.B. *and Panthi, K.K., 2018c. Evaluation on the minimum principal stress state and potential hydraulic jacking from the shotcrete lined pressure tunnel - A case from Nepal. Rock Mechanics and Rock Engineering (under review).*

Stress state analysis at the UTHP area

In this paper, a comprehensive assessment is carried out by developing a full rock stress model so that a reliable value of minimum principal stress along the unlined pressure tunnel can be estimated. To address the complex geotectonic and topographic environment of the UTHP project area, a final rock stress model (FRSM) concept as suggested by Stephansson and Zang (2012) is heavily utilized. The FRSM concept considers stepwise evaluation of the in-situ stress state analysis integrating the best estimate stress model (BESM), stress measurement methods (SMM) and integrated stress determination methods (ISD). The analysis carried out in this paper reveals that the in-situ stress state at the project area has high degree of spatial variation even at the similar overburden due to the presence of complex topography and the presence of local shear and weakness zones. The analysis further demonstrates that a presence of local shear / weakness zone has considerable de-stressing effect, which leads to the reduction of in-situ minimum principal stress magnitude. The analysis finally shows that the reduction in the minimum principal stress along the pressure tunnel increases the risk for the potential hydraulic jacking and leakage at the vicinity of the shear zone along old shotcrete lined pressure tunnel alignment.

4.1.5 Paper V

Basnet, C.B. *and Panthi, K.K., 2018d. Detailed assessment on the use of unlined or shotcrete lined pressure tunnel in the Himalayan rock mass conditions: A case study from Nepal. Bulletin of Engineering Geology and the Environment (under review).*

Detailed assessment of shotcrete lined pressure tunnel of the UTHP

This paper studies the both old and new shotcrete lined pressure tunnel of the UTHP in detail. The pressure tunnel alignments are assessed with the Norwegian confinement criteria, rock engineering aspects and minimum principal stresses from both measurement and numerical simulation. It has been found that the good quality rock mass with tight joints is suitable for unlined /shotcrete lined tunnel provided that the stress requirement is fulfilled. Even though the Norwegian confinement criteria show headrace tunnel alignment is safe for unlined tunnel concept, the detailed rock engineering assessment and stress state analysis indicated that some critical locations along the headrace tunnel alignment are vulnerable for the unlined or shotcrete lined tunnel concept. This is specially the case for about 700m downstream stretch of the newly excavated headrace tunnel from where there is a high risk for the potential hydraulic jacking to occur, which may lead to the excessive water leakage. The paper further argues that there is a need for the modification on the Norwegian confinement criteria in order to make them applicable in the Himalayan rock mass conditions.

4.1.6 Paper VI

Basnet, C.B. *and Panthi, K.K., 2018e. Hydraulic jacking and leakage assessment in an unlined or shotcrete lined pressure tunnel - A case study from the Nepal Himalaya. To be submitted.*

Hydraulic jacking and leakage assessment

This paper first performs the qualitative assessment of the possibility of hydraulic jacking and water leakage at the headrace tunnel of the UTHP. For that fluid flow analysis through the rock mass is carried out using the UDEC model at different selected locations along the unlined or shotcrete lined pressure tunnel. The result of fluid flow analysis carried out at the study locations show that there is higher risk of hydraulic jacking and water leakage at the tunnel stretch downstream of chainage 7+300 m than the upstream side. Furthermore, a quantitative assessment of the leakage is also carried out in this paper. Panthi's approach is used to calculate the specific leakage from the headrace tunnel of the UTHP. The average

specific leakage from the headrace tunnel of the UTHP from chainage 2+914 m to 7+960 m is estimated about 2.7 l/min/m. The result of leakage estimation further suggests that the stretch of tunnel segments with high leakage values should be sealed before the test water filling. The stretch of the tunnel vulnerable to water leakage is particularly downstream of the chainage 5+700 m to the end of headrace tunnel.

4.1.7 Paper VII

Panthi, K.K. and ***Basnet, C.B.,*** *2018a. State-of-art Design Guidelines in the Use of Unlined Pressure Tunnels / Shafts for Hydropower Scheme. 10th Asian Rock Mechanics Symposium, ISRM International Symposium.*

Modification of the confinement criteria

In this paper, the state-of-the-art design guidelines for the use of unlined / shotcrete lined pressure tunnels are suggested with the belief that the vast hydropower resources still untapped in the Himalayan region will be even more cost effective, technically sound and long-term sustainable solution. In this regard, a state-of-art modification in the Norwegian confinement criterion is proposed in order to fit into different topographical, geological and geo-tectonic environments. The finding of this paper is that the lateral rock cover calculated from the Norwegian confinement criterion should be multiplied by a factor, which varies from 1.6 to almost 3 to address another valley in addition to a single valley that prevails in the Scandinavia.

4.2 Supplementary results

4.2.1 Roughness estimation at the UTHP

Using the methodology of roughness evaluation (Paper I), the roughness of the shotcrete lined tunnel of the UTHP is evaluated. At the headrace tunnel of the UTHP, altogether 62 actual tunnel cross-sections are available to measure the mean over-break thickness (t_m) and other geometrical parameters. The tunnel sections were mapped after a layer of shotcrete lining was applied in the walls and the crown of the tunnel. The invert is designed to be lined with the concrete. The physical roughness of shotcrete lined part (ε_{sc}) is calculated from the over-break thickness using Eq. 9. On the other hand, the physical roughness of the concrete lining at the invert (ε_c) is taken same as that considered in Paper I for both CHP and MKHP cases. From these roughnesses, the resulting roughness for whole tunnel periphery (ε_R) is calculated using Eq. 10. Finally, the Manning's roughness coefficient for the shotcrete lined tunnel with invert

concrete lining is calculated using Eq. 11. The statistical distribution of different roughness values are presented in Table 1.

Table 1. Manning's roughness coefficient of shotcrete lined tunnel with invert concrete lining of the UTHP

Statictical values	t_m m	ε_{sc} m	ε_c m	ε_R m	M_R $m^{1/3}/s$
Min.	0.078	0.083	-	0.060	35
Max.	0.256	0.206	-	0.148	42
Mean	0.149	0.135	0.0033	0.097	38
Sd.	0.038	0.027	-	0.019	2

Table 1 shows that the mean value of the Manning's roughness coefficient for the shotcrete lined tunnel of the UTHP is 38, which in other two projects (the CHP and the MKHP) was estimated as 39 and 38, respectively. It seems that the estimated roughness values of the UTHP are more or less similar to that of other two projects. The estimated roughness values can further be used to calculate the headloss along the whole tunnel alignment using Eq. 1. However, the headloss measurement during the operation of the tunnel is always recommended to verify the calculated headloss.

4.2.2 Different topographical conditions prevailing at the UTHP

The ground conditions, mentioned by Basnet and Panthi (2018b), for the applicability of the confinement criteria are mostly related to the topography in addition to other geological and tectonic factors. The topographies prevailing in the Himalaya are generalized as three different topographical conditions by Panthi and Basnet (2018a). In the UTHP, three similar topographies are identified along headrace tunnel alignment as shown in Fig. 7a. In the figure, 'Zone I' represents single valley topography, Zone II represents two valleys topography and Zone III represents multiple valley topography. All three zones are commonly encountered in most of the tunnel alignments in the Himalaya (Panthi and Basnet, 2018a). The extent of stress attenuations is different in each of the three zones having less attenuation in Zone I compared to other zones and Zone III has obviously largest attenuation due to multiple deep valleys. This situation is manifested in Fig. 7 (Fig. 7b, Fig. 7c and Fig. 7d) where the magnitude of minimum principal stresses at different sections is attenuated towards the valley slopes. The extent of the attenuation is obviously different for different topographical conditions. The stress magnitudes in Fig. 7 are extracted from the stress state analysis carried out in Paper V (Basnet and Panthi, 2018d).

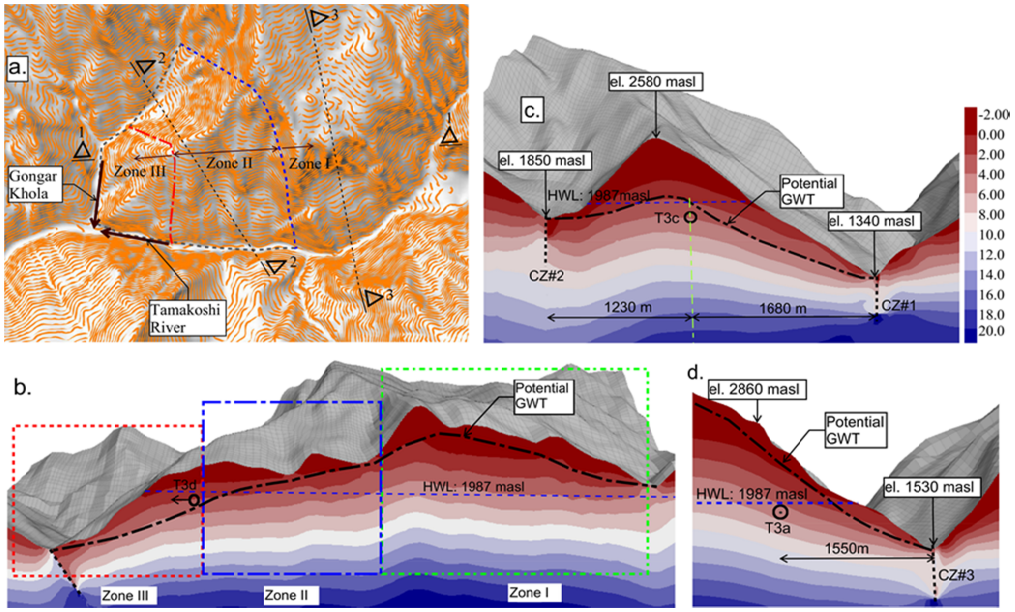

Fig. 7. a. Categories of different topographic zones based on the vulnerability of hydraulic jacking and leakage at the UTHP; b. Section 1-1; c. Section 2-2; d. Section 3-3 (Note: minimum principal stress shown in the sections is in MPa)

Furthermore, on the basis of the assessment carried out for the Norwegian failure and successful cases (Paper II) and the Tamakoshi area (Paper IV and V), Table 2 lists out typical ratings for different parameters at different topographical conditions. These ratings will certainly help to locate the unlined or shotcrete lined pressure tunnel in a favorable ground condition.

Table 2. Rating for different parameters at different zones

Zones	Destressing	Confinement	Joint frequency	Joint aperture / opening	Frequency of weakness zones	Depth of GWT from slope topography
Zone I	Low	High	Low	Low	Low	Low
Zone II	Medium	Medium	Medium	Medium	Medium	Medium
Zone III	High	Low	High	High	High	High

4.2.3 Seismic influence in the in-situ stress state

The whole Himalaya region is very dynamic and has been witnessing large number of various scaled earthquakes. The UTHP area is relatively close (about 13 km) to the epicenter of 7.3 M_w (moment magnitude scale) aftershock occurred on 12th of May 2015. The impact of this seismic event to the in-situ stress state of the UTHP area is studied by Panthi and Basnet

(2018b). For that, both static and dynamic analysis was carried out in FLAC^{3D} model. The model was first validated for static analysis with the help of measured stresses at different locations. The final result of the static analysis in terms of the magnitude of minimum principal stress is shown in Fig. 8a. The model was then run for dynamic analysis where the peak ground acceleration (PGA) computed by USGS (2015) was used to validate the model.

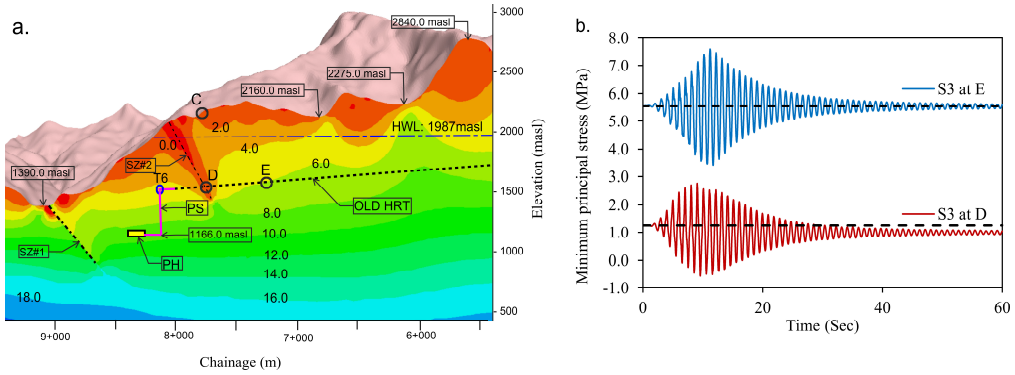

Fig. 8. a. Minimum principal stress (MPa) along old headrace tunnel (OLD HRT) of the UTHP after static analysis; b. Minimum principal stress recorded over the dynamic time period during dynamic analysis (Panthi and Basnet, 2018b)

Fig. 8b shows the minor principle stress recorded during the dynamic time period at two different locations; i.e. D and E which are shown in Fig. 8a. The figure demonstrates that there is high fluctuation in the stress values during highest shaking period. The stress value at location E eventually dampens and reaches to its original value, which belongs to the point where intact rock mass exist and is far from the shear zone (SZ#2). However, at location D where SZ#2 is situated, the stress dampens to a new stress value and is reduced from the original value. This indicates that the weakness and fault zones are vulnerable areas during seismic events and permanent change in the stress state are eminent.

4.2.4 Methodology for the design of unlined or shotcrete lined pressure tunnel

A design methodology has been finally developed as an outcome in order to select the favorable location of unlined or shotcrete lined pressure tunnel and shaft (Fig. 9). The methodology also incorporates the comprehensive design consideration in unlined pressure tunnels. During the application of the methodology, a continuous feedback system is necessary in order to improve and modify the existing design criteria.

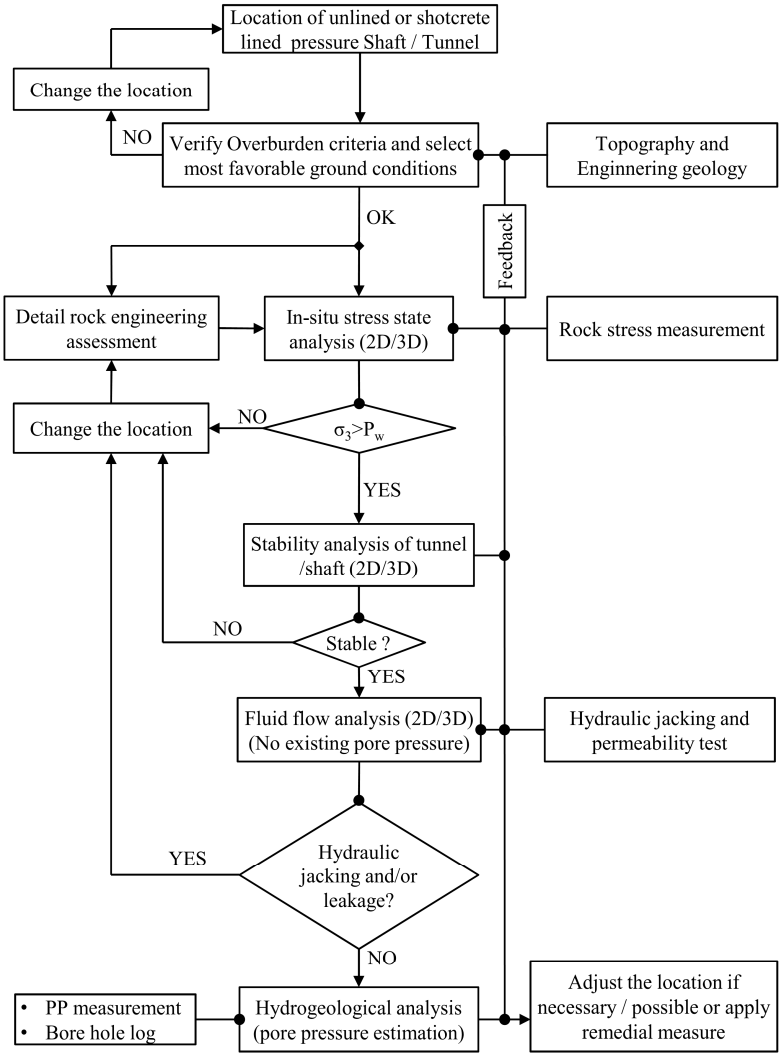

Fig. 9. Flow chart showing the methodology for the planning and design of unlined or shotcrete lined pressure tunnel (Note: PP is pore pressure).

4.3 Limitations

The findings of this PhD research work, especially related to the Himalaya, are based on three project cases. This indicates that there is still possibility of enhancing the proposed concepts presented in this PhD thesis with the consideration of more cases of unlined or shotcrete lined pressure tunnels in the hydropower projects of the Himalaya.

5 Conclusions

This PhD research draws following conclusions in the end of the study.

- The shotcrete lined tunnels are one of the economically attractive solutions in the waterway system of the hydropower projects.
- The Norwegian confinement criteria for the design of unlined or shotcrete lined tunnels are valid only in favorable ground conditions for their applicability. The unfavorable ground conditions on the other hand needs further analysis.
- A comprehensive stress state analysis should be carried out in the area of complex topography, geology and tectonics.
- The unlined or shotcrete lined pressure tunnel are possible in Himalayan rock mass conditions.
- It is however required to modify the exiting Norwegian confinement criteria in order to fit them into the Himalayan conditions.
- The modification requirement is mainly due to the fact that the safe location of the unlined pressure tunnels and shafts will mainly depend on the topographic complexity, tectonic environment and presence of weakness / fault zones.
- The proposed modified equation in most of the cases will provide a satisfactory location of the unlined pressure tunnel given that the ground conditions are favorable for unlined or shotcrete lined tunnels. It is, however, always of benefit to carry out stress measurement during construction before deciding on the exact location from where an unlined or shotcrete lined pressure tunnel is to start.
- Fluid flow and leakage analyses should be carried out in a jointed rock mass and at the area of weakness zones to ensure the safety against hydraulic jacking and water leakage.

6 Future research

This PhD thesis emphasizes that the stress database is very important for the reliability of the numerical analysis. However, the stress database of the Himalaya in general is limited. This indicates that the database should be enhanced by conducting more measurements in future. Focus should be given to demarcate the different tectonic blocks of the Himalaya in terms of magnitude and direction of the tectonic stresses. The tectonic stress information can then be used in the numerical models so that in-situ stress state at the area of unlined or shotcrete lined pressure tunnels can be estimated more accurately. In addition, more case studies of the unlined or shotcrete lined pressure tunnel located at different topographic and geo-tectonic environments can be included in the analysis to enhance the outcome of this thesis in future.

References

Basnet, C.B. and Panthi, K.K., 2018a. Roughness evaluation in shotcrete-lined water tunnels with invert concrete based on cases from Nepal. *Journal of Rock Mechanics and Geotechnical Engineering*; 10(1): pp.42-59.

Basnet, C.B. and Panthi, K.K., 2018b. Analysis of unlined pressure shafts and tunnels of selected Norwegian hydropower projects. *Journal of Rock Mechanics and Geotechnical Engineering*, 10(3): pp.1-27.

Basnet, C.B. and Panthi, K.K., 2018c. Evaluation on the minimum principal stress state and potential hydraulic jacking from the shotcrete lined pressure tunnel - A case from Nepal. *Rock Mechanics and Rock Engineering*, under review.

Basnet, C.B. and Panthi, K.K., 2018d. Detailed assessment on the use of unlined or shotcrete lined pressure tunnel in the Himalayan rock mass conditions: A case study from Nepal. *Bulletin of Engineering Geology and the Environment*; under review.

Benson, R., 1989. Design of unlined and lined pressure tunnels. *Tunneling and Underground Space Technology*; 4(2): 155-70.

Bergh-Christensen, J., 1975. Failure of unlined pressure tunnel at Askara Power Plant. In: Proceedings of the Bergmekanikkdagen.(Rock mechanics day) (in Norwegian): pp.15.1-15.8.

Bergh-Christensen J., Dannevig N.T., 1971. Engineering geological evaluations of the unlined pressure shaft at the Mauranger Hydropower Plant. *Technical report*. Oslo, Norway: Geoteam A/S.

Brekke, T.L., Ripley, B.D., 1987. Design guidelines for pressure tunnels and shafts. Technical report No. EPRI-AP-5273. *Department of Civil Engineering, California University at Berkeley*.

Broch, E., 1982. The development of unlined pressure shafts and tunnels in Norway. *Proceedings of the International Symposium, International Society for Rock Mechanics (ISRM)*; pp.545-54.

Broch E., 1984. Unlined high pressure tunnels in areas of complex topography. *International Water Power and Dam Construction*. 36(11): pp.21-23.

Broch, E., 2013. Underground hydropower projects - Lessons learned in home country and from projects abroad. *Norwegian Tunneling Society*; pp.11-19.

Buen, B. and Palmstrom, A., 1982. Design and Supervision of Unlined Hydro Power Shafts and Tunnels with Head up to 590 Meters. *ISRM International Symposium*. International Society for Rock Mechanics.

Colebrook, C.F., 1958. The flow of water in unlined, limed and partly lined rock tunnels. *Proceedings of the Institution of Civil Engineers*; 11(1): pp.103-32.

DGM, 1994. Geological Map of Nepal (scale 1:1,000,000). *Department of Geology and Mines*, Nepal.

ITASCA, 2018. ITASCA Consulting Group, Inc. (https://www.itascacg.com).

Johansen, T., 1984. Norwegian tunneling. Oslo, Norway: FHS.

Louis, C., 1969. A study of groundwater flow in jointed rock and its influence on the stability of rock masses. Imperial College. *Rock Mechanics Research Report*, 10, pp.1-90.

Martin, C.D., Kaiser, P.K. and McCreath, D.R., 1999. Hoek-Brown parameters for predicting the depth of brittle failure around tunnels. *Canadian Geotechnical Journal*; 36(1): pp.136-151.

Nilsen, B., & Thidemann, A., 1993. Rock engineering. Norwegian Institute of Technology, Division of Hydraulic Engineering, *Hydropower development series*; 9.

Palmstrom, A., 1987. Norwegian design and construction of unlined pressure shafts and tunnels. *Proceedings of the International conference on Hydropower*, Oslo, Norway, pp. 87-111.

Palmstrom A. and Broch E., 2017. The design of unlined hydropower tunnels and shafts: 100 years of Norwegian experience. *International Journal on Hydropower and Dams*; 3: pp.1-9.

Panthi, K.K., 2006. Analysis of engineering geological uncertainties related to tunneling in Himalayan rock mass conditions. *PhD Thesis, NTNU*, Trondheim, Norway.

Panthi, K.K. and Nilsen, B., 2007. Predicted versus actual rock mass conditions: A review of four tunnel projects in Nepal Himalaya. *Tunnelling and underground space technology*; 22(2): pp.173-184.

Panthi, K.K. and Nilsen, B., 2010. Uncertainty analysis for assessing leakage through water tunnels: A case from Nepal Himalaya. *Rock mechanics and rock engineering*; 43(5): pp. 629-639.

Panthi, K.K., 2012. Evaluation of rock bursting phenomena in a tunnel in the Himalayas. *Bulletin of Engineering Geology and the Environment*; 71(4): pp.761-769.

Panthi, K.K., 2014. Norwegian design principle for high pressure tunnels and shafts: Its applicability in the Himalaya. *Journal of Water, Energy and Environment*; 14: pp.36-40.

Panthi, K.K., 2015. Himalayan rock mass and possibility of limiting concrete lined pressure tunnel length in hydropower projects in the Himalaya. *Geosystem Engineering*; 18(1): pp.45-50.

Panthi, K.K. and Basnet, C.B., 2017. Design review of the headrace system for the Upper Tamakoshi project, Nepal. *The International Journal on Hydropower and Dams*; 24(1): pp.60-67.

Panthi, K.K. and Basnet, C.B., 2018a. State-of-the-art design guidelines in the use of unlined pressure tunnels / shafts for hydropower scheme. *10th Asian Rock Mechanics Symposium (ARMS10)*, the ISRM International Symposium.

Panthi, K.K. and Basnet, C.B., 2018b. A dynamic stress state analysis at the pressure tunnel of Upper Tamakoshi HPP, Nepal. *Third International Conference on Rock Dynamics and Applications (RocDyn-3)*; pp.251-257.

Rowley, D.B., 1996. Age of initiation of collision between India and Asia: A review of stratigraphic data. *Earth and Planetary Science Letters*; 145(1): pp.1-13.

Selmer-Olsen, R., 1969. Experience with unlined pressure shafts in Norway. *Proc. Int. Symposium On Large Permanent Underground Openings*, Oslo.

Selmer-Olsen, R., 1974. Underground openings filled with high-pressure water or air. *Bulletin of the International Association of Engineering Geology*; 9(1): pp.91-95.

Shen, Y., Gao, B., Yang, X. and Tao, S., 2014. Seismic damage mechanism and dynamic deformation characteristic analysis of mountain tunnel after Wenchuan earthquake. *Engineering Geology*; 180: pp.85-98.

Solvik, O., 1984. Unlined tunnel hydraulics. *Hard rock underground engineering*; FHS, Olso, Norway.

Stephansson, O. and Zang, A., 2012. ISRM suggested methods for rock stress estimation—part 5: establishing a model for the in situ stress at a given site. *ISRM Suggested Methods for Rock Characterization, Testing and Monitoring*: 2007-2014 (pp. 187-201).

USGS, 2015. U.S. Geological Survey: ShakeMap of M 7.3 aftershock - 19km SE of Kodari, Nepal: (https://earthquake.usgs.gov/earthquakes/eventpage/us20002ejl#shakemap)

Vogt, JHL., 1922. Pressure tunnels and geology. Technical Report No. 93. Oslo, Norway: NGU.

Part II

Main Publications

Authors' contributions in the main publications

The PhD research concept was developed by the supervising professor while applying for the research fund of this PhD research project.

Papers	Main contributions	
	1st Author	2nd Author
Paper I	Field measurements, data collection, analysis and calculations, manuscript writing, follow-up during editing and publication.	Concept formulation, data allocation, manuscript review and editing etc.
Paper II	Data collection, laboratory testing, analyses and calculations, manuscript writing, follow-up during editing and publication.	Concept formulation, translation of Norwegian articles to English, data allocation, manuscript review and editing, etc.
Paper III	Concept formulation, data collection, manuscript writing, issues finalization, follow-up during publication, etc.	Data collection, calculations and artworks, manuscript writing, follow-up during editing etc.
Paper IV	Data collection, detailed analyses and calculations, manuscript writing, follow-up during editing and submission.	Concept formulation, data allocation, manuscript review and editing etc.
Paper V	Field mapping, data collection, laboratory testing, detailed analyses, assessment and calculation, manuscript writing, follow-up during editing and submission.	Concept formulation, data allocation, manuscript review and editing etc.
Paper VI	Field mapping, data collection, laboratory testing, detailed analyses and calculations, manuscript writing, follow-up during editing.	Concept formulation, data allocation, manuscript review and editing etc.
Paper VII	Concept formulation, manuscript writing, review and editing, and follow-up during publication, etc.	Analysis, calculations and artworks, manuscript writing, follow-up during editing etc.

Paper I

Title:

Roughness evaluation in shotcrete lined water tunnels with invert concrete based on cases from Nepal

Authors:

Basnet, Chhatra Bahadur

Panthi, Krishna Kanta

Published in:

Journal of Rock Mechanics and Geotechnical Engineering (2018)

Volume 10(1), pages 42-49

Journal of Rock Mechanics and Geotechnical Engineering 10 (2018) 42–59

Contents lists available at ScienceDirect

Journal of Rock Mechanics and Geotechnical Engineering

journal homepage: www.rockgeotech.org

Full Length Article

Roughness evaluation in shotcrete-lined water tunnels with invert concrete based on cases from Nepal

Chhatra Bahadur Basnet*, Krishna Kanta Panthi

Department of Geosciences and Petroleum, Norwegian University of Science and Technology, Sem Saelands Vei 1, NO-7491, Trondheim, Norway

ARTICLE INFO

Article history:
Received 18 April 2017
Received in revised form
19 June 2017
Accepted 18 July 2017
Available online 21 November 2017

Keywords:
Shotcrete-lined water tunnels
Friction loss
Physical and hydraulic roughnesses
Tunnel over-break

ABSTRACT

Most of the existing roughness estimation methods for water tunnels are related to either unlined or concrete/steel-lined tunnels. With the improvement in shotcrete technology, advancement in tunneling equipment and cost and time effectiveness, future water tunnels built for hydropower projects will consist of rock support with the extensive use of shotcrete lining in combination with systematic bolting and concrete lining in the tunnel invert. However, very little research has been performed to find out tunnel surface roughness for shotcrete-lined tunnels with invert concrete, which is important in calculating overall head loss along the waterway system to achieve an optimum and economic hydropower plant design. Hence, the main aim of this article is to review prevailing methods available to calculate tunnel wall roughness, and to use existing methods of head loss calculation to back-calculate roughness of the shotcrete-lined tunnels with invert concrete by exploiting measured head loss and actual cross-sectional profiles of two headrace tunnels from Nepal. Furthermore, the article aims to establish a link between the Manning coefficient and the physical roughness of the shotcrete-lined tunnel with invert concrete and to establish a link between over-break thickness and physical roughness. Attempts are also made to find a correlation between over-break thickness and rock mass quality described by Q-system and discussions are conducted on the potential cost savings that can be made if concrete lining is replaced by shotcrete lining with invert concrete.

1. Introduction

The waterway tunnels represent the most significant source of construction cost for hydropower projects, especially for run-of-the-river plants. Reducing and optimizing the cost of waterway systems is therefore a major issue to make hydropower projects financially attractive. One of the economic solutions is to use unlined or shotcrete-lined pressure tunnels or combination of both for the waterway system if the rock mass and applied shotcrete and/or systematic bolting guarantee long-term stability and safety (Panthi, 2015). Originally, the application of unlined shafts and tunnels as waterway systems came in practice in Norway with the philosophy that accepts minor falls of rock blocks during the operation period provided that head loss is within permissible limits (Broch, 1982). The basic criteria to be satisfied for unlined or shotcrete-lined pressure shafts and tunnels are safety against hydraulic splitting, hydraulic efficiency (frictional head loss) and long-term stability (Brekke and Ripley, 1987; Benson, 1989). Frictional head loss depends on both cross-sectional area and roughness of tunnel periphery in consideration (Rahm, 1958), because rougher tunnel wall surfaces will result in higher head loss and larger cross-sectional areas result in smaller head loss. An alternative way to reduce the head loss can be the use of concrete or steel lining to make the tunnel surfaces smoother without increasing tunnel size. However, lining a tunnel with concrete or steel will demand considerable additional cost (Huval, 1969; Westfall, 1996).

Tunnel shape also influences hydraulic efficiency of the water tunnel. In tunnel boring machine (TBM) tunneling, the tunnel cross-section is circular (i.e. hydraulically ideal shape) with smooth rock surfaces. However, it is not always feasible to use TBM as an excavation method since the success of TBM application is largely dependent on the geological conditions and length of the tunnel to be excavated. Hence, the drill-and-blast method of tunnel excavation is popular and extensively used due to flexibility in making decisions if unforeseen geological conditions arise and it can be

* Corresponding author.
E-mail address: Chhatra.basnet@ntnu.no (C.B. Basnet).
Peer review under responsibility of Institute of Rock and Soil Mechanics, Chinese Academy of Sciences.

https://doi.org/10.1016/j.jrmge.2017.07.006

used in any length of tunnel to be excavated, provided that ventilation requirements during construction are met. However, tunnel walls excavated using drill-and-blast method have an undulating surface of varying smoothness and the shape of tunnel will be determined mostly by construction necessities and easiness (Lysne et al., 2003). The most practical tunnel shapes in drill-and-blast tunneling are inverted D and horse-shoe (Cuesta, 1988; Panthi, 2015). In waterway tunnels, excavated tunnel profiles may either be left unlined or shotcrete-lined or concrete/steel-lined (or a combination of different linings). The shotcrete-lined tunnels end up more or less with the excavated shape and surface as shown in Fig. 1.

As seen in Fig. 1, there are undulations in the contour surface in a tunnel excavated using the drill-and-blast method due to the presence of grooves and projections. The frequency distribution and amplitude of these undulations signify resistance to water flow and are defined by the term surface/physical roughness. These undulations are the result of over-break of the rock mass beyond the designed tunnel profile (Maerz et al., 1996). The larger the over-break area is, the more the tunnel surface will be undulated and rough. Hence, over-break is the key parameter to define roughness of the tunnel surface. According to various researches, over-break in drill-and-blast tunnels is the result of look-out and deviation in contour holes, blasting energy, rock mass condition and in situ stress situation (Nilsen and Thidemann, 1993; Mandal and Singh, 2009; Kim and Bruland, 2015). Longer blast rounds develop greater longitudinal over-break leading to an increase in roughness of the tunnel surface. Similarly, the rock mass condition influences over-break intensity and roughness. In Fig. 2a, the blasted tunnel surface is relatively smooth in the case of a homogeneous rock mass, whereas, if rock mass is jointed, the surface roughness is partially determined by the jointing pattern (Fig. 2b). In addition, there might be some localized enlarged over-break due to the presence of faults or weakness zones (Figs. 1b and 2c), which will further increase the roughness. Fig. 2a is seldom achieved in the jointed rock mass, thus Fig. 2b and c represents the most common contour profile types in blasted tunnels. Over-break in Fig. 2a and b may be defined as normal over-break, whereas localized enlarged area in Fig. 2c may be expressed as excessive over-break. Such localized enlarged areas may also be formed due to stress induced rock spalling and bursting in hard rock (Panthi, 2012).

Now the question arises as how the physical roughness can be used to calculate frictional head loss along the waterway tunnel. Both the Darcy–Weisbach and Manning formulae use coefficient of resistance, known as hydraulic roughness, in order to calculate frictional head loss. However, the hydraulic roughness in the equations is not equivalent to the physical roughness directly measured from the tunnel surface. Before 1980, according to Bishwakarma (2012), it was a common practice to calculate hydraulic roughness from the relative variation of cross-sectional area along the tunnel length using different methods proposed by Rahm (1958), Priha (1969), Reinius (1970), Wright (1971) and others. Later in the 1990s, the concept was updated with the introduction of physical roughness of the tunnel, which is related to both surface undulations and area variation (Bruland and Solvik, 1987; Ronn and Skog, 1997), and the physical roughness was converted to the hydraulic roughness in order to fit into the head loss equations. It is a common practice to calculate hydraulic roughness using the relationship proposed by Colebrook (1958) considering physical roughness as equivalent sand roughness. Bruland and Solvik (1987) extended their research and proposed a new relationship between physical roughness and hydraulic roughness where the physical roughness in their definition does not correspond to the sand roughness. On the other hand, the total physical roughness defined by Ronn and Skog (1997) corresponds to the sand roughness and fits into Colebrook (1958)'s equation. More recently, attempts have also been made to relate measured physical roughness to hydraulic roughness for bored tunnels (Pegram and Pennington, 1998; Hákonardóttir et al., 2009). Regardless of the type of method used, a correct definition of physical roughness and its relation with hydraulic roughness are the key issues to define unlined or shotcrete-lined tunnel hydraulics.

Existing methods of estimating tunnel roughness are used only after the tunnel is excavated and the geometrical data of actual tunnel surface are available. In parallel to these methods, attempts have also been made to predict tunnel roughness before tunnel excavation based on over-break in tunnels (Colebrook, 1958; Huval, 1969; Priha, 1969; Kim, 2009), even though it is difficult to define over-break intensity and its relation to physical roughness. In this perspective, this article attempts to establish a new relationship between physical roughness and over-break thickness by analyzing actual tunnel profiles of the shotcrete-lined headrace tunnel of the Chilime hydropower project (CHP) in Nepal. Similarly, the article also attempts to establish a correlation between physical roughness and the Manning coefficient (hydraulic roughness) and proposes modifications on the methods proposed by Colebrook (1958) and Solvik (1984). Furthermore, the modified equations are used to predict roughness and hence the head loss and results are

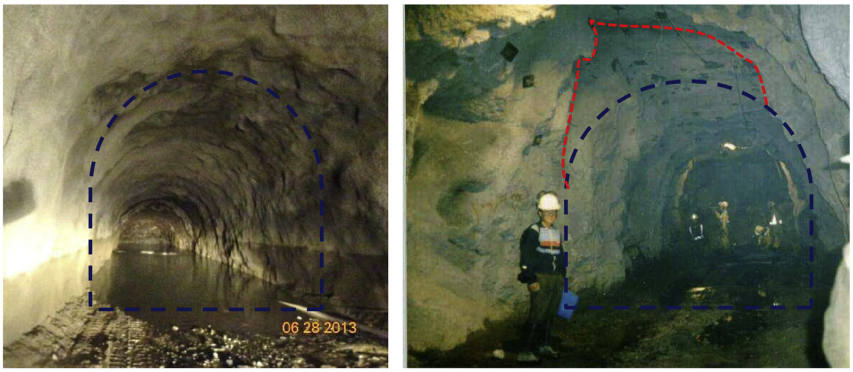

a. Relatively good quality tunnel contour (Upper Tamakoshi Project, Nepal)

b. Relatively poor quality tunnel contour with excessive over-break (Khimti Project, Nepal)

Fig. 1. Tunnel contour quality after blasting and shotcreting.

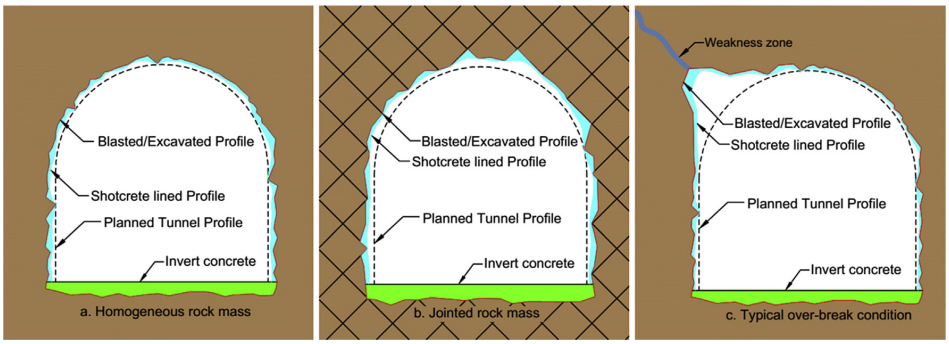

Fig. 2. Quality of tunnel contour in different geological conditions.

compared with the head loss measured at both headrace tunnels of the CHP and Modi Khola hydropower project (MKHP), respectively.

2. Relevant theory

In the waterway system of hydropower projects, part of the potential energy is lost while transferring water from the headwater system to the powerhouse. There are mainly two reasons for this energy loss. First, the flowing water experiences resistance from the surface in which it flows due to a boundary layer developed in the interface of fluid and flow surface. The boundary layer is essentially formed due to viscosity of the fluid and condition of the surface. An energy loss is then produced by shear stress along the said boundary layer, which is called friction loss (Hager, 2010). In addition, a part of energy is also lost as a singular loss, due to obstructions to the flow from different essential structural components built across the waterway system. Hence, the total energy loss, i.e. total head loss (H_1), in the waterway system consists of two components:

$$H_1 = H_f + H_s \tag{1}$$

where H_f is the frictional head loss and H_s is the singular loss. The frictional head loss depends on flow surface condition and length of waterway system. On the other hand, singular loss typically consists of entrance loss, loss due to changes in cross-sections in the direction of flow, bend loss, exit loss and losses due to local disturbances caused by gates, trash racks, niches, rock traps, etc.

2.1. Roughness and frictional head loss

The flow surface of a waterway system is typically made up of different materials, such as gravel, concrete, rock, steel, and plastic. The resistance to flow is more pronounced in rough surfaces which have large undulations such as unlined or shotcrete-lined tunnel surfaces. The extent of undulations (protrusions and grooves) which has resistance to water flow can be expressed as the term roughness. Because of the spatial variation of these undulations along the surface, the roughness shall be generalized as equivalent roughness and is denoted as 'ε' in this article. Since 'ε' represents physical undulations of the surface, it is considered as physical roughness in the case of unlined or shotcrete-lined tunnel surfaces. However, the frictional head loss is calculated considering a coefficient of resistance called hydraulic roughness (f or M), which depends upon physical roughness and/or hydraulic radius. It is important to note here that the friction factor (f) and the Manning coefficient (M) are hydraulic roughness, 'ε' in steel and concrete is equivalent sand roughness and 'ε' in an unlined or shotcrete-lined tunnel is physical roughness that corresponds with equivalent sand roughness. Hence, in this article, the term roughness in general refers to all of the mentioned roughnesses.

As summarized in Table 1, the Darcy–Weisbach formula (Eq. (2)) is used to calculate frictional head loss in any pressurized waterway. While using Eq. (2), the friction factor (f) is calculated by using different formulae for different flow conditions. According to Colebrook (1958), Eq. (3) can be used to calculate friction factor for the pipe flow when the Reynold's number is $R \geq 2300$, whereas Eq. (4) is used in case of flow in rough pipes ($R\sqrt{f} \geq 800R_h/\varepsilon$, where R_h is the hydraulic radius). Alternatively, equivalent sand roughness of steel pipes and concrete conduits can be back-calculated by using Eqs. (2) and (3) if the frictional head loss is known beforehand. Colebrook (1958) also emphasized that unlined or shotcrete-lined tunnel hydraulics can be represented by the flow in hydraulically rough pipes. On the other hand, the Manning formula (Eq. (5)) is mainly used in unlined or shotcrete-lined tunnels due to its simplicity where the Manning coefficient can be calculated by using different relationships such as Eq. (6). If carefully used, the Manning formula shows a good correlation with the Darcy–Weisbach formula, but this applies only for a specific range of applications according to Solvik (1984). Following the study of Colebrook (1958), Solvik (1984) developed Eq. (7) giving an application range of the Manning formula for frictional head loss calculation based on the inverse of relative roughness ($4R_h/\varepsilon$) of the closed conduit.

2.2. Singular losses

Different types of singular losses across the waterway system of hydropower projects are caused by entrance loss, trash rack loss,

Table 1
List of equations for the calculation of friction loss and roughness.

Equation (No.)		Equation (No.)	
$H_f = \frac{fLv^2}{2g(4R_h)}$	(2)	$H_f = \frac{Lv^2}{M^2R_h^{4/3}}$	(5)
$\frac{1}{\sqrt{f}} = -2\log_{10}\left(\frac{\varepsilon}{14.8R_h} + \frac{2.51}{R\sqrt{f}}\right)$	(3)	$M = \left(\frac{8g}{fR_h^{1/3}}\right)^{1/2}$	(6)
$\frac{1}{\sqrt{f}} = 2\log_{10}\left(3.72\frac{4R_h}{\varepsilon}\right)$	(4)	$M = \frac{25.4}{\varepsilon^{0.167}}$	(7)

Note: L is the length of conduit, v is the flow velocity, and g is the acceleration due to gravity.

gate loss, bend loss, transition loss, niche loss, rock trap loss, exit loss and other similar factors. Table 2 shows all the equations that are relevant to calculating these singular losses. Each of these losses can be expressed as the function of velocity head and the coefficient ξ as defined by Eq. (8), where ξ_i is the head loss coefficient for a particular singular loss and v_i is the velocity of flow at the location considered. The total singular loss in whole waterway system is the sum of total number (n) of singular losses presented in the system (Eq. (9)).

For entrance and exit losses, the coefficients (ξ_1 and ξ_2) will be equal to 0.4–0.5 and 1, respectively (Lysne et al., 2003). Similarly, the coefficient of loss due to trash rack can be calculated using Eq. (10) suggested by Penche (2004). The typical arrangement of trash rack and rack types that are being used at the inlet and other locations of the waterway system and their respective coefficients are shown in Fig. 3 for the readers' reference.

In addition, there will be head loss at the gate location due to the presence of gate slots. The gate loss coefficient can be calculated using the relationship given by Hager (2010) for slide gates. The discharge coefficient (C_d) and the head loss coefficient (ξ_4) of the gate with flat edge (i.e. edge rounding r_v is zero) can be calculated using Eqs. (11) and (12), respectively, where Ø is the relative opening of the gate as shown in Fig. 4.

Also, bend loss is one of the significant parts of singular losses along the waterway system and it is even more pronounced in sharp bends with small radius. Fig. 5 shows the bend loss coefficient (ξ_{90}) as the function of ratio between bend radius (R_b) and width of the tunnel at bend (D) for 90° bend (Lysne et al., 2003). For bends with other angles, a reduction factor has also been proposed (Fig. 5, right). The bend loss coefficient for different bend angles can be calculated by multiplying bend loss coefficient of 90° bend with a reduction factor described by Eq. (13).

The waterway systems have changes in cross-sectional area due to different shapes and tunnel linings. These changes result in transitions between two different sections and both expansion and contraction transitions are present as typically indicated in Fig. 6a and b, respectively. In Fig. 6, HL is the head loss from section 1 to section 2 and the velocity in smaller sections is considered to calculate head loss due to both expansion and contraction. According to Hager (2010), the loss coefficient in expansion can be expressed by Eq. (14), where experimentally measured values of $\phi_e(\delta)$ are represented as a function of angle δ (Eqs. (15) and (16)). Similarly, Hager (2010) proposed a relationship for loss coefficient in contraction (Eq. (17)).

Additional niches are excavated in certain intervals along the headrace tunnel length in order to provide an extra space for laybys, vehicle parking, turning, storage of immediate construction materials and equipment. Lysne et al. (2003) studied the head loss due to niches and proposed a chart for head loss coefficient of niches, which is termed as loss coefficient due to the expansion of tunnel, ξ_7 (Fig. 7).

In general, there is a rock trap at the end of unlined or shotcrete-lined tunnels in order to trap fallen rock blocks and coarse sand particles produced along the tunnel length and transported by the flow. The rock trap is constructed with the expansion of tunnel area at the invert. Therefore, it is considered similar to the niche in terms of head loss coefficient and the same chart (Fig. 7) is used in the analysis.

Table 2
List of equations for singular losses calculation.

Equation (No.)		Equation (No.)	
$h_{si} = \xi_i \frac{v_i^2}{2g}$	(8)	$\xi_5 = R_f \xi_{90}$	(13)
$H_s = \sum_{i=1}^{n} h_{si}$	(9)	$\xi_{6e} = \phi_e(\delta)\left(1 - \frac{1}{\phi}\right)^2$	(14)
$\xi_3 = C_R \left(\frac{S}{b}\right)^{4/3} \sin\alpha$	(10)	$\phi_e(\delta) = \frac{\delta}{90} + \sin(2\delta) \quad (0 \le \delta \le 30^\circ)$	(15)
$C_d = 0.61 + 0.73\varnothing^2$	(11)	$\phi_e(\delta) = \frac{5}{4} - \frac{\delta}{360^\circ} \quad (30^\circ \le \delta \le 90^\circ)$	(16)
$\xi_4 = \left(\frac{1}{C_d\varnothing} - 1\right)^2$	(12)	$\xi_{6c} = \frac{1}{2}(1-\phi)\left(\frac{\delta}{90^\circ}\right)^{1.83(1-\phi)^{0.4}}$	(17)

Note: h_{si} is the singular loss of the ith type, ξ_3 is the loss coefficient of trash rack, C_R is the rack coefficient, S is the bar thickness, b is the width between bars, α is the angle of inclination from horizontal, ξ_5 is the bend loss coefficient, R_f is the reduction factor, ξ_{90} is the bend loss coefficient of 90° bend, ξ_{6e} is the loss coefficient in expansion, $\phi_e(\delta)$ is the loss coefficient depending only on expansion angle, δ is the expansion/contraction angle, ϕ is the area ratio, and ξ_{6c} is the loss coefficient in contraction.

3. Methodology for roughness evaluation

Initially, data and information from two hydropower projects (MKHP and CHP) were collected. Both projects have low-pressure headrace tunnels up to SSs. The remaining waterway segments from the SSs to the powerhouses are high-pressure shafts and tunnels. The CHP has a steel-lined penstock shaft and the MKHP has a combination of a concrete-lined horizontal pressure tunnel, a concrete-lined vertical shaft and a steel-lined horizontal penstock

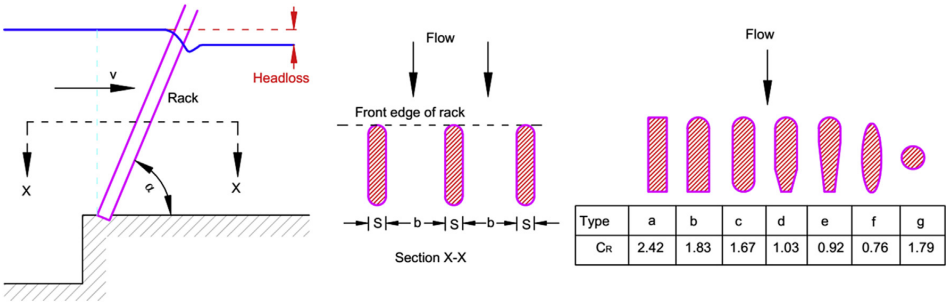

Type	a	b	c	d	e	f	g
C_R	2.42	1.83	1.67	1.03	0.92	0.76	1.79

Fig. 3. Head loss coefficient in trash rack (drawn based on Penche, 2004).

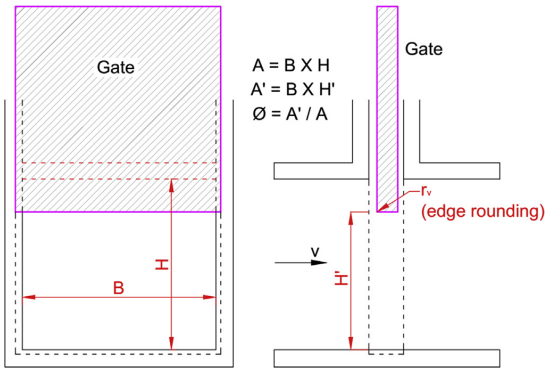

Fig. 4. Slide type gate arrangement in the conduit.

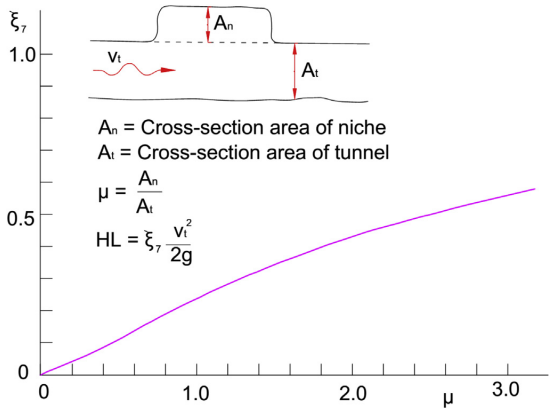

Fig. 7. Head loss coefficient in tunnel expansion (drawn based on Lysne et al., 2003).

tunnel. The authors carried out head loss measurement in December 2015 at both low-pressure headrace tunnels and high-pressure shafts and tunnels in both projects.

Fig. 8 shows the methodology used in predicting the roughness of tunnels at these two hydropower projects. As a first step of analysis (inside the black dotted rectangle in Fig. 8), the roughnesses of the steel, concrete and shotcrete-lined sections of the tunnel and shaft (including invert concrete lining) have been back-calculated using the equations presented in Tables 1 and 2. In the back calculation, the measured head loss, discharge and geometry are known parameters and roughness is an unknown parameter. The calculated roughnesses of steel- and concrete-lined tunnels are considered as fixed entities for calculating the roughness of shotcrete-lined headrace tunnels with invert concrete as and when necessary. From the results of this back calculation, a new relationship between the Manning coefficient and physical roughness of a shotcrete-lined tunnel with invert concrete is proposed.

In the second step, statistical analysis is carried out to determine the extent of undulations in the surface of shotcrete-lined tunnel by using geometrical information of the selected cross-sections of the CHP. As a result of the analysis, a relationship has been developed between the physical roughness and over-break in the walls and the crown of the shotcrete-lined tunnel. By using this relationship, the physical roughness has been calculated from the data of actually measured over-break of all shotcrete-lined sections of the headrace tunnel documented in the as-built drawing of both

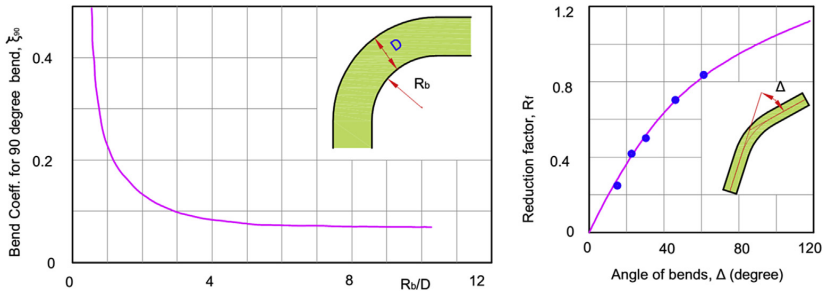

Fig. 5. Bend loss coefficient chart (drawn based on Lysne et al., 2003).

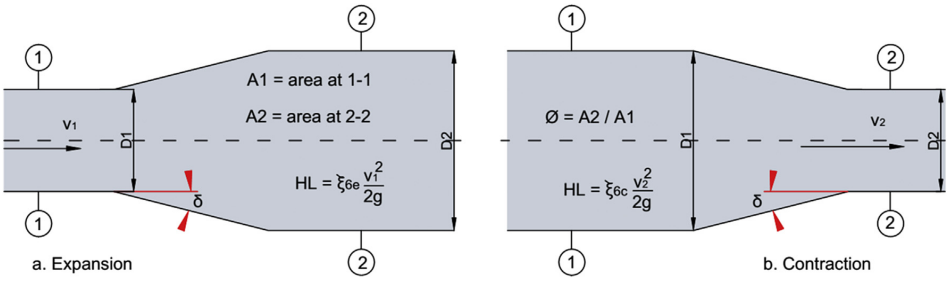

Fig. 6. Transition between different sections (expansion and contraction). v_1 and v_2 represent the flow velocities at sections 1 and 2, respectively; and D_1 and D_2 represent the diameters at sections 1 and 2, respectively.

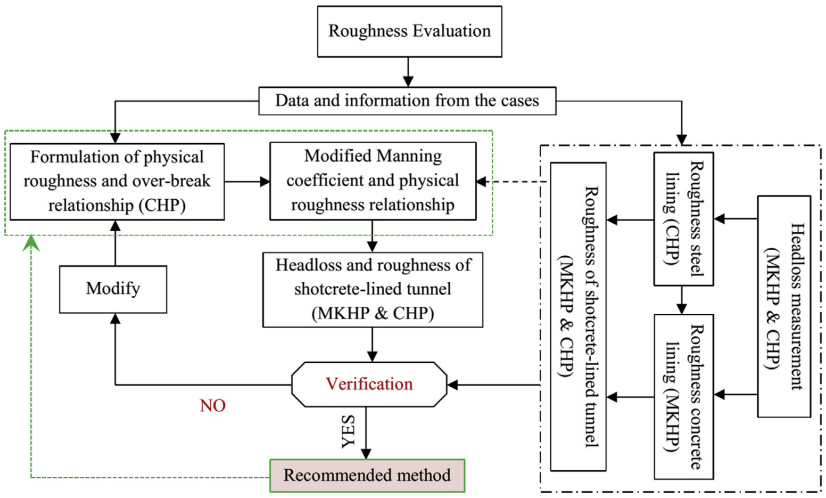

Fig. 8. Methodology for roughness prediction in shotcrete-lined tunnels with invert concrete lining.

projects. Since both headrace tunnels have shotcrete sections with invert concrete, the composite physical roughness of the whole cross-section is calculated as the weighted average of the shotcrete and concrete-lined sections. Further, the Manning coefficient (hydraulic roughness) is calculated from the physical roughness for each section using the proposed equation. Finally, frictional head loss in shotcrete-lined tunnels with invert concrete for both projects is calculated by using Eq. (5) and the established Manning coefficient. A new roughness prediction method is then proposed after verification of this calculated head loss with the one measured in the field.

4. Case studies

The locations of two hydropower projects are shown in the geological map of Nepal (Fig. 9). As seen in the figure, both the CHP

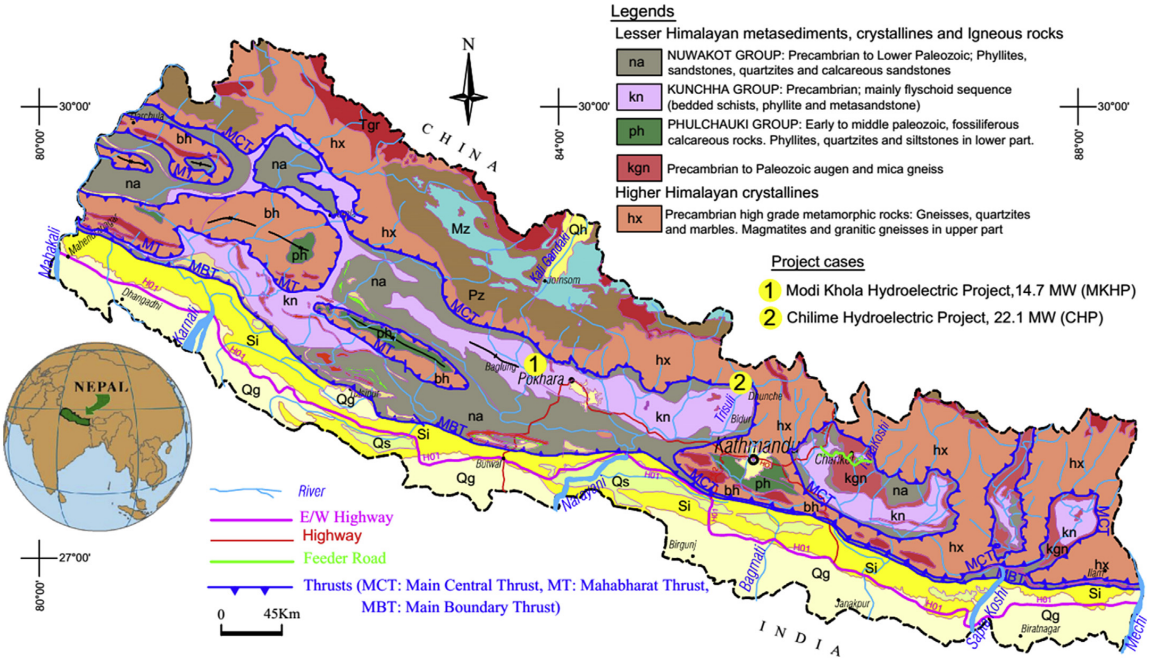

Fig. 9. Project locations in geological map of the Nepal Himalaya.

and MKHP are located in the Lesser Himalaya meta-sedimentary rock formations. The drill-and-blast method of excavation was used for the construction of all underground works of both projects.

4.1. Modi Khola hydroelectric project

The MKHP is located in central-west part of Nepal at Nayapul, Parbat district, which is about 45 km to the northwest of Pokhara (Fig. 9). Water from Modi Khola at Nayapul is diverted to the right bank and all project components are built on the same bank. The headworks components of this project consist of a diversion weir, an open concrete canal, desanding basins and a regulating poundage. The regulating poundage is used for head and discharge regulation. From the poundage to the powerhouse, water is transferred through a headrace tunnel, a vertical pressure shaft and a horizontal pressure tunnel and to the semi-underground powerhouse located at Patichaur. The project has a surface powerhouse with an installed capacity of 14.7 MW generated by utilizing 27.5 m^3/s design discharge and a gross head of 71 m. The main rock types in the project area are quartzite and phyllitic schist (Shrestha and Panthi, 2014). The headrace tunnel mainly passes through quartzite.

The total length of the headrace tunnel is 1507 m, which extends from the regulating pond (RP) to the surge shaft (SS) of the project. The headrace tunnel is composed of different sections of concrete linings and shotcrete linings (Fig. 10). The designed shape of the headrace tunnel is an inverted D. The cross-sectional area of concrete-lined section is very close to constant. On the other hand, the cross-sectional area of shotcrete-lined section varies due to blasting effect. However, the invert of the whole headrace tunnel is lined with concrete.

As shown in Fig. 10, there are three stretches of tunnel downstream of the SS, i.e. a 42 m long horizontal inverted D shaped headrace tunnel, connecting the SS with the top of the vertical shaft, a vertical shaft of circular shape with a transition between horizontal tunnel, a circular tunnel before the start of the curve at the top, and a pressure tunnel from the bottom of vertical shaft to the powerhouse. The pressure tunnel consists of a circular concrete-lined tunnel and a circular steel-lined tunnel. Typical cross-sections of the tunnel with different lining conditions are shown in Fig. 11.

Each of three different linings indicated in Fig. 11 has different roughnesses against water flow. Even though this article mainly focuses on the roughness of shotcrete-lined tunnel with invert concrete, it is necessary to find out the roughness of both concrete and steel linings for calculation of the roughness from measured head loss.

4.2. Chilime hydroelectric project

The CHP is located in Chilime and Syabrubesi Village Development Committees in Rasuwa District in Central Nepal (Fig. 9). The project has an installed capacity of 22.1 MW with the design discharge of 7.5 m^3/s and gross head of 345 m. Water from Chilime River is diverted to the right bank of the river and reaches the regulating pound followed by desanding basin, conduits and canals. The main purpose of the poundage is to regulate water level and to function as peaking reservoir. Water from the poundage to underground powerhouse is transported through the underground headrace system consisting of a pressure conduit, headrace tunnel and inclined penstock shaft. The water is then discharged back to the Bhotekoshi River through a tailrace tunnel (Fig. 12). Geologically, the project area lies in the Lesser Himalaya meta-sediments and the main rock types in the project area are quartzite and mica schist (CHC, 2005).

There exists a 425 m long pressure conduit with a syphon from the inlet gate downstream of the RP to the headrace tunnel inlet portal, of which 395 m is concrete box and the rest is circular steel pipe. The total length of headrace tunnel (HRT) from inlet portal to SS is 2827 m. The headrace tunnel consists of tunnel segments with concrete lining and shotcrete lining with invert concrete, and steel lining. Concrete lining segments of the headrace tunnel have two different shapes, i.e. horse-shoe and inverted D shapes. The inclined shaft and pressure tunnel from SS to powerhouse are embedded with steel penstock pipe, which has a total length of 650 m.

Fig. 13 shows typical sections of the headrace system representing each lining system. These sections are the basis for the calculation of flow velocity and hydraulic radius of each headrace system, which are used chainage-wise as lining types for head loss calculation.

5. Analysis of roughness

Shotcrete-lined pressure tunnels are feasible only if the economic loss caused by the friction head loss is much less than the cost needed for full concrete or steel lining. The head loss and hence

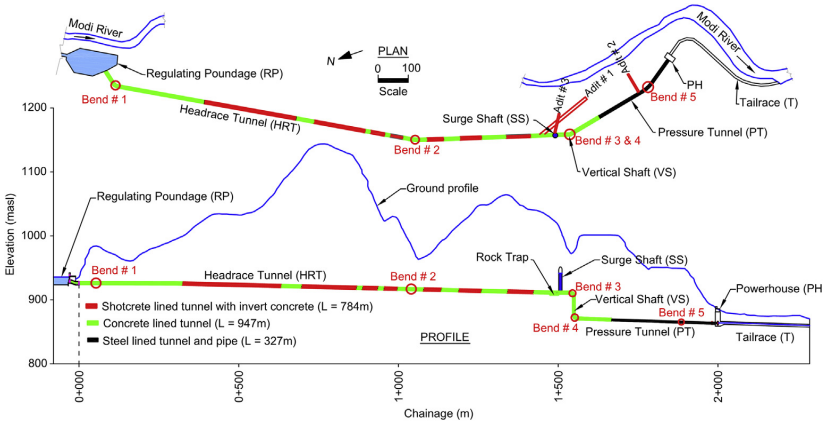

Fig. 10. Plan and profile along the MKHP, Nepal (drawn based on Shrestha and Panthi, 2014). masl represents meter above sea level.

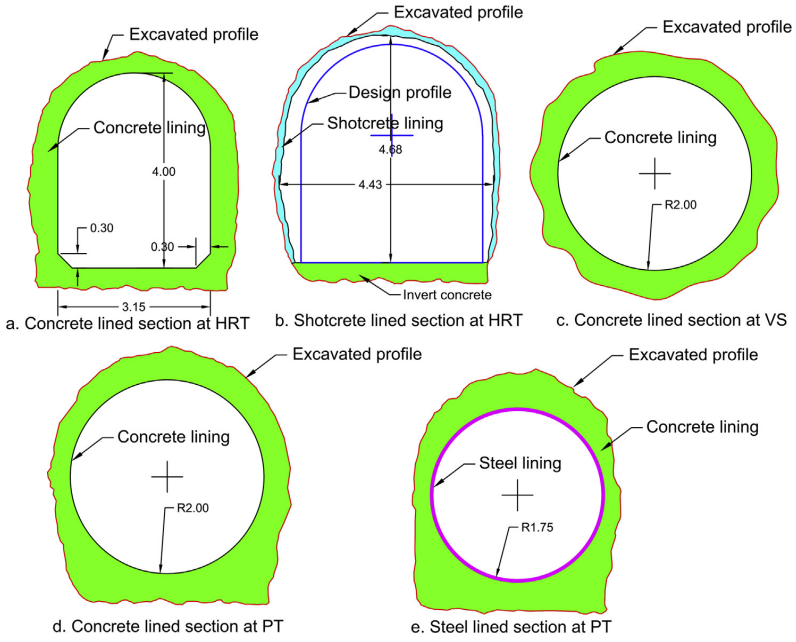

Fig. 11. Typical sections at different stretches of tunnel in the MKHP (unit in meter) (drawn based on Sharma, 2001).

the friction loss have to be measured once the hydropower project enters to the operation phase and the loss has to be verified whether it is within the design limit. The roughness of different linings in tunnels can be back-calculated from measured head loss. However, roughness needs to be predicted before and during the excavation of the tunnel in order to cope with design and contractual issues.

5.1. Head loss measurement

Head loss measurement was carried out in both the MKHP and CHP. In each project, the head loss has been measured in two stretches: one is from the RP to the SS and another is from the SS to the upstream of powerhouse inlet valve (USPIV). The schematic diagram of measurement locations including project components is shown in Fig. 14. The water level at the SS was measured multiple

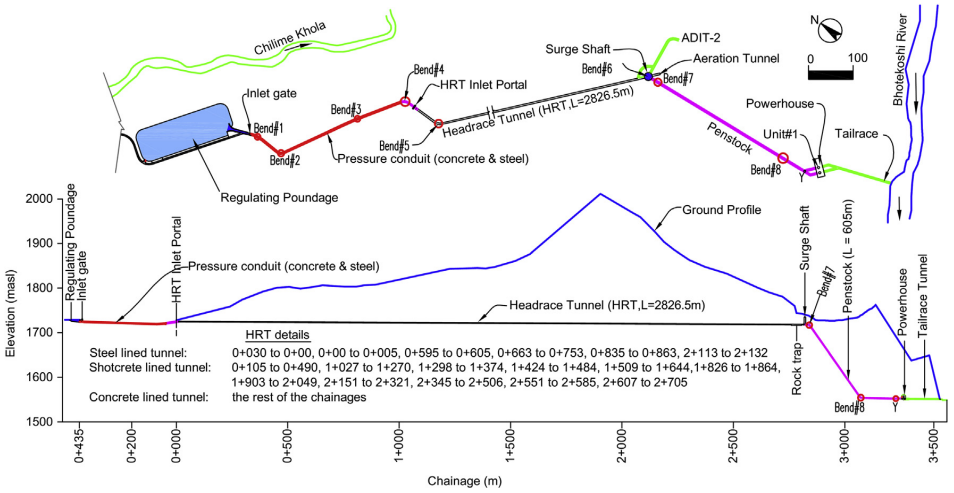

Fig. 12. Plan and profile along waterway alignment of the CHP (Source: Chilime Hydropower Company Ltd.).

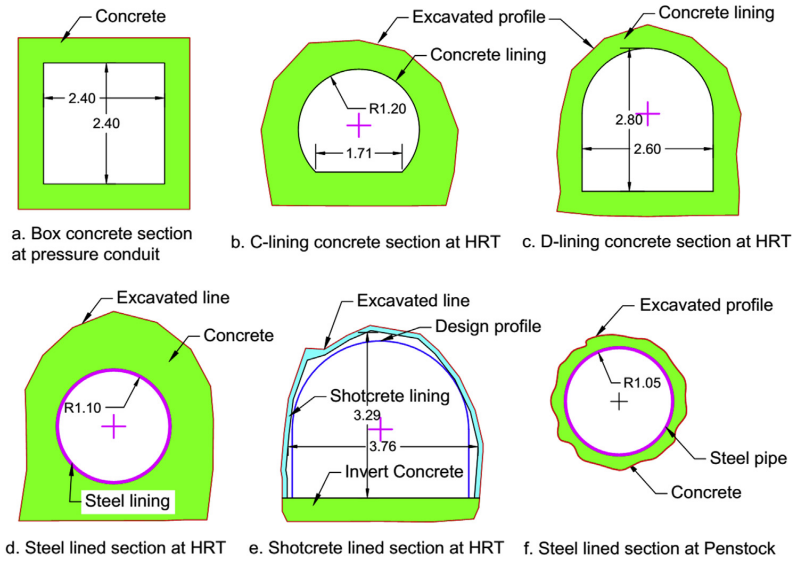

Fig. 13. Typical sections at different stretches of waterway systems of the CHP (unit in meter).

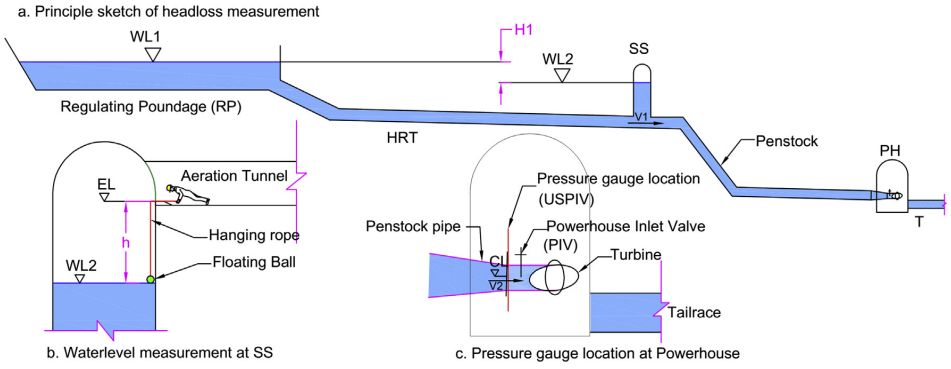

Fig. 14. Typical sketch of head loss measurement locations and details.

times using a floating ball hanging from the invert of the aeration tunnel at the SS. At the time of measurement, the water level at the RP and pressure at the USPIV were recorded from the data monitoring system of the projects and maintained constant throughout the measurement. The constant values were achieved by maintaining constant discharge and constant power production.

Head loss in different stretches has been calculated using the equations listed in Table 3. Head loss from the RP to the SS is calculated using Eq. (18), where H_1 is the water level difference between the RP and the SS (Eq. (19)) and V_1 is the velocity of water in the tunnel at the location of the SS (Eq. (20)), Q is the water discharge in m^3/s and A_1 is the cross-sectional area of the tunnel at the SS location in m^2.

Water level at the SS is calculated using Eq. (21), where EL is the elevation at the invert of aeration tunnel and h is the vertical height

Table 3
List of equations used to calculate head loss at different stretches.

Equation (No.)	Equation (No.)
$HL_1 = H_1 - \frac{V_1^2}{2g}$ (18)	$WL_2 = EL - h$ (21)
$H_1 = WL_1 - WL_2$ (19)	$HL_2 = WL_1 - \left(CL + \frac{100P_r}{\gamma_w} + \frac{V_2^2}{2g}\right) - HL_1$ (22)
$V_1 = \frac{Q}{A_1}$ (20)	$V_2 = \frac{Q_1}{\pi d^2/4}$ (23)

between WL_2 and EL, which is measured with the help of a floating ball hanging as shown in Fig. 14b. EL is taken from as-built drawing of the SS provided from the respective projects. Furthermore, the head loss from the SS to USPIV is calculated by using Eq. (22), where CL is the center elevation level at the USPIV (Fig. 14c), P_r is the pressure in bar at the USPIV, V_2 is the flow velocity at the USPIV and γ_w is the unit weight of water (9.81 kN/m^3). Finally, Eq. (23) is used to calculate V_2 from the discharge at the USPIV (Q_1) and pipe diameter (d). Even though both projects have two turbine units, only one unit was in operation in the MKHP at the time of measurement. This gives Q_1 in the MKHP as the total discharge of the plant.

During the measurement, total power production (P_w) was also recorded from the control panel at the powerhouse. Using Eqs. (18)–(23) and input data in Table 4, both HL_1 and HL_2 are calculated for each measurement for both projects (Table 5). As one can see in Table 5, there were 8 measurements at the MKHP and 12 measurements at the CHP.

5.2. Roughness from measured head loss

One of the major parameters to calculate the roughness from measured head loss is frictional head loss. The frictional head loss in the considered tunnel stretch has been calculated after subtracting all other losses from total measured head loss. Once the frictional head loss, water discharge and tunnel geometry are known, roughness is the only parameter to be calculated which is unknown in the head loss equations (Eqs. (2) and (5)). As shown in Fig. 12, at the CHP, there is a steel penstock lining from the SS to the USPIV. The roughness of the steel penstock lining is back-calculated from this section. At the MKHP, both steel and concrete linings are used in part of pressure tunnel and vertical shaft (Fig. 10). In this stretch, the roughness of the concrete-lined tunnel is back-calculated with the help of the established roughness of the steel lining. By fixing the roughness of the concrete and steel linings, the roughness of shotcrete-lined tunnel with invert concrete sections is calculated along the headrace tunnels of both the CHP and MKHP.

5.2.1. Roughness for steel lining

The roughness of steel penstock-lined tunnel is back-calculated from measured head loss (HL_2 in Table 5) between the SS and the USPIV of the CHP. Singular losses in this part are caused by bellmouth at the outlet of SS, 4 reducers, bends #6-#8 and Y-furcation near the powerhouse (Fig. 12). Bellmouth and reducer loss coefficients are calculated using Eq. (17) considering contraction case and Y-furcation loss coefficient is taken as 0.35 based on the authors' experience and information given in Mosonyi (1965). Head loss due to bellmouth, reducers and Y-furcation is calculated using input data given in Tables 6 and 7.

There are altogether three bends in the penstock, but along unit #1 in the powerhouse, there is no bend from Y-furcation. As shown in Fig. 12, the SS itself is along the bend and loss due to this bend is considered in penstock part. Unit #1 is taken into account in the calculation and hence effective bends in the penstock are bends #6, #7 and #8 (Table 7).

Based on Tables 6 and 7, the total singular loss (H_s in Eq. (9)) in this particular case will be 0.197 m (= 0.161 m + 0.036 m). Furthermore, friction loss in steel-lined part (H_{fs}) is calculated by subtracting H_s from each value of HL_2 in Table 5. Eqs. (2) and (3) are merged and the roughness for steel lining (ε_s) is established for the first friction loss for the given length of tunnel, geometry of tunnel and discharge (ε in Eq. (3) is ε_s). Here, ε_s is considered as a constant parameter irrespective of the size of tunnel, but the friction factor of

Table 6
Bellmouth, reducers and Y-furcation losses from the SS to the USPIV of CHP. Total head loss = 0.161 m.

Loss types	Length (m)	D_1 (m)	D_2 (m)	δ (°)	ϕ	ξ	v (m/s)	Head loss (m)
Bellmouth	2.4	2.85	2.1	8.88	0.54	0.01	1.6	0.001
Reducer 1	2.75	2.1	1.8	3.12	0.73	0.004	2.18	0.001
Reducer 2	1.9	1.8	1.7	1.51	0.89	0.003	2.45	0.001
Reducer 3	2.9	1.7	1.6	0.99	0.89	0.002	2.76	0.001
Reducer 4	0.8	1.13	0.9	8.18	0.63	0.01	4.53	0.01
Y-furcation			1.13			0.35	2.87	0.147

Table 4
Input data for the head loss measurement of both MKHP and CHP.

Project	Q (m^3/s)	P_w (MW)	WL_1 (masl)	EL (masl)	A_1 (m^2)	Q_1 (m^3/s)	P_r (bar)	d (m)	CL (masl)
MKHP	11.61	5	935.45	952.16	19.34	11.61	6.82	1.7	863.7
CHP	5.5	16.12	1734.39	1751.1	6.7	2.88	33.66	0.9	1386.91

Table 5
Head loss (in meter) at the waterway systems of both MKHP and CHP.

No.	CHP					MKHP				
	h	WL_2	H_1	HL_1	HL_2	h	WL_2	H_1	HL_1	HL_2
1	18.02	1733.08	1.31	1.275	2.041	17.216	934.944	0.506	0.491	0.625
2	18.03	1733.07	1.32	1.285	2.031	17.206	934.954	0.496	0.481	0.635
3	18.06	1733.04	1.35	1.315	2.001	17.215	934.945	0.505	0.49	0.626
4	18.06	1733.04	1.35	1.315	2.001	17.213	934.947	0.503	0.488	0.628
5	18.07	1733.03	1.36	1.325	1.991	17.21	934.95	0.5	0.485	0.631
6	18.03	1733.07	1.32	1.285	2.031	17.205	934.955	0.495	0.48	0.636
7	18.04	1733.06	1.33	1.295	2.021	17.209	934.951	0.499	0.484	0.632
8	17.98	1733.12	1.27	1.235	2.081	17.2	934.96	0.49	0.475	0.641
9	18.05	1733.05	1.34	1.305	2.011					
10	18.08	1733.02	1.37	1.335	1.981					
11	18.02	1733.08	1.31	1.275	2.041					
12	18.03	1733.07	1.32	1.285	2.031					
Min	17.98	1733.03	1.27	1.235	1.991	17.2	934.944	0.49	0.475	0.625
Max	18.07	1733.12	1.36	1.325	2.081	17.216	934.96	0.506	0.491	0.641
Mean	18.036	1733.064	1.326	1.291	2.025	17.209	934.951	0.499	0.484	0.632
SD	0.0288	0.0288	0.0288	0.0288	0.0288	0.0054	0.0054	0.0054	0.0054	0.0054

Note: Min, Max and SD represent minimum, maximum and standard deviation, respectively.

steel pipe f_s slightly changes with the size and again Eq. (3) is used to calculate f_s for different sizes. Similarly, Manning coefficient of steel pipe M_s is calculated by using Eq. (6) for each f_s and the result is shown in Table 8.

Following the same calculation steps as in Table 8, ε_s for all head loss measurements (H_{fs}) is calculated and presented in Table 9. The table also shows average values of f_s and M_s for each length and size of the penstock pipe for all measurements. Further, the mean value of ε_s shown in Table 9 will be used as the fixed roughness for steel lining.

5.2.2. Roughness for concrete lining

As shown in Fig. 10, the MKHP has both concrete lining and steel lining from the SS to the USPIV. In this stretch, friction loss in concrete-lined tunnel (H_{fc}) is calculated by subtracting singular losses and friction loss in steel-lined tunnel from HL_2. For singular losses, the calculation process is the same as that for the previous case. Calculated values of reducer loss, bend loss and Y-furcation loss are presented in Table 10.

Friction loss in the steel-lined pressure tunnel of the MKHP is calculated for the given length, size and established roughness of steel lining. The roughness of steel-lined pressure tunnel is equal to 0.526 mm (mean value of ε_s in Table 9) and friction loss is equal to 0.2 m. Total fixed loss is then 0.605 m, which is the sum of total singular loss and friction loss in steel-lined tunnel. Furthermore, friction loss in the concrete lining (H_{fc}) section is calculated by subtracting the total fixed loss from measured head loss (HL_2) of the MKHP. For given geometry and length of concrete-lined tunnel, the roughness of the concrete lining (ε_c) is back-calculated from H_{fc} by using Eqs. (2) and (3), following the same calculation steps as in Table 8 for each measurement of H_{fc}. In addition to this, average values of f_c and M_c are also calculated as that in Table 8 and shown in Table 11.

Table 11 shows the final result of the roughness of the concrete-lined tunnel of the MKHP for all eight measurements. The final value of ε_c is the average of all eight measurements and is used as a fixed value for further calculations.

5.2.3. Roughness for shotcrete-lined tunnel

Both the CHP and MKHP have shotcrete-lined headrace tunnels with invert concrete (Figs. 11b and 13e). Roughness of shotcrete-lined tunnel is back-calculated from frictional head loss for stretches with shotcrete lining. The back-calculated roughness is the equivalent roughness of shotcrete linings in the walls and crown and concrete lining in the invert.

Since the headrace tunnel of the MKHP has both concrete lining and shotcrete lining, the total head loss HL_1 is the sum of friction losses in shotcrete and concrete-lined tunnels and singular losses in the system. The total singular losses and friction loss in concrete-lined segment are considered as fixed losses for the given discharge. Table 12 shows input data required to calculate head loss in trash rack, gate, niches, rock trap and bends.

In addition, there are a total of 18 transitions between concrete to shotcrete and shotcrete to concrete linings. The loss coefficients of these transitions are estimated by using Eqs. (14) and (17). The detailed calculations of head loss due to transitions are made and the final results with all other singular losses are presented in Table 13.

Another fixed loss in the system, the frictional loss in the concrete-lined tunnel (H_{fc}), is calculated using Eqs. (2) and (3) with the established value of ε_c and given geometry and length of concrete linings. The total H_{fc} is equal to 0.197 m and the total fixed loss, including singular losses, becomes 0.275 m. Finally, friction loss in shotcrete-lined tunnel (H_R) is calculated by subtracting the total fixed loss from measured head loss (HL_1) of the MKHP. A chainage-wise calculation spreadsheet for 18 shotcrete-lined tunnel sections is prepared with input parameters to calculate ε_R, f_R and M_R for each H_R following exactly the same calculation process as given earlier in

Table 7
Bend loss calculation in the stretch from the SS to the USPIV of CHP. Total head loss = 0.036 m.

Bend	D (m)	R_b (m)	R_b/D	ξ_{90}	Δ (°)	R_f	ξ_5	v (m/s)	Head loss (m)
#6	2.1	12.5	6	0.08	55	0.78	0.0624	1.6	0.008
#7	1.6	12.5	7.8	0.08	54	0.78	0.0624	2.76	0.024
#8	2.6	7.5	2.9	0.1	46	0.7	0.07	1.05	0.004

Note: Δ represents the bend angle.

Table 8
Roughness of steel lining (ε_s = 0.551 mm) between the SS and the USPIV of CHP for the first measurement. Total H_{fs} = 1.84 m.

No.	L (m)	D (m)	R_h (m)	v (m/s)	f_s	M_s (m$^{1/3}$/s)	H_{fs} (m)
1	55.45	2.1	0.53	1.6	0.014	82	0.05
2	119.84	1.8	0.45	2.18	0.015	83	0.24
2	119.88	1.7	0.43	2.45	0.015	83	0.33
4	282.85	1.6	0.4	2.76	0.015	83	1.05
5	27	1.13	0.28	2.87	0.017	85	0.17

Table 9
Roughness of steel lining (ε_s) between the SS and the USPIV of CHP.

No.	HL_2 (m)	H_{fs} (m)	ε_s (mm)	Avg. f_s	Avg. M_s (m$^{1/3}$/s)
1	2.04	1.84	0.551	0.015	83
2	2.03	1.83	0.537	0.015	83
3	2	1.8	0.497	0.015	84
4	2	1.8	0.497	0.015	84
5	1.99	1.79	0.485	0.015	84
6	2.03	1.83	0.537	0.015	83
7	2.02	1.82	0.524	0.015	84
8	2.08	1.88	0.609	0.016	82
9	2.01	1.81	0.511	0.015	84
10	1.98	1.78	0.472	0.015	85
11	2.04	1.84	0.551	0.015	83
12	2.03	1.83	0.537	0.015	83
Min	1.98	1.78	0.472	0.015	82
Max	2.08	1.88	0.609	0.016	85
Mean	2.02	1.82	0.526	0.015	84
SD	0.03	0.03	0.035	0	1

Note: Avg. means average.

Table 10
The singular losses in the SS to the USPIV of MKHP. Total singular losses = 0.405 m.

Reducers						Bends					Y-furcation		
No.	L (m)	D_1 (m)	D_2 (m)	δ (°)	Head loss (m)	No.	D (m)	R_b (m)	Δ (°)	Head loss (m)	D_2 (m)	ξ	Head loss (m)
1	10	4.96	4	2.75	0.006	#3	4	10	90	0.009	1.7	0.35	0.39
2	1.5	4	3.5	9.46		#4	4	10	89				
3	1.5	3.5	3.2	5.71		#5	3.5	10	25				
4	2.3	1.7	1.3	4.97									

Table 11
Roughness of concrete-lined tunnel of MKHP.

No.	HL_2 (m)	H_{fc} (m)	ε_c (mm)	Avg. f_c	Avg. M_c (m$^{1/3}$/s)
1	0.625	0.021	0.911	0.014	74
2	0.635	0.031	4.382	0.02	62
3	0.626	0.022	0.86	0.014	75
4	0.628	0.024	1.445	0.015	71
5	0.631	0.027	2.446	0.017	67
6	0.636	0.032	5.016	0.02	61
7	0.632	0.028	2.899	0.018	66
8	0.641	0.037	8.722	0.024	57
Min	0.625	0.021	0.86	0.014	57
Max	0.641	0.037	8.722	0.024	75
Mean	0.632	0.028	3.335	0.018	67
SD	0.005	0.005	2.487	0.003	6

concrete and steel linings, which are calculated as 0.18 m, 0.13 m and 0.64 m, respectively. These losses are calculated in detail by using project data and information and previous calculation procedures. By subtracting the fixed losses from HL_1, the friction loss in the shotcrete-lined tunnel (H_R) is calculated, which is shown in Table 14. In order to calculate the roughness of shotcrete-lined tunnel, a chainage-wise calculation spreadsheet is prepared for 299 tunnel cross-sections and the same calculation process is also employed as that for the MKHP.

As shown in Table 14, the hydraulic roughness from both Darcy–Weisbach (Eqs. (2), (4) and (6)) and Manning formulae (Eqs. (5) and (7)) corresponds very well in both projects. Table 14 also shows the minimum, maximum and mean values of different roughnesses.

Table 12
Geometrical and technical data for singular losses in the HRT of MKHP.

Trash rack					Gate		Niches			Rock trap		Bend			
Type	s (mm)	b (mm)	α (°)	C_R	ϕ	Remarks	Number	A_n (m^2)	A_t (m^2)	A_n (m^2)	A_t (m^2)	No.	D (m)	R_b (m)	Δ (°)
a	10	25	78	2.42	1	Fully opened	2	12	16.3	3.45	11.55	#1	2.95	50	56
												#2	3.15	100	10

Table 8, where Eq. (3) is replaced by Eq. (4). The outcome of these calculations is presented in Table 14. Additionally, M_R and ε_R are also calculated by using Eqs. (5) and (7), respectively, and the results from the two different approaches are compared.

In the case of the CHP, the total head loss (HL_1) is the sum of singular losses and friction losses in concrete box culvert, steel pipe, steel-lined tunnel, concrete-lined tunnel and shotcrete-lined tunnel. Fixed losses in this case are singular losses and friction losses in

Table 13
Singular losses in the HRT of MKHP. Total singular loss = 0.078 m.

Loss types	No.	A (m^2)	v (m/s)	ξ	H_s (m)
Trash rack	1	21.5	0.493	0.7	0.009
Entrance	1	21.5	0.493	0.5	0.006
Gate	1	12.25	0.87	0.06	0.002
Bend	2				0.004
Niches	2	16.3	0.65	0.2	0.009
Transitions					0.044
Rock trap	1	11.55	0.92	0.1	0.004

5.2.4. Manning coefficient and physical roughness

The physical roughness, ε_R, from both the Darcy–Weisbach and Manning approaches in Table 14, has some deviation in the results for both projects, which indicates that modification in Eq. (7) is needed in order to define ε_R as a physical roughness equivalent to sand roughness given by Eq. (4). In this endeavor, an attempt is made to establish a modified relationship between Manning coefficient (M_R) from Eq. (5) and equivalent sand roughness (ε_R) derived from the Darcy–Weisbach and Colebrook relationships (Eqs. (2) and (4)) using 20 results presented in Table 14 (Fig. 15).

As Fig. 15 indicates, in comparison to the M_R values for shotcrete-lined tunnel with invert concrete lining back-calculated in Table 14, Eq. (7) gives lower M_R values for the same values of ε_R. Therefore, the authors suggest that the relationship between M_R and ε_R for shotcrete-lined tunnels with invert concrete is defined by Eq. (24), which shows a good fit in Fig. 15:

$$M_R = \frac{24}{\varepsilon_R^{1/5}} \tag{24}$$

Table 14
Roughness of shotcrete-lined tunnel with invert concrete in the HRT of CHP and MKHP.

No.	CHP						MKHP					
	H_R (m)	Eqs. (2), (4) and (6)			Eqs. (5) and (7)		H_R (m)	Eqs. (2), (4) and (6)			Eqs. (5) and (7)	
		ε_R (mm)	f_R	M_R (m$^{1/3}$/s)	M_R (m$^{1/3}$/s)	ε_R (mm)		ε_R (mm)	f_R	M_R (m$^{1/3}$/s)	M_R (m$^{1/3}$/s)	ε_R (mm)
1	0.32	48.82	0.043	44	44	37.56	0.215	98.24	0.051	39	39	80.13
2	0.33	53.02	0.045	43	43	41.17	0.205	87.43	0.049	40	40	69.48
3	0.36	66.4	0.048	41	41	53.37	0.214	96.96	0.051	39	39	79.02
4	0.36	66.4	0.048	41	41	53.37	0.212	95.99	0.051	39	39	76.83
5	0.37	71.56	0.05	41	41	57.92	0.209	91.43	0.05	39	39	73.62
6	0.33	53.12	0.045	43	43	41.17	0.204	85.87	0.049	40	40	68.47
7	0.34	57.43	0.046	43	43	45	0.208	90.31	0.05	39	39	72.57
8	0.28	33.51	0.038	47	47	25.22	0.199	80.38	0.048	40	40	63.56
9	0.35	61.72	0.047	42	42	49.07						
10	0.38	76.29	0.051	40	40	62.72						
11	0.32	48.54	0.043	44	44	37.56						
12	0.33	53.01	0.045	43	43	41.17						
Min	0.28	33.51	0.038	40	40	25.22	0.199	80.38	0.048	39	39	63.6
Max	0.38	76.29	0.051	47	47	62.72	0.215	98.24	0.051	40	40	80.1
Mean	0.34	57.49	0.046	43	43	45.44	0.209	90.83	0.05	39	39	73
SD	0.03	11.75	0.004	2	2	10.36	0.005	5.76	0.001	0	0	5.3

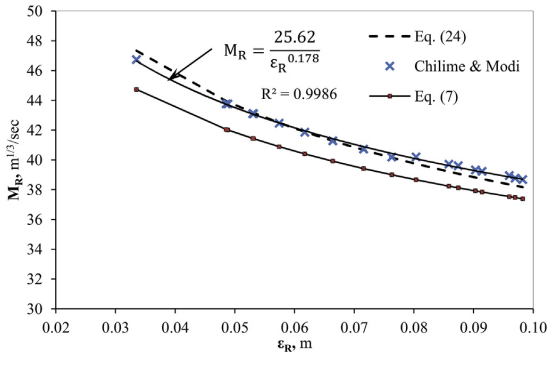

Fig. 15. Relationships between M_R and ε_R based on different approaches.

The benefit of this equation is its simplicity in comparison to the one with Darcy–Weisbach and Colebrook equations. Moreover, Darcy–Weisbach and Colebrook equations do not consider different lining scenarios in the same cross-section of the tunnel. However, the authors emphasize that Eq. (24) is derived based on 20 datasets from two shotcrete-lined tunnels with invert concrete and it should be tested with many other tunnels with similar lining conditions, which are becoming more common in the Himalayan region and other part of the world such as the Andes.

5.3. Physical roughness in relation to over-break

If a correlation between the average over-break thickness and the undulations in actual tunnel profile is established, it may be possible to predict roughness. With this concept in mind, an attempt has been made to find a correlation between roughness and mean over-break thickness using actual cross-section data of the headrace tunnel of the CHP where the tunnel cross-sections are mapped at either every 5 m or 10 m. These records of tunnel cross-sections are used to establish a correlation between over-break and physical roughness of the tunnel surface. The achieved correlation is further tested with the over-break and roughness properties of the MKHP headrace tunnel.

The cross-section profile of a blasted tunnel seldom meets the profile assumed in a design profile and differs from it with an undulating wall surface as shown in Fig. 16. A shotcrete-lined tunnel follows almost similar surface conditions as in an unlined tunnel

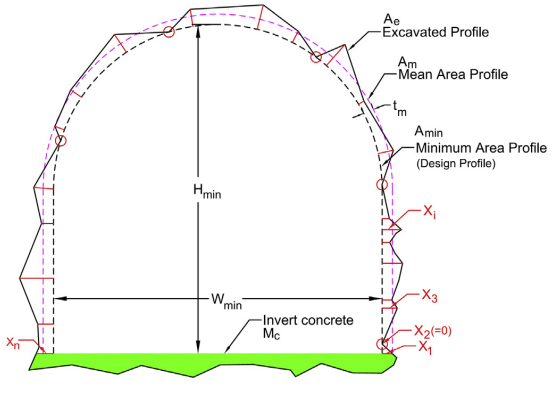

Fig. 16. Roughness of unlined or shotcrete-lined tunnel with invert concrete.

and hence has similar undulation along the tunnel periphery excluding the invert, which is mostly concrete-lined in the Himalayan water tunnels.

Hence, the roughness of a shotcrete lining (walls and crown in Fig. 16) can be calculated using undulation depth measured from the minimum area profile as shown in Fig. 16. In case of excavated tunnel sections, the minimum area profile may or may not coincide with the designed area profile depending on the quality of the contour blast. However, the shape of the minimum area profile is the same as that of designed profile (i.e. inverted D in this article). Since the minimum area profile follows innermost projections of the excavated profile or the shotcrete-lined profile, the undulation depth (X_i), which is measured perpendicular to the minimum area profile, is always equal to or greater than zero. There is statistical variation of undulation depth around the tunnel profile which demands that a single representative value of undulation depth is needed to estimate the equivalent sand roughness. According to Adams et al. (2012), depending on the type of undulating surface, different statistical parameters (calculated from the undulation depth) can be used to convert the undulation depth to the equivalent sand roughness. One of such parameters is the square root of variance of the undulation depth (Pegram and Pennington, 1998; Adams et al., 2012). In this article, the square root of the variance of X_i is assumed to be equal to the physical roughness (equivalent sand roughness) of the unlined or shotcrete-lined profile of the tunnel in question and is expressed by

$$\varepsilon_{sc} = \sqrt{\sum_{i=1}^{n} \frac{(X_i - \overline{X})^2}{n}} \tag{25}$$

where n is the number of undulation depths, and $\overline{X}$ is the average of undulation depths.

The mean area (A_m) shown in Fig. 16 is equal to the actually excavated area or area after shotcrete lining (A_e) of the tunnel in question. The mean area profile of the tunnel can be drawn to match the profile of the minimum area (A_{min}) maintaining uniform thickness (t_m) around walls and crown. The thickness (t_m) is therefore the mean over-break thickness for the cross-sectional profile in question and is calculated by

$$t_m = \frac{-p_{min} + \sqrt{p_{min}^2 + 2\pi\Delta A}}{\pi} \tag{26}$$

where p_{min} is the perimeter of walls and crown of the minimum area profile and ΔA is the over-break area ($=A_e - A_{min}$).

At the CHP, 299 tunnel cross-section profiles were surveyed at either every 5 m or every 10 m of shotcrete-lined headrace tunnel with invert concrete lining. Out of these cross-sectional profiles, 68 sections from chainage 0 + 105 m to 0 + 490 m are taken as representative cases for the measurement of roughness in walls and crown. The tunnel stretch is selected as representative considering the fact that it is the longest tunnel stretch where shotcrete lining is continuous. In this stretch, X_i is measured in each cross-section and the number of measurements is governed by the extent of undulations presented in the profile in question and varied from 11 to 16 measurements for each section. ε_{sc} and t_m are calculated for each section by using Eqs. (25) and (26), respectively, and the values are used to find out whether there exists any correlation between these two properties (Fig. 17).

As Fig. 17 indicates, the correlation between ε_{sc} and t_m is found satisfactory with a regression coefficient (R^2) exceeding 80%. More importantly, Eq. (27) is proposed based on the result achieved,

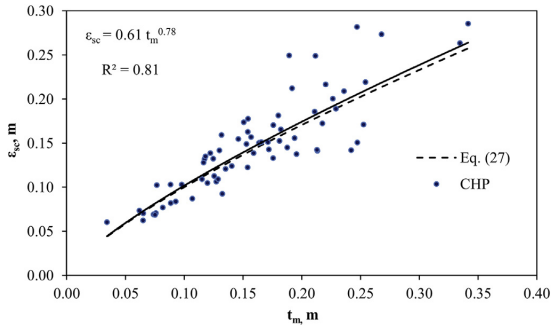

Fig. 17. Correlation between roughness and mean over-break thickness.

which is slightly modified with the one shown in Fig. 17, to improve the readability of the equation without any impact on the calculation results:

$$\varepsilon_{sc} = \frac{1}{1.7} t_m^{1/1.3} \tag{27}$$

It is important to note that Eq. (27) represents only the walls and crown of a shotcrete-lined tunnel. Since there is concrete lining in the invert, the whole cross-section becomes composite lining, which should be analyzed accordingly. In this respect, the roughness of the composite lining is considered as the weighted average with respect to perimeter and can be defined by

$$\varepsilon_R = \frac{\varepsilon_{sc} p_{min} + \varepsilon_c W_{min}}{p_{min} + W_{min}} \tag{28}$$

where the roughness of invert concrete lining ε_c is equal to 3.34 mm, i.e. the same as that of a concrete-lined tunnel (mean value in Table 11). It is considered as a fixed parameter over the entire length of the shotcrete-lined tunnel.

The proposed Eqs. (24) and (27) are further used in all shotcrete-lined sections of headrace tunnels of both the MKHP and CHP to calculate both physical and hydraulic roughnesses. In this regard, all 299 measured cross-sectional profiles from the CHP and 18 cross-section profiles from the MKHP are exploited. For each section, ε_{sc} is first calculated by using Eq. (27) for respective measured t_m. Furthermore, Eq. (28) is used to calculate ε_R and finally M_R is calculated using Eq. (24) suggested by the authors. Furthermore, frictional head loss is calculated by using Eq. (5) and exploiting respective M_R values, cross-sections and length of tunnel (Table 15).

As Table 15 indicates, there is fairly good match between measured and calculated head losses with approximately 15% deviation at the CHP. However, the results obtained for the MKHP are extremely good with a deviation of only 3%.

Furthermore, Eq. (24) is inserted in the chart drawn by Solvik (1984), for both the Manning and Darcy–Weisbach formulae as shown in Fig. 18. As Fig. 18 indicates, the proposed Manning formula for shotcrete-lined tunnel with invert concrete fits very well with the Darcy–Weisbach equations for the inverse of relative physical roughness range between 20 and 100, which is very logical since the Manning coefficient for shotcrete-lined tunnels with invert concrete in general should vary between 35 and 50 depending on the quality of tunnel contour excavation.

Hence, it is concluded that the proposed equations, such as Eq. (24), can be used in shotcrete-lined tunnels with invert concrete to estimate the Manning coefficient and Eq. (27) can be used to predict physical roughness of shotcrete-lined surface. However, the authors highlight that the suggested equations are based on only two waterway systems and recommend that these equations are further verified using data from other projects.

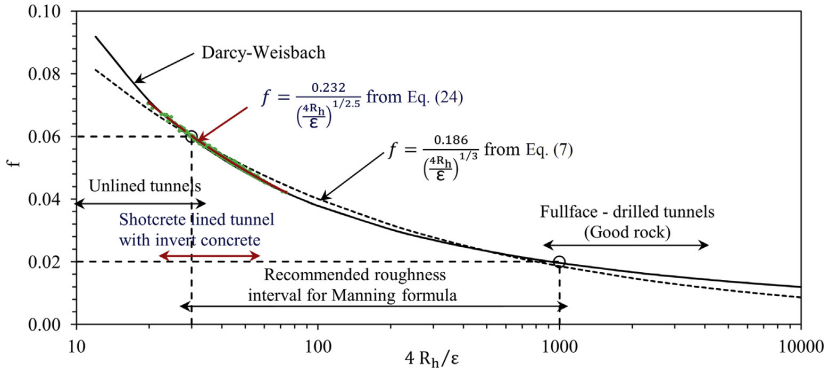

Fig. 18. Comparison of Darcy–Weisbach and Manning formulae (updated in Solvik, 1984).

Table 15
Head loss and roughness of shotcrete-lined tunnel with invert concrete of both CHP and MKHP, calculated using proposed equations.

Variance	CHP							MKHP						
	t_m (m)	ε_{sc} (m)	ε_R (m)	M_R ($m^{1/3}/s$) (Eq. (24))	M_R ($m^{1/3}/s$) (head loss)	H_R (m) (calculated)	H_R (m) (measured)	t_m (m)	ε_{sc} (m)	ε_R (m)	M_R ($m^{1/3}/s$) (Eq. (24))	M_R ($m^{1/3}/s$) (head loss)	H_R (m) (calculated)	H_R (m) (measured)
Min	0.03	0.04	0.03	33	40	0.393	0.341	0.1	0.1	0.07	34	39	0.216	0.209
Max	0.37	0.27	0.2	49	47			0.31	0.24	0.18	41	40		
Mean	0.14	0.13	0.09	39	43			0.15	0.13	0.1	38	39		
SD	0.05	0.04	0.03	2	2			0.05	0.03	0.02	1	0		

5.4. Roughness from existing methods

The existing methods, such as those proposed by Rahm (1958), Priha (1969) and Reinius (1970), for calculating tunnel roughness were also tested to calculate the roughness of shotcrete-lined tunnel of the CHP. Altogether, 299 cross-sections of shotcrete-lined tunnel are used for the calculation. Regarding the MKHP, available cross-sections are not enough to apply these existing methods. Hence, Table 16 shows only the result for the CHP.

The roughness obtained from the existing methods is higher than that from the actual head loss measurement at the CHP. It is important to highlight that the existing methods (Rahm, 1958; Priha, 1969; Reinius, 1970) of roughness calculation were mainly established using data sources from unlined tunnels, and hence result in higher roughness predictions than appropriate for the tunnels with shotcrete and invert concrete lining. On the other hand, roughness obtained by using the equations proposed by the authors is closer to the back-calculated value based on the measured head loss of the CHP. Therefore, we claim that, for the composite lining consisting shotcrete and invert concrete, the proposed equations (Eqs. (24) and (27)) have better reliability.

6. Over-break (excavation) vs. rock mass quality

The extent of over excavation on the tunnel excavated using the drill-and-blast method depends upon the quality of rock mass along the tunnel in question, type of blast methods (wedge cut/burn cut), length of drill holes, type and amount of explosive used and professional quality and awareness of the tunneling team involved in tunnel excavation work. As discussed above, the tunnel roughness is greatly influenced by the quality of excavation. In the following, the authors try to assess to what extent the rock mass quality influences the over-break thickness expressed by t_m. The average or smoothened over-break thickness (t_m) of 299 and 77 excavated tunnel cross-sections for the CHP and MKHP, respectively, has been calculated. The calculated over-break thickness (t_m) is then plotted against mapped values of rock mass class defined by Q-system of rock mass classification (Fig. 19).

As Fig. 19 indicates, there is no clear correlation between over-break thickness (t_m) and rock mass quality class. Even though the rock types along these two headrace tunnels are similar and represented by jointed quartzite, the variation in t_m values at the CHP is found to be more pronounced in all rock mass classes than that at the MKHP. This is most likely related to professional quality and awareness of the tunneling team involved during the excavation. However, Fig. 19 depicts one very important piece of information, which explains that the variation in over-break thickness in poor rock mass (Class IV) is higher than that of other rock mass quality classes. The authors believe that this is quite logical since the rock mass with Class IV according to Q-system typically has more than three joint sets and is blocky in nature. On the other hand, Class V represents very poor quality rock mass, where blasting length in each round is reduced (in general less than 1.5 m) to make sure that there is no tunnel collapse immediately after blasting. Lower blasting round length reduces protrusion depth and therefore a reduced t_m value. Another finding of this analysis is that the average over-break thickness seems to be between 0.1 m and 0.2 m in the blasted tunnels excavated using the drill-and-blast tunneling technique.

Table 16
Roughness of shotcrete-lined tunnel with invert concrete using existing methods in CHP.

Source	f_R	M_R (m$^{1/3}$/s)
Rahm (1958)	0.062	36
Priha (1969)	0.071	34
Reinius (1970)	0.056	38
Equations by authors	0.053	39
From head loss	0.046	43

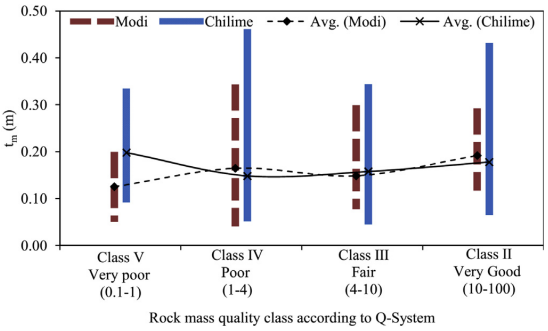

Fig. 19. Smoothened over-break thickness (t_m) against rock quality class according to Q-system of rock mass classification at CHP and MKHP.

7. Cost optimization

Traditionally, using a fully concrete-lined waterway system has been proven to be a costly solution due to extra need for construction resources and time. Therefore, innovative solutions are needed to reduce the fully concrete-lined length of the pressure tunnel system (in particular, low- to medium-pressure headrace and tailrace tunnels). On the other hand, innovative applied solutions must guarantee long-term stability and sustainability, cost effectiveness and construction time savings. Tunnel rock support, consisting of sprayed concrete and systematic bolting, is applied to almost all waterway tunnels constructed today in the Himalayan region. This is mainly to secure tunnel stability and also to guarantee the safety of working crew at the tunnel face. Hence, applied support should be capable of withstanding any type of tunnel collapses including block fall (Panthi, 2015).

The basis of cost optimization is hence the use of shotcrete-lined headrace and tailrace tunnels with invert concrete instead of traditional concrete-lined tunnels. However, the construction cost of such tunnels should guarantee reduced construction cost and time. In addition, the waterway system should also be able to generate similar or higher financial revenue than that of concrete-lined tunnels. Regarding the waterway system, the main long-term revenue loss can be related to the frictional head loss. To evaluate this economic impact, in the following, a range of hydraulic roughness values for shotcrete and concrete-lined tunnels have been chosen for each lining type. Hydraulic roughness in concrete lining (M_c) is considered to vary from 60 to 75 and in a shotcrete-lined tunnel with invert concrete (M_R), it is considered to range from 35 to 50. The shape of the tunnel was chosen as inverted D with equal width and height for both concrete-lined and shotcrete-lined tunnels in order to ensure a hydraulically efficient shape of the tunnel (Lysne et al., 2003). The ratio between the area of a concrete-lined tunnel (A_c) and the area of a shotcrete-lined tunnel with invert concrete (A_{sc}) for equal head loss can be expressed by

$$\frac{A_c}{A_{sc}} = \left(\frac{M_R}{M_c}\right)^{3/4} \tag{29}$$

The area ratio is calculated for all possible combinations within the given range of roughness, as presented in Fig. 20. The contour

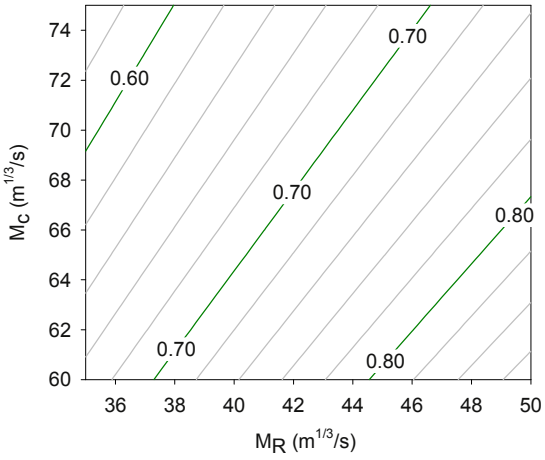

Fig. 20. Area ratio (A_c/A_{sc}) for different roughness values for the same hydraulic head loss.

lines in the figure are an area ratio that helps to find equivalent area of concrete-lined tunnel for a known area of shotcrete-lined tunnel and vice versa.

After having equivalent areas, the quantities of excavation and rock support have been calculated for each lining case. It is considered that there is a need for initial rock support consisting of sprayed concrete and systematic bolting to achieve construction safety in the tunnel. Even though the extent of this initial support is dependent on the quality of rock mass, it is considered that on average, 10 cm fiber reinforced shotcrete and rock bolts (3 m long @1.5 m × 1.5 m spacing) are required as initial tunnel support. The final lining required for shotcrete-lined tunnel is assumed as 40 cm thick reinforced concrete lining in the invert and 5 cm extra shotcrete lining and 20% extra rock bolts. The concrete-lined tunnel on the other hand is assumed to have 40 cm thick reinforced concrete along the tunnel periphery including tunnel invert. For cost calculation, the unit rate for each item has been fixed based on present market rates prevailing in Nepal (Himal Hydro, 2016) and adjusted with global market rates based on international experience. Table 17 shows the adjusted unit rate for different main items.

Table 17
Unit rate of different support items.

Item	Unit	Rate (USD)
Tunnel excavation	m^3	45
Fiber reinforced shotcrete	m^3	410
Rock bolts	m	24
Reinforced concrete	m^3	300

All possible area and roughness ratios have been calculated within the given range of roughness. Construction cost per meter tunnel is calculated for both shotcrete-lined and concrete-lined tunnels with varying area ratio where the area of shotcrete-lined tunnel varies from 10 m^2 to 80 m^2. Fig. 21 shows the possible cost saving as a fraction of excavation cost per meter shotcrete-lined tunnel with invert concrete for different area ratios and roughness ratios.

As Fig. 21a indicates, a cost saving is possible to achieve for all sized shotcrete-lined tunnels against concrete-lined tunnels as long as the area ratio is over 0.5. The figure also indicates that the cost savings are more pronounced in tunnels with smaller cross-sectional area. Fig. 21b indicates the cost savings for different tunnel cross-sectional areas in the form of ratio of roughness for shotcrete-lined and concrete-lined tunnels, which may also be used as a basis for cost optimization.

8. Conclusions

As has been demonstrated in this article, shotcrete-lined waterway tunnels (both headrace and tailrace tunnels) with invert concrete will be innovative and optimal cost effective options for the future hydropower projects in the Himalayan region. However, one should make sure that the long-term stability and safety of the waterway system are achieved and tunnel segments crossing serious weakness/fault zones are fully concrete-lined. Suggested relationships between the Manning coefficient (hydraulic roughness) and the physical roughness (Eq. (24)), and between the physical roughness and the over-break thickness (Eq. (27)) of tunnels excavated using drill-and-blast methods can be used to predict head loss along

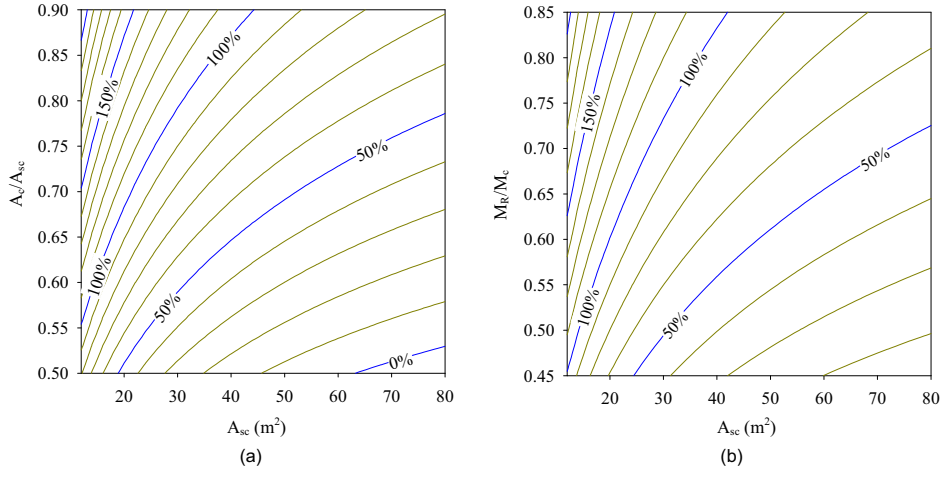

Fig. 21. Contour lines showing possible cost saving as a fraction of excavation cost per meter of shotcrete-lined tunnel with invert concrete. (a) Area ratio, and (b) Roughness ratio.

the shotcrete-lined tunnels with invert concrete. These relationships may be used for predicting tunnel roughness both before and after excavation of a waterway tunnel in question. The strength of the suggested relationships is their simplicity and the relationships are directly linked with the roughness of actual tunnel periphery. However, the authors note that the proposed equations are based on only two tunnel cases and hence assume that there may be some discrepancies in the outcome of the proposed method compared to the reality. Similarly, it is also concluded that there is no distinct correlation between over-break thickness (directly linked with the roughness of the tunnel periphery) and rock mass quality class defined by Q-system of rock mass classification. However, the study indicates that the rock mass quality under Class IV (poor rock mass) seems more vulnerable to the deviation on the over-break thickness. Finally, the study demonstrates the financial attractiveness of the use of shotcrete-lined waterway tunnels with invert concrete lining versus fully concrete-lined tunnels.

Conflicts of interest

The authors wish to confirm that there are no known conflicts of interest associated with this publication and there has been no significant financial support for this work that could have influenced its outcome.

Acknowledgements

The authors are grateful to the project operation team of the Modi Khola and Chilime hydroelectric projects for giving access to measure the head loss and for providing project background data and information and also giving permission to use these two projects as cases for this research, which will be a milestone in the use of unlined or shotcrete-lined pressure tunnel concept in the Himalayan region.

Notations

ξ	Loss coefficient for singular losses
ν	Kinematic viscosity (1.3×10^{-6} m^2/s for water at 10 °C)
A	Cross-sectional area of tunnel (m^2)
D	Diameter of pipe/circular tunnel (m)
f	Friction factor (hydraulic roughness)
f_s	Friction factor of steel pipe
f_c	Friction factor of concrete
f_{sc}	Friction factor of shotcrete lining
f_R	Friction factor of shotcrete-lined tunnel with invert concrete
g	Acceleration due to gravity (9.81 m/s^2)
H_f	Frictional head loss (m)
H_{fc}	Frictional head loss in concrete-lined tunnel/culvert (m)
H_{fs}	Frictional head loss in steel pipe (m)
H_R	Frictional head loss in shotcrete-lined tunnel with invert concrete (m)
ε	Equivalent sand roughness/physical roughness of the conduit (m)
ε_s	Equivalent sand roughness of steel pipe (m)
ε_c	Equivalent sand roughness of concrete (m)
ε_{sc}	Physical roughness of shotcrete lining (m)
ε_R	Physical roughness of shotcrete-lined tunnel with invert concrete (m)
L	Length of conduit (m)
M	Manning coefficient (m$^{1/3}$/s) (hydraulic roughness)
M_s	Manning coefficient of steel pipe (m$^{1/3}$/s)
M_c	Manning coefficient of concrete (m$^{1/3}$/s)
M_{sc}	Manning coefficient of shotcrete lining (m$^{1/3}$/s)
M_R	Manning coefficient of shotcrete-lined tunnel with invert concrete (m$^{1/3}$/s)
P	Wetted perimeter (m)
P_r	Water pressure (bar)
R	Reynold's number, vD/ν
R_h	Hydraulic radius, A/P (m)
v	Flow velocity (m/s)

References

Adams T, Grant C, Watson H. A simple algorithm to relate measured surface roughness to equivalent sand-grain roughness. International Journal of Mechanical Engineering and Mechatronics 2012;1(2):66–71.
Benson R. Design of unlined and lined pressure tunnels. Tunneling and Underground Space Technology 1989;4(2):155–70.
Bishwakarma MB. Computation of head losses in hydropower tunnels. Dam Engineering 2012;23(2):1–15.
Brekke TL, Ripley B. Design guidelines for pressure tunnels and shafts. 1987. Research Project 1745-17, EPRI, Section 5-Detailed design. Technical Report.
Broch E. The development of unlined pressure shafts and tunnels in Norway. In: ISRM international symposium. International society for rock mechanics; 1982.
Bruland A, Solvik Ø. Analysis of roughness in unlined tunnels. In: Proceedings of the international conference on underground hydropower plants; 1987. p. 22–5.
Chilime Hydropower Company Ltd. (CHC). Project completion report. CHC; 2005.
Colebrook CF. The flow of water in unlined, limed and partly lined rock tunnels. Proceedings of the Institution of Civil Engineers 1958;11(1):103–32.
Cuesta L. Unlined hydroelectric tunnels. In: ISRM international symposium. Isrm; 1988.
Hager WH. Wastewater hydraulics: theory and practice. Springer; 2010.
Hákonardóttir KM, Tómasson GG, Kaelin J, Stefánsson B. The hydraulic roughness of unlined and shotcreted TBM-bored tunnels in volcanic rock: In Situ observations and measurements at Kárahnjúkar Iceland. Tunnelling and Underground Space Technology 2009;24(6):706–15.
Huval CJ. Hydraulic design of unlined rock tunnels. Journal of the Hydraulics Division 1969;95(4):1235–46.
Himal Hydro. Archive of the present market rate of tunneling works in the Himalaya. Himal Hydro and General Construction Ltd.; 2016.
Kim Y. Tunnel contour quality index in a drill and blast tunnel: definition, analysis and effects. Norwegian University of Science and Technology; 2009. PhD Thesis.
Kim Y, Bruland A. A study on the establishment of tunnel contour quality index considering construction cost. Tunnelling and Underground Space Technology 2015;50:218–25.
Lysne DK, Glover B, Støle H, Tesaker E. Hydraulic design. Department of hydraulic and environmental engineering. Norwegian University of Science and Technology; 2003.
Maerz N, Ibarra J, Franklin J. Overbreak and underbreak in underground openings, Part 1: measurement using the light sectioning method and digital image processing. Geotechnical & Geological Engineering 1996;14(4):307–23.
Mandal S, Singh M. Evaluating extent and causes of overbreak in tunnels. Tunnelling and Underground Space Technology 2009;24(1):22–36.
Mosonyi E. Water power development. Akademiai Kiado; 1965.
Nilsen B, Thidemann A. Rock engineering. Division of Hydraulic Engineering, Norwegian Institute of Technology; 1993.
Panthi KK. Evaluation of rock bursting phenomena in a tunnel in the Himalayas. Bulletin of Engineering Geology and the Environment 2012;71(4):761–9.
Panthi KK. Himalayan rock mass and possibility of limiting concrete-lined pressure tunnel length in hydropower projects in the Himalaya. Geosystem Engineering 2015;18(1):45–50.
Pegram GGS, Pennington MS. Hydraulic roughness of bored tunnels. Journal of the South African Institution of Civil Engineering 1998;40(4):9–14.
Penche C. Guide on how to develop a small hydropower plant. European Small Hydropower Association; 2004.
Priha S. Hydraulic properties of small unlined rock tunnels. Journal of the Hydraulics Division 1969;95(4):1181–210.
Rahm L. Friction losses in Swedish rock tunnels. In: International water power & dam construction; 1958. p. 457–64.
Reinius E. Head losses in unlined rock tunnels. In: International water power & dam construction; 1970. p. 246–52.
Ronn P, Skog M. New method for estimation of head loss in unlined water tunnels. In: Proceedings of the 3rd international conference on hydropower. Rotterdam: A.A. Balkema; 1997. p.675–82.
Sharma RH. Modi Khola hydroelectric project. Construction report. Himal Hydro and General Construction Ltd.; 2001.
Shrestha PK, Panthi KK. Groundwater effect on faulted rock mass: an evaluation of Modi Khola pressure tunnel in the Nepal Himalaya. Rock Mechanics and Rock Engineering 2014;47(3):1021–35.
Solvik O. Unlined tunnel hydraulics. In: Hard rock underground engineering. Olso, Norway: Furuholmen-Astrup Høyer-Selmer (FHS); 1984.
Westfall DE. Water conveyance tunnels. In: Tunnel engineering handbook. Springer; 1996. p. 298–310.
Wright DE. The hydraulic design of unlined and lined-invert rock tunnels. Construction Industry Research and Information Association; 1971.

Chhatra Bahadur Basnet is conducting his PhD research at the Department of Geosciences and Petroleum, Norwegian University of Science and Technology (NTNU), Norway. His current research work is related to unlined pressure tunnels in hydropower projects. He holds MSc degree in Hydropower Development from NTNU. He has more than six years of working experience in planning, design, and construction supervision of numbers of hydropower projects in Nepal.

Krishna Kanta Panthi is an Associate Professor in Geological Engineering at the Department of Geosciences and Petroleum, Norwegian University of Science and Technology (NTNU) since 2008. He holds the degrees of PhD in Rock Engineering, MSc in Hydropower Engineering and MSc in Tunneling. He has approximately 25 years of experience in design, construction management and research of tunneling, hydropower, slope stability and mining projects. He is the author of many scientific papers published in renowned international journals.

Paper II

Title:

Analysis of unlined pressure shafts and tunnels of selected Norwegian hydropower projects

Authors:

Basnet, Chhatra Bahadur

Panthi, Krishna Kanta

Published in:

Journal of Rock Mechanics and Geotechnical Engineering (2018)

Volume 10 (3), pages 486-512

Journal of Rock Mechanics and Geotechnical Engineering 10 (2018) 486–512

Contents lists available at ScienceDirect

Journal of Rock Mechanics and Geotechnical Engineering

journal homepage: www.rockgeotech.org

Full Length Article

Analysis of unlined pressure shafts and tunnels of selected Norwegian hydropower projects

Chhatra Bahadur Basnet*, Krishna Kanta Panthi

Department of Geoscience and Petroleum, Norwegian University of Science and Technology, Sem Saelands Vei 1, NO-7491, Trondheim, Norway

ARTICLE INFO

Article history:
Received 19 September 2017
Received in revised form
7 December 2017
Accepted 25 December 2017
Available online 24 February 2018

Keywords:
Hydropower projects
Unlined pressure shafts and tunnels
Minor principal stress
Hydraulic jacking
Water leakage

ABSTRACT

Norwegian hydropower industry has more than 100 years of experiences in constructing more than 4000 km-long unlined pressure shafts and tunnels with maximum static head of 1047 m (equivalent to almost 10.5 MPa) reached at unlined pressure tunnel of Nye Tyin project. Experiences gained from construction and operation of these unlined pressure shafts and tunnels were the foundation to develop design criteria and principles applied in Norway and some other countries. In addition to the confinement criteria, Norwegian state-of-the-art design principle for unlined pressure shaft and tunnel is that the minor principal stress at the location of unlined pressure shaft or tunnel should be more than the water pressure in the shaft or tunnel. This condition of the minor principal stress is prerequisite for the hydraulic jacking/splitting not to occur through joints and fractures in rock mass. Another common problem in unlined pressure shafts and tunnels is water leakage through hydraulically splitted joints or pre-existing open joints. This article reviews some of the first attempts of the use of unlined pressure shaft and tunnel concepts in Norway, highlights major failure cases and two successful cases of significance, applies Norwegian criteria to the cases and reviews and evaluates triggering factors for failure. This article further evaluates detailed engineering geology of failure cases and also assesses common geological features that could have aggravated the failure. The minor principal stress is investigated and quantified along unlined shaft and tunnel alignment of six selected project cases by using three-dimensional numerical model. Furthermore, conditions of failure through pre-existing open joints by hydraulic jacking and leakage are assessed by using two-dimensional fluid flow analysis. Finally, both favorable and unfavorable ground conditions required for the applicability of Norwegian confinement criteria in locating the unlined pressure shafts and tunnels for geotectonic environment different from that of Norway are highlighted.

1. Introduction

Norway has built more than 200 underground powerhouses and 4200 km-long hydropower tunnels in the past 100 years (Broch, 2013). Experiences gained in design, construction and operation of waterway system have led to the development of innovative ideas. One of these ideas is the application of unlined high-pressure tunnels and shafts in hydropower schemes. It is estimated that over 95% of the waterway length of Norwegian hydropower schemes is left unlined (Johansen, 1984; Panthi, 2014). The earliest attempt to apply such concept in Norway was in Herlandsfoss project in 1919 (Vogt, 1922), and up to now, more than 4000 km-long unlined pressure shafts and tunnels with maximum static head of 1047 m have been in successful operation. Panthi and Basnet (2016) collected the information about most of the unlined tunnel projects and explained a brief history of development of unlined shaft and tunnel concept in Norway. They generalized the layout of such unlined shafts and tunnels in different hydropower schemes in four different arrangements, which are being practiced in Norway since the start of unlined pressure tunnel concept (Fig. 1). The arrangements shown in Fig. 1 are prepared based on the layout of a number of successful unlined shafts and tunnels in different hydropower schemes of Norway.

Apart from Norway, the unlined pressure tunnels are constructed worldwide where the layout planning, design and construction experiences from Norway are extensively used in

* Corresponding author.
E-mail address: chhatra.basnet@ntnu.no (C.B. Basnet).
Peer review under responsibility of Institute of Rock and Soil Mechanics, Chinese Academy of Sciences.

https://doi.org/10.1016/j.jrmge.2017.12.002

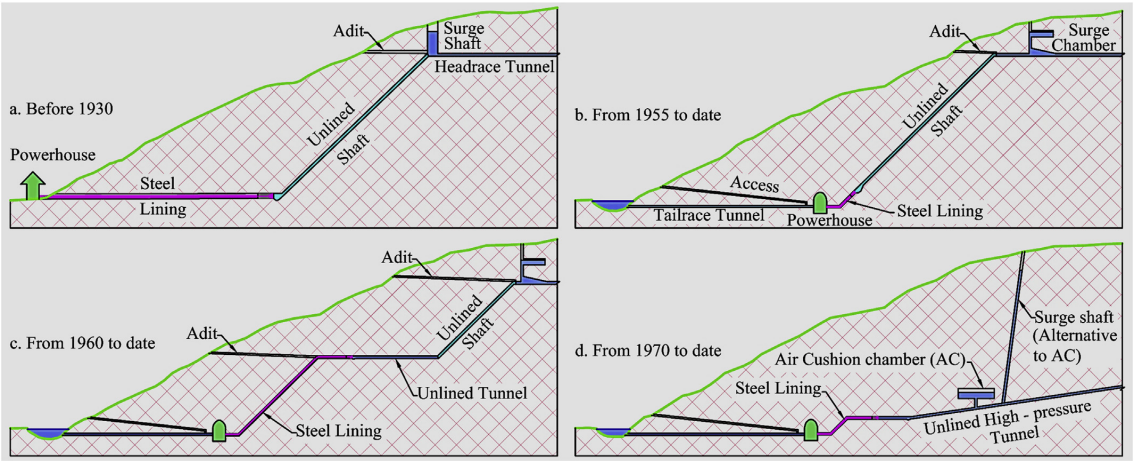

Fig. 1. Locations of unlined high-pressure shafts and tunnels in different hydropower schemes of Norway.

different geological and tectonic environments. Some examples of unlined pressure tunnels around the world are mentioned here. In Colombia, Chivor and Gauvio projects were planned with unlined pressure tunnels where Norwegian design principles were used in the design process (Broch, 1984; Broch et al., 1987). In Tanzania, unlined high-pressure tunnel of Lower Kihansi hydropower project was designed by using Norwegian criteria (Marwa, 2004). Palmstrom and Broch (2017) highlighted that two of the hydropower projects with unlined tunnels are in operation in Chile after the repair work of the collapses occurred after the waterway system is filled and power plants come in operation. Similarly, according to Norconsult (2017), the Las Lajas project in Chile is planned to use 9.5 km-long unlined pressure tunnel. In Portugal, Venda Nova II (Lamas et al., 2014) and Venda Nova III (Esteves et al., 2017) have successfully employed unlined pressure tunnels and both projects are in operation without any significant problem. In China, there is growing rate of use of unlined tunnels in the hydropower projects (Liu, 2013). In Nepal, Upper Tamakoshi Hydroelectric with unlined pressure tunnel is under construction (Panthi and Basnet, 2017) and is expected to be water-filled within two years of time.

The principle behind the idea of unlined pressure tunnel concept is that the rock mass itself works as a natural concrete against the pressure exerted by water column in the tunnel (Broch and Christensen, 1961; Selmer-Olsen, 1969; Broch, 1982). It is well known that Norway is geologically considered as a hard rock province, since two thirds of the country is situated in the Precambrian rocks consisting of gneisses (the most dominant rock type), granites, gabbros and quartzites. This hard rock province offers stiff rocks, which could work against the high water pressure without failure. However, about one third of the landscape is made up of rocks of Cambro-Silurian age (mainly Caledonian mountain range) consisting of different mixes of rock types such as gneisses, schists, phyllites, greenstones and marbles of varying degree of metamorphism as well as granites, gabbros, sandstones, shales, dolomites and limestones (Johansen, 1984). It is worthy to note here that waterway systems of many Norwegian hydropower schemes are aligned along the rock mass of the Caledonian mountain range, which do not represent as stiff rock mass as that of the Precambrian formations. The typical feature of Norwegian landscape is that the last deglaciation left the rock surface without any appreciable weathered material on the top of the surface, but there is a tendency of a frequent jointing in the rock mass near the surfaces. Selmer-Olsen (1969) explained that this condition may lead to higher permeability of rock mass at a depth ranging from 5 m to 40 m, which could cause water leakage. On the other hand, more stabilized tectonic setting (relatively few tectonic activities in comparison to other mountainous regions) helped to increase confinement in the rock mass even near surface. In general, favorable engineering geological and geotectonic environment of the Scandinavian landscape has favored the use of unlined pressure tunnel concept in Norway.

The successful history of the operation of unlined pressure shafts and tunnels in Norway is almost 99% with very few stability problems along the waterway system excluding some exceptions where problems were registered during the initial phase of the development of unlined concepts. The detailed studies of the failure were carried out and the lessons learned from the failure were helpful in developing certain design principles and criteria for unlined high-pressure tunnels and shafts (Broch and Christensen, 1961; Selmer-Olsen, 1969, 1974, 1985; Broch, 1982). In addition to the design criteria for confinement, a concept came in practice after the 1970s that nowhere along the unlined shafts and tunnels, the minor principal stress should be less than the pressure due to static water head. In order to use this concept in practice, a set of standard two-dimensional (2D) finite element charts were prepared in 1971–1972 for valley side slope from 14° to 75° (Nilsen and Thidemann, 1993). Bergh-Christensen (1982), Bergh-Christensen and Kjolberg (1982), Buen and Palmstrom (1982) and Benson (1989) emphasized the necessity of more detailed study on the engineering geological and stress state conditions. The in situ stress measurement program became popular means to verify the assumptions made during the design of unlined concept in Norway as well as in other parts of the world (Bergh-Christensen, 1982, 1986; Myrset and Lien, 1982; Vik and Tunbridge, 1986; Palmstrom, 1987; Hartmaier et al., 1998; Panthi and Basnet, 2017). The risk of hydraulic jacking along the pre-existing joints and fractures and possibility of leakage were always the major issues in the design of unlined tunnels and shafts (Barton et al., 1987; Brekke and Ripley, 1987). Hydraulic jacking test and fluid flow analysis through the joints could also be used to

assess the risk of hydraulic jacking and leakage (Ming and Brown, 1988; Edvardsson and Broch, 2002).

The above description clearly indicates that the detailed geological assessment, stress state analysis, hydraulic jacking, leakage analysis and in situ rock stress measurement should be carried out in addition to the use of design criteria for confinement and standard finite element charts. In this article, detailed geological assessment of seven major failure cases, stress state analysis of four failures and two successful cases and hydraulic jacking and leakage assessment of four failure cases have been carried out. The reliable application of standard 2D finite element charts is limited due to the uniqueness of each project in terms of topography and geology. In recent years, more sophisticated 2D computer programs are being used to model the project-specific topography and geology. However, 2D model in general fails to quantify the effect of complex topography and complex geology including intersecting faults and zones of weakness in the in situ stress state. In order to cope with this limitation, three-dimensional (3D) computer programs (FLAC^{3D}) is used in this article for the quantification of in situ stress state. In addition, 2D fluid flow model (UDEC) is used to assess the hydraulic jacking and water leakage through the pre-existing joints.

2. Brief description of the cases

As mentioned above, most of the unlined pressure tunnels and shafts in Norway are successfully operated without serious instability problems excluding few exceptions, which became the basis for the development of design principles and criteria. The Herlandsfoss was the first hydropower scheme built in 1919 to use unlined pressure shaft concept and followed by Skar and Svelgen built in 1920 and 1921, respectively (Vogt, 1922). Mixed experience was gained from these three projects with Skar completely failed and other two were brought in operation after needed mitigation measures. Most of the unlined pressure tunnels and shafts were successfully designed and operated until the failure that occurred at Byrte project in 1968 and at Askara project in 1970. The failure that took place at these two projects was instrumental in enhancing the design principles. Even though all unlined pressure shafts and tunnels follow the established design principles and criteria, there are still cases of failures even in modern time where further investigations were needed with substantial mitigation measures applied after the first water filling. The examples of such projects are Bjerka, Fossmark and Holsbru. However, the maximum static water head of 1047 m was successfully applied at unlined pressure tunnel of Nye Tyin project in 2004, which is the world record to date. Ten selected cases of the unlined pressure shaft and tunnel projects (eight failed and two highest head projects successfully implemented and operated) are listed in Table 1 for the purpose of detailed investigations and analysis in this paper.

The locations of the selected projects are shown in the overall geological map of Norway in Fig. 2. The projects such as Svelgen and Askara are located in Devonian sandstone whereas Byrte and Bjerka projects are situated in Archean and Proterozoic basements. The rest of the selected projects are situated in Caledonian rock formations. Each of the rock formations has different rock types, geological conditions and tectonic environments. The strength properties of different rocks are tested in the laboratory mostly by SINTEF and the database was published in SINTEF (1998).

The detailed geological conditions differ from project to project even though the projects are situated in same geological formations. Hence, the geological conditions are project-specific and have to be studied in detail for each project. The detailed information was collected for each selected project from the available project reports and the published articles. For in situ stress state analysis, the magnitude and orientation of horizontal stresses are needed. Fejerskov and Lindholm (2000) studied the mechanism of stress generation of the Norwegian continental shelf and compiled the stress database. Similarly, Hanssen (1997) also compiled the stress data including stress measurement in some of the hydropower projects. The required stress data were collected from Nilsen and Thidemann (1993), Fejerskov (1996), Hanssen (1997) and Myrvang (2017). The magnitude and orientation of horizontal stresses in and nearby the locations of selected projects are then superimposed in the geological map of Norway, as shown in Fig. 2.

3. Norwegian confinement criteria

According to Broch (1982), unlined pressure shafts and tunnels built in the 1950s and 1960s were designed using following rule of thumb:

$$h > cH \tag{1}$$

Table 1
Selected cases of unlined pressure shafts and tunnels in Norway.

Project	Location	Year	Gross head (m)	Maximum discharge (m^3/s)	Installed capacity (MW)	Maximum head in unlined shaft/tunnel (m)	Rock type	Failure condition and applied solution
Herlandsfoss	Osteroy, Hordaland	1919	136	6	12	136 (T)	Mica schist	Partly failed and steel lined
Skar	Tingvoll, More og Romsdal	1920	149	1	3.3	129 (T)	Granitic gneiss	Completely failed and steel lined
Svelgen	Bremanger, Sogn og Fjordane	1921	225	6.5	12	152 (S)	Sandstone	Minor leakage and concrete lined
Byrte	Tokke, Telemark	1968	295	8	20	295 (S)	Granitic gneiss	Partly failed and steel lined
Askara	Bremanger, Sogn og Fjordane	1970	690	11.4	85	200 (T)	Sandstone	Partly failed and steel lined
Bjerka	Hemnes, Nordland	1971	370	6.3	20	72 (T)	Gneiss	Partly failed and steel lined
Fossmark	Vaksdal, Hordaland	1985	440	2.38	9	380 (T)	Granite	Partly failed and steel lined
Naddevik	Ardal, Sogn og Fjordane	1987	963	–	112	963 (S)	Dark gneiss	Successfully operated
Nye Tyin	Ardal, Sogn og Fjordane	2004	1050	–	360	1047 (T)	Dark gneiss, granitic gneiss, phyllite and metasandstone	Successfully operated
Holsbru	Ardal, Sogn og Fjordane	2012	692	8.6	49	63 (T)	Dark gneiss	Leakage

Note: T = Tunnel; S = Shaft.
Sources: Vogt, 1922; Selmer-Olsen, 1969; Bergh-Christensen, 1975; Valstad, 1981; Broch, 1982; Buen, 1984; Vik and Tunbridge, 1986; Garshol, 1988; Panthi and Basnet, 2016.

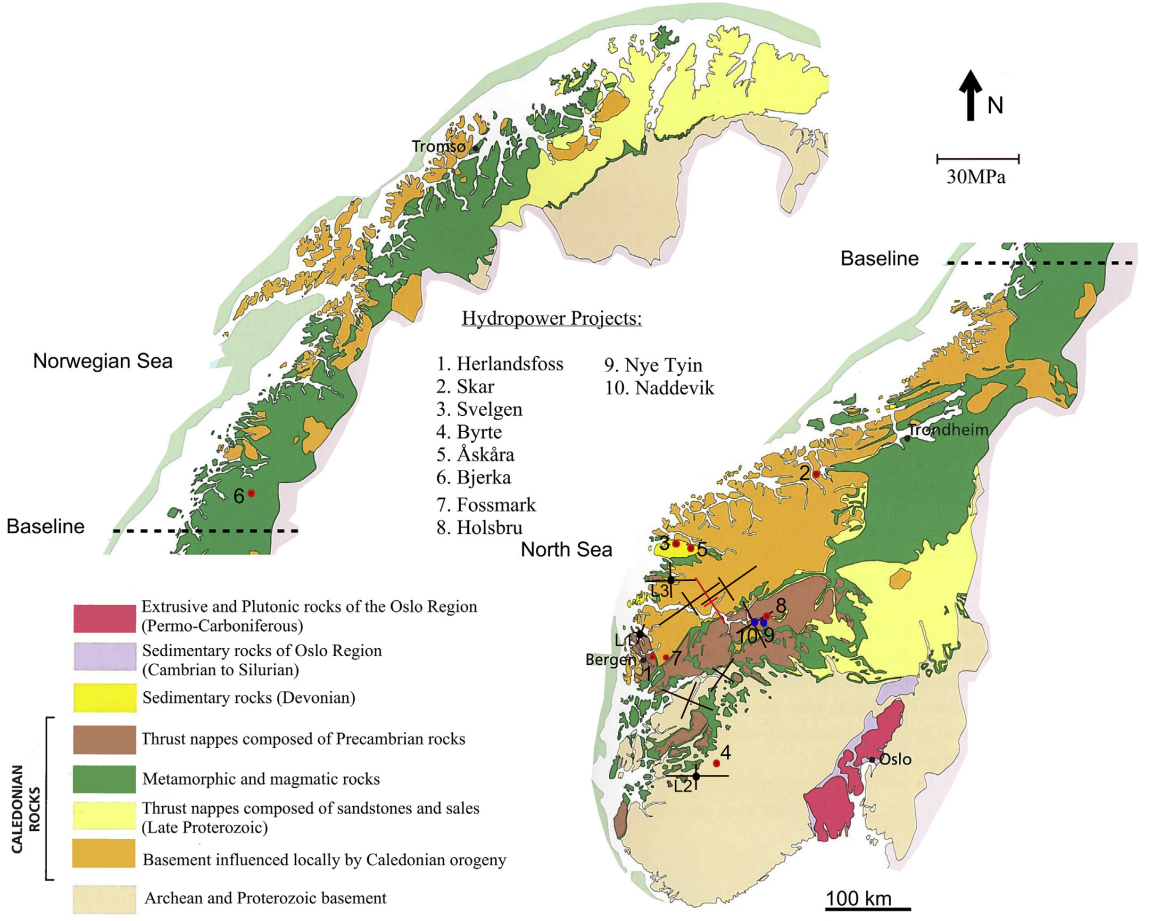

Fig. 2. Locations of the hydropower projects in the geological map of Norway with direction and magnitude of horizontal rock stresses superimposed (Map source: NGU, 2017).

where h is the minimum required rock cover over the shaft alignment, H is the hydrostatic head acting over the shaft alignment, and c is a constant that has a value of 0.6 for valley sides with inclinations up to 35° and 1 for valley sides slope exceeding 35°.

After the failure of unlined pressure shaft at Byrte in 1968 where the pressure shaft had an inclination of 60°, the rule of thumb expressed by Eq. (1) was upgraded as (Broch, 1982):

$$h > \frac{H}{\rho \cos \alpha} \tag{2}$$

$$\rho = \frac{\rho_r}{\rho_w} \tag{3}$$

where ρ_w is the density of water, ρ_r is the density of the rock, ρ is the relative density of the rock, and α is the inclination of shaft/tunnel with respect to horizontal plane. It is highlighted that if the shaft has an inclination more than 60°, Eq. (2) is no longer valid. In such situations, the shaft should be placed inside the line representing minimum depth for a 45° shaft (Selmer-Olsen, 1969).

The above design criterion was used in the design of unlined shafts in Norway until the failure at Askara in 1970. This failure led to the establishment of a new concept proposed by Bergh-Christensen and Dannevig (1971) that considers the shortest perpendicular distance (L) from the valley inclination line (Fig. 3), which is expressed by

$$L > \frac{H}{\rho \cos \beta} \tag{4}$$

where β represents the angle of valley side slope with respect to horizontal plane. Since then, both Eqs. (2) and (4) are considered as the state-of-the-art Norwegian rule of thumb for the confinement criterion of unlined/shotcrete-lined pressure shafts and tunnels.

It would be of great interest to check whether the cases mentioned above (Table 1) fulfill the design criteria expressed by Eqs. (2) and (4). The profiles along shaft and tunnel alignment for all these cases excluding Holsbru project are shown in Fig. 4 for the geometrical reference of locations to be investigated. However, all profiles shown in Fig. 4 represent critical sections defined by the needed rock cover and slope inclinations except for Askara,

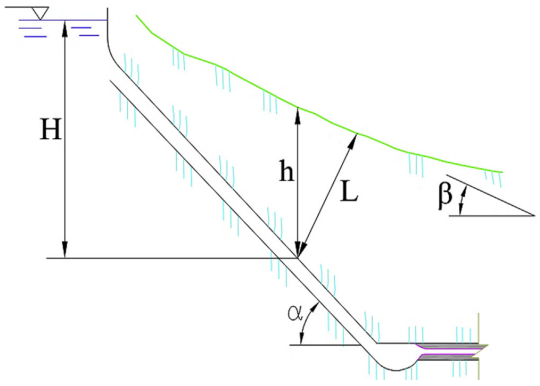

Fig. 3. Definition for the rule of thumb (Broch, 1982).

Naddevik and Nye Tyin projects. In these projects, respective critical sections are taken from 3D topography and the required geometrical information is extracted. While defining the valley side slope angle and measuring the available vertical rock cover (h') and available shortest distance (L'), a correction of valley side slope for protruding noses as recommended by Broch (1984) is applied. The details of the calculation including available factor of safety are presented in Table 2.

As seen in Table 2, the required vertical rock cover and shortest distance from the valley side slope at different locations of selected projects are calculated. The calculated values are compared with the actually available values to calculate the factor of safety (FoS_1 and FoS_2). In theory, the factor of safety should be greater than one for no failure to occur at the selected location of the unlined shaft and tunnel. It is interesting to note that there are locations (Sv-A, Bj-A, Br-A, Br-B, Br-C, As-A, Fo-B, Fo-C, Fo-D, Fo-E, Fo-F and Holsbru) where even though the factor of safety is greater than one, the failure/leakage was experienced after the water filling was carried out. On the other hand, in some locations (Hf-C, Sv-B and Br-D), no

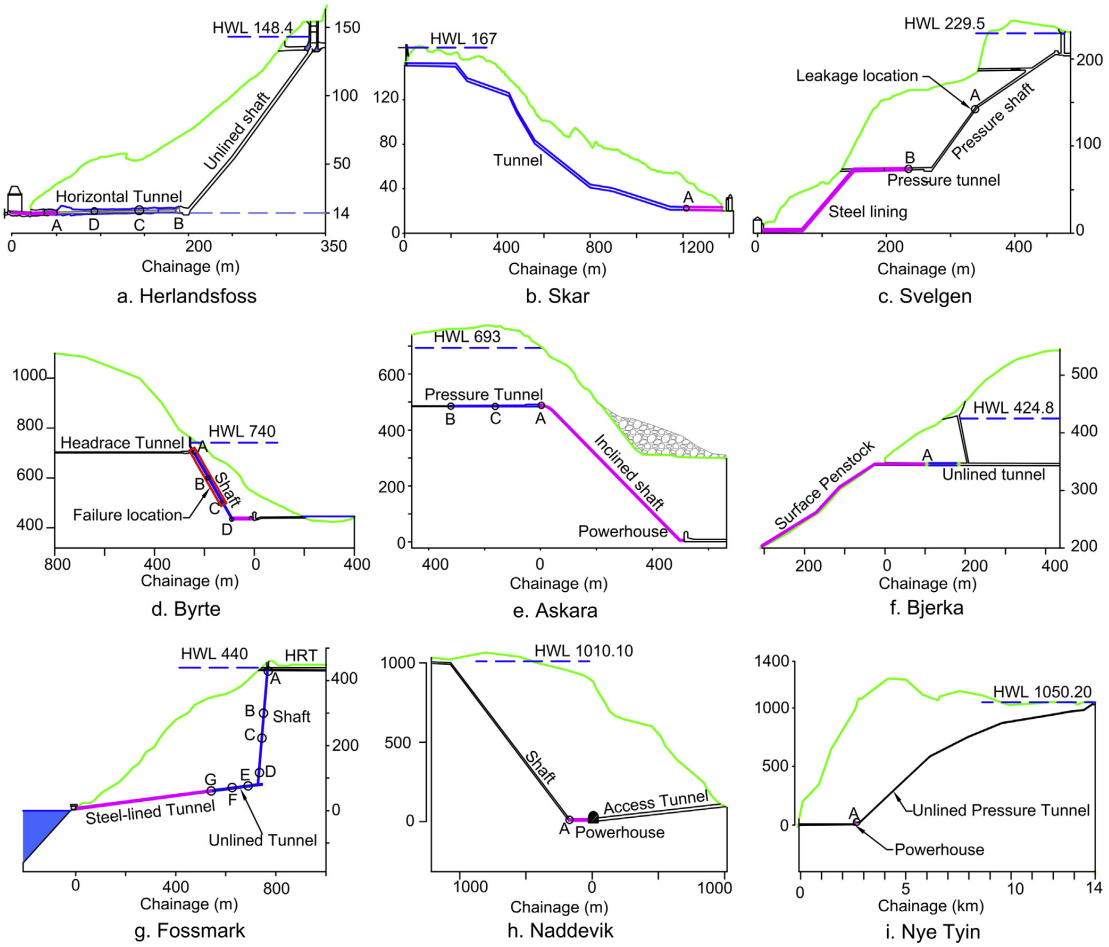

Fig. 4. Overview of profiles along the unlined shaft/tunnel of different hydropower projects in Norway. The vertical axis represents the elevation in masl (meter above sea level). HWL is the head water level.

Table 2
Analysis of the cases based on the design criteria defined by Eqs. (2) and (4).

Project	Location	H (m)	ρ_r (t/m^3)	h' (m)	α (°)	β (°)	L' (m)	L'/H	h (m)	L (m)	FoS_1 (h'/h)	FoS_2 (L'/L)	Remarks
Herlandsfoss	Hf-B	136	3.05	56	0	26	51	0.38	45	50	1.26	1.03	No failure
	Hf-C	136	3.05	31	0	26	32	0.24	45	50	0.7	0.65	No failure
	Hf-D	136	2.77	19	0	28	17	0.13	49	56	0.39	0.31	Failure
Skar	Sk-A	129	2.65	30	8	10	25	0.19	49	49	0.61	0.51	Failure
Svelgen	Sv-A	84	2.65	38	27	25	40	0.48	36	35	1.07	1.14	Minor leakage
	Sv-B	152	2.65	54	0	25	48	0.32	57	63	0.94	0.76	No failure
Byrte	Br-A	37	2.64	45	60	40	40	1.08	28	18	1.61	2.19	Failure
	Br-B	116	2.64	100	60	40	70	0.6	88	57	1.14	1.22	Failure
	Br-C	210	2.64	147	60	40	114	0.54	159	104	0.92	1.1	Failure
	Br-D	295	2.64	200	60	40	125	0.42	223	146	0.89	0.86	No failure
Askara	As-B	200	2.71	273	0	26	241	1.21	74	82	3.7	2.94	No failure
	As-C	200	2.71	265	0	35	216	1.08	74	90	3.59	2.4	No failure
	As-A	200	2.71	200	0	55	130	0.65	74	129	2.71	1.01	Failure
Bjerka	Bj-A	72	2.64	61	0	25	58	0.81	27	30	2.24	1.93	Failure
Fossmark	Fo-A	9	2.64	12	84	31	8	0.89	5	4	2.49	2.01	No failure
	Fo-B	135	2.64	132	84	31	114	0.84	72	60	1.83	1.91	Failure
	Fo-C	213	2.64	205	84	31	177	0.83	114	94	1.8	1.88	Failure
	Fo-D	318	2.64	304	84	31	262	0.82	170	141	1.78	1.86	Failure
	Fo-E	364	2.64	334	6	31	288	0.79	139	161	2.41	1.79	Failure
	Fo-F	373	2.64	292	6	31	252	0.68	142	165	2.06	1.53	Failure
	Fo-G	380	2.64	250	6	31	215	0.57	145	168	1.73	1.28	No failure
Naddevik	Nd-C	963	2.74	905	48	35	740	0.77	525	429	1.72	1.72	No failure
Nye Tyin	Nt-F	1047	2.84	838	1	18	875	0.84	369	388	2.27	2.26	No failure
Holsbru	Tunnel end	63	2.65	76	0	30	65	1.03	24	27	3.2	2.37	Leakage

failure occurred even though the factor of safety is less than one. The remaining locations (Hf-B, Hf-D, Sk-A, Br-C, As-B, As-C, Fo-A, Fo-G, Nd-A and Nt-A) that fulfill the design criteria had no failure evidence. Based on Eq. (4), NGI (1972) has recommended two demarcation curves (Fig. 5) expressed by the ratio of shortest length (L') to static head (H) with the valley slope angle (β) that should principally fulfill the criterion for no leakage to occur along those locations of the pressure tunnels falling above these two curves. The analyzed datasets of Table 2 are plotted in Fig. 5 to test the criterion. As seen in Fig. 5, the results achieved are mixed, indicating some locations lying above these two curves where have experienced substantial leakage and some locations lying below these two curves with no leakage.

This indicates that the design criterion expressed by Eq. (4) does not necessarily fulfill the demand for leakage conditions through the unlined pressure tunnels and shafts and needs to be carefully assessed for each individual case, since each alignment of the waterway is unique in itself. It is important that a comprehensive engineering geological assessment should be carried out while designing the unlined pressure tunnels.

4. Engineering geology of the cases

The Norwegian confinement criteria for the design of unlined tunnels and shafts are developed mainly based on 2D geometry of the topography. The rule of thumb does not take into account the

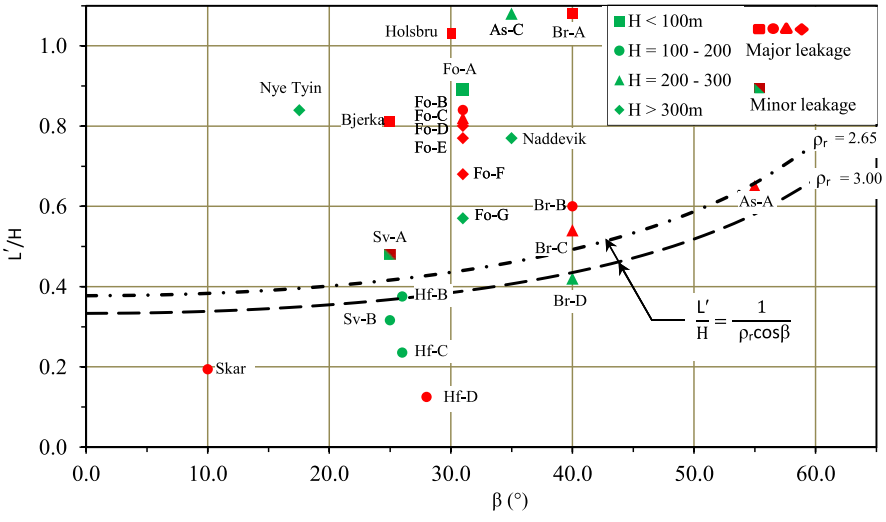

Fig. 5. Unlined pressure shafts and tunnels in valley side with various inclinations, β.

engineering geology and full overview of the in situ stress state of the area. The engineering geology includes rock types, strength properties of the rock and rock mass, joints and their characteristics, faults and zones of weakness presented along the shaft and tunnel alignment. In general, the stress state of the area is influenced by the 3D topography, weakness and fault zones, and the geotectonics and geological environment of the area. In the following, detailed engineering geology of the selected projects is assessed which is further used to quantify the input parameters required for the stress state analysis and hydraulic jacking assessment of the cases.

4.1. Herlandsfoss project

Herlandsfoss project has 1400 m-long headrace tunnel, surge shaft, inclined unlined shaft dipping approximately at 40°, and 175 m-long horizontal penstock tunnel near the powerhouse located at surface (Fig. 6). As indicated in Figs. 6 and 7, the main rock types in the project were registered as hornblende schist and mica schist and lay in the Caledonian nappe complex (Fig. 2). Hornblende schist was found to be massive and of good quality compared with the mica schist. A band of talcose mica schist passing through the southwest side of downstream valley was highly fractured.

The failure of unlined pressure tunnel of this project is explained in detail by Panthi and Basnet (2016) and the failure location at initially planned unlined tunnel is shown in Figs. 6 and 7. The failure resulted in excessive water leakage out from the tunnel, which was inferred as the occurrence of hydraulic jacking along the foliation joints of the highly schistose mica schist. The location of leakage area in the surface topography is also shown in Fig. 6. This hydraulic jacking that took place at the pressure tunnel led to extended existing joints in the rock mass and also new fractures were developed along the spring line of the unlined pressure tunnel over a distance of about 50 m from the initial cone area 'A'. It is worthwhile here to study this failure location in detail, since the failure had been noticed only in relatively weak mica schist even though the Norwegian criteria for confinement are not fulfilled in the nearby location with relatively stronger hornblende schist (Table 2).

The rock mass and jointing information is assessed and collected in the literature (e.g. Vogt, 1922; Broch and Christensen, 1961; NGI, 1972). Mica schist between chainage 55 m and 98 m was observed to be highly schistose and rich in chlorite and muscovite. The rock mass was found to be extremely schistose and was formed along the foliation joints, which has orientation of about N55°–60°W/46°–48°SW. The extent of schistosity was so high that even man's fingers could separate the fresh rock mass. In addition, the tunnel alignment met six marked calcite filled shear zones with strike ranging from N20°E to N40°E and dip ranging from 60°SE to 85°SE (Figs. 6 and 7). The shear zones presented had a width of 2–3 m and the joint spacing ranged between 5 cm and 20 cm, which were filled with calcite clay of 1–3 mm in thickness. Selmer-Olsen (1969) indicated that hornblende schist has some joints cross-cutting across the foliation planes. Broch and Christensen (1961) pointed out that the hydraulic jacking occurred along the joint sets 2–4 and along some foliation joints (Figs. 6 and 7) presented in schistose mica schist between chainage 55 m and 98 m.

4.2. Byrte project

Byrte project has low-pressure headrace tunnel, surge shaft, unlined pressure shaft (60° inclination), about 80 m-long steel lined horizontal tunnel, underground powerhouse and about 200 m-long tailrace tunnel, as shown in Fig. 8. Main rock type in the project is granitic gneiss. The rock mass consists of several systems of joint sets and minor faults/zones of weakness with strike approximately parallel to the valley side slope (Selmer-Olsen, 1969). There is also a wide clay-filled fault at Byrte Lake, which is called 'Byrte fault' (Figs. 8 and 9).

Fig. 9 shows the profile along the tunnel and shaft alignment with geological information included. According to Selmer-Olsen (1969), many cracks were observed in the rock mass both in the shaft and powerhouse cavern during the operation of power plant

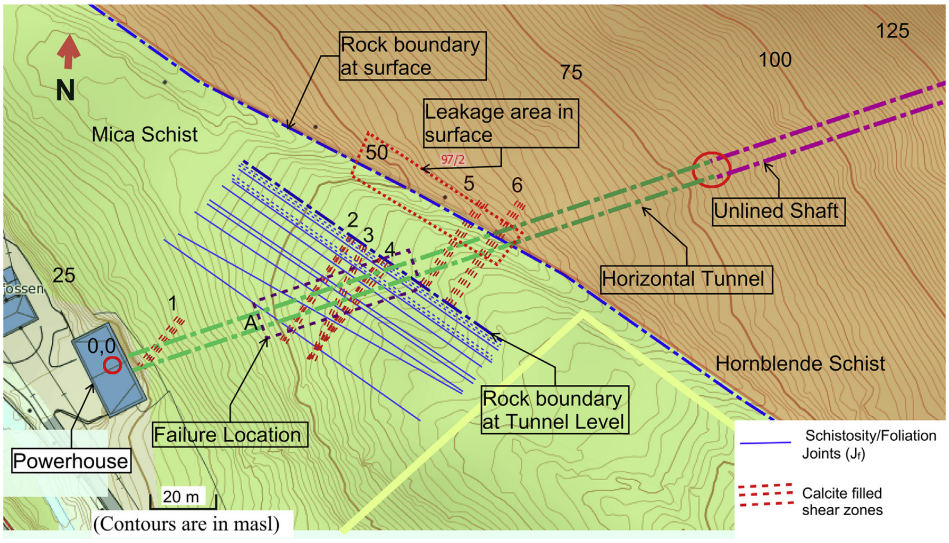

Fig. 6. The Herlandsfoss project details at failure location and rock formation (Contour map source: www.norgeskart.no).

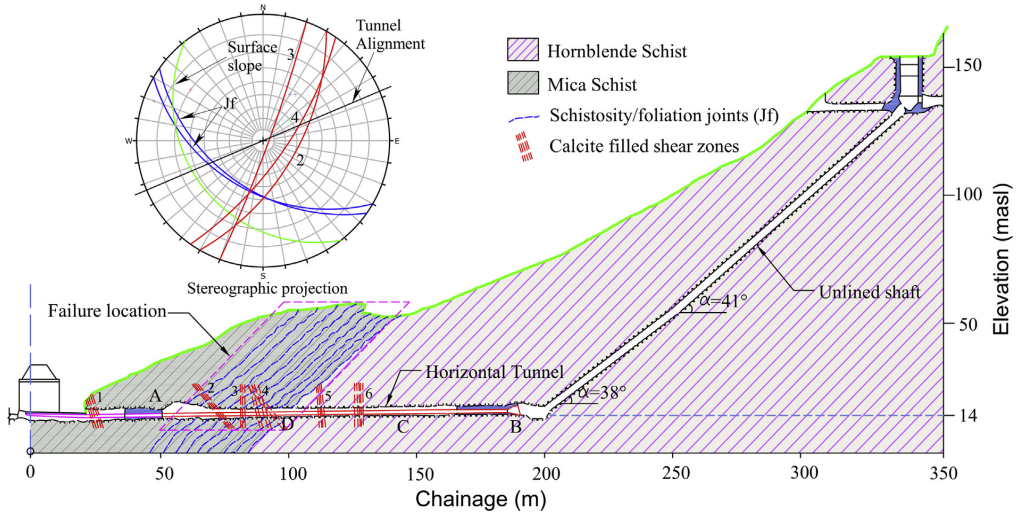

Fig. 7. Profile along the tunnel alignment and failure location of Herlandsfoss project.

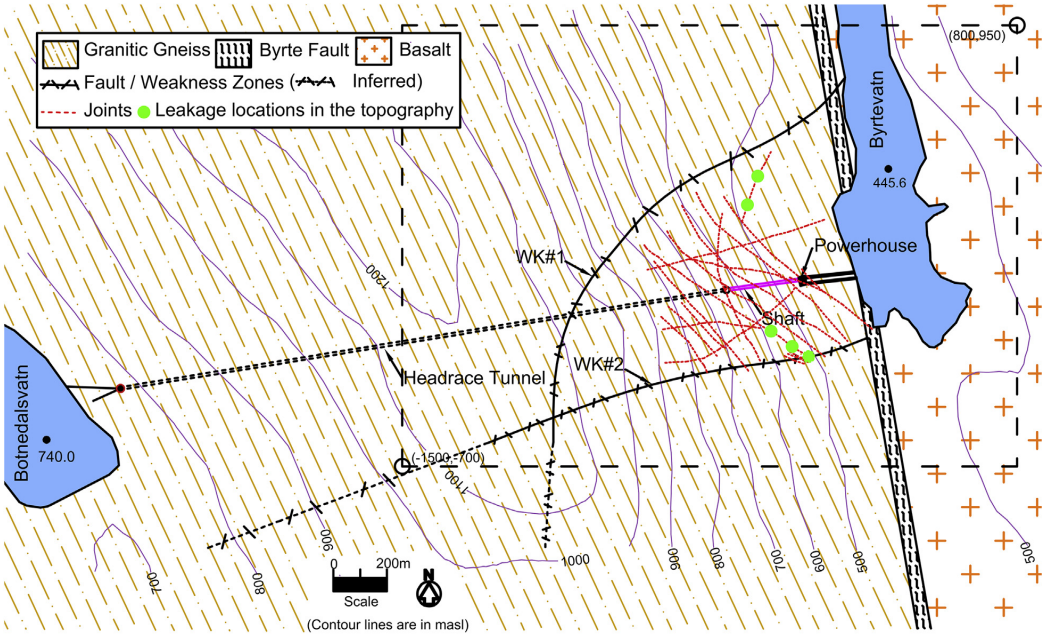

Fig. 8. Byrte project area with rock types, faults/zones of weakness, joints, and leakage locations.

at 300 m gross head. The cracks were marked above the zone of weakness (WK#1) in the shaft and to the right side of the zone of weakness along pressure tunnel to the powerhouse (NVE, 1970). There were no cracks along the shaft below the zone of weakness and the rock mass in this area was also observed as relatively massive and strong. Hence, it can be concluded that rock mass above the zone of weakness has more fractures and joints. Furthermore, leakage was experienced in underground powerhouse cavern and several springs also appeared at the surface topography indicating considerable leakage through the rock mass. The leakage locations in the surface topography are located in Fig. 8.

There are two joint systems in the project area. One of the joint sets, Joint#b in Fig. 9, has an average orientation of about N25°W/65°NE, which is almost parallel to the foliation joints. There are some representative joints shown in Fig. 9 (red color) along the

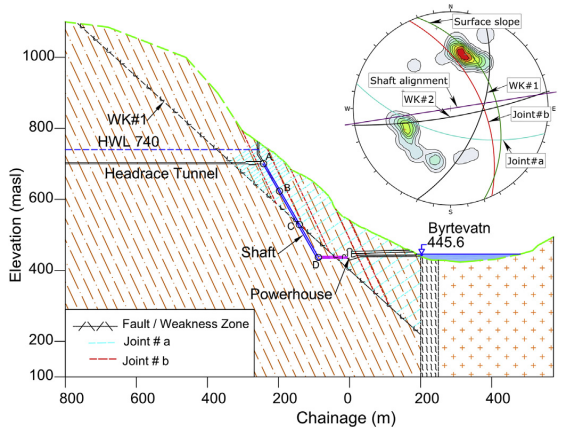

Fig. 9. Profile along the alignment of Byrte project and stereographic projection of joints, zones of weakness and shaft alignment.

shaft and tunnel alignment where hydraulic jacking occurred, since these joints have an opening of about 1–3 mm with almost no clay filling. Another joint set, Joint#a in Fig. 9, has an average orientation of about N75°W/60°SW with a spacing ranging between 10 m and 30 m and has joint opening of 0.5–3 mm. The joints observed in the area mostly open and the filled material if existed was washed away. In addition to these two joint sets, clay filled zones of weakness (WK#1 and WK#2) are also presented in Fig. 8. According to Selmer-Olsen (1969), the clay filled zone WK#1 in Fig. 9 constituting weak rock mass did not manage to sustain the hydrostatic head acting on it and hydraulic jacking occurred along this zone as well.

4.3. Askara project

The location and longitudinal profile of unlined tunnel and other project components of Askara project are shown in Figs. 10 and 11. Main rock type in the project is Devonian sandstone with bedding plane (Jb) striking about N30°E and dipping approximately 20°–25°SE (Bergh-Christensen, 1975). The rock mass in the tunnel area consisted of a series of crushed zones that are parallel to bedding stratification. The vertical distance between these zones varies between 50 m and 150 m. One of the crushed zones along the stratification separates two rock masses in different qualities. The rock mass below the zone is less fractured, massive and impermeable, and that above the zone is jointed. In addition to the bedding planes, there are two more distinct joint sets in the area. The orientation of one of the joint sets (J1) is about N55°–60°E/85°SE and that of another joint set (J2) is about N20°–25°W. The joint set J2 is almost vertical (Fig. 10).

After the failure of unlined tunnel occurred, the waterway system was drained and inspection was carried out. According to Bergh-Christensen (1975), during the inspection, it was observed that the cross joints nearby location *A* opened by about 3–4 cm between the tunnel sections *A* and *B* (Fig. 11). The opening in the joints clearly demonstrated the occurrence of hydraulic jacking.

The splitted joints crushed zones were studied in detail based on 3D maps and description of failure by Bergh-Christensen (1975). At the time of failure, the joints had opening from 10 cm to 50 cm at the location of heavy leakage in the surface. There were also moderate leakages where joints had about 1.5 cm-wide open cracks, which were completely washed out. During the excavation of pressure tunnel, the joint set (J1) was registered as dominant

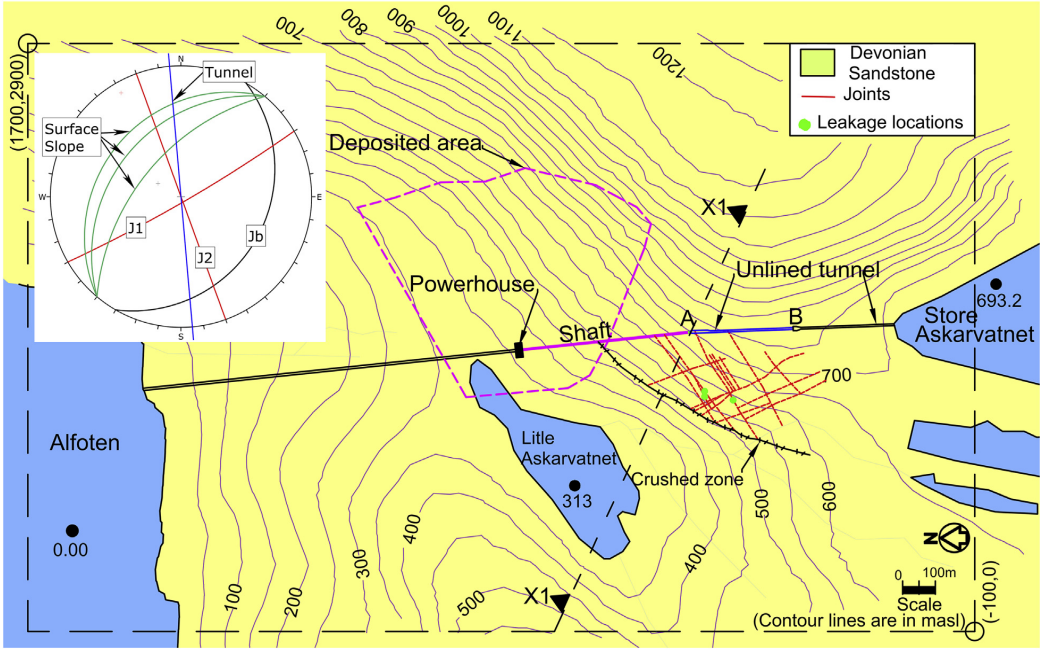

Fig. 10. Askara project area with rock type, crushed zone, joints (stereographic projection), and leakage locations.

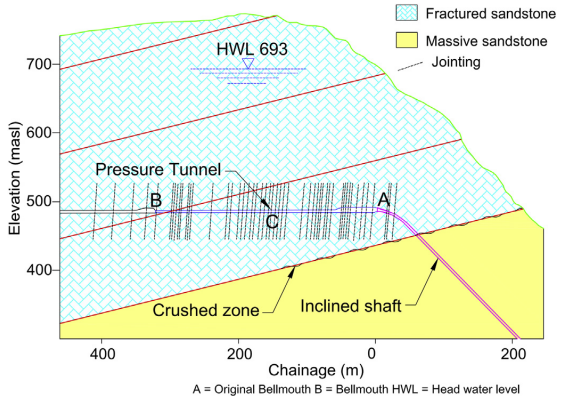

Fig. 11. Section through pressure tunnel of Askara power plant (Redrawn from Bergh-Christensen, 1975).

jointing system, which had 0.5–2 cm-wide opening filled with silt material. The joints were consistently becoming narrower, usually a few millimeter wide, beyond the chainage about 240 m from section *A* towards section *B* (Fig. 11). The narrower joints were filled with clay material. Similarly, another joint set (J2) in the outer part of the mountain was filled with silt and clay material.

4.4. Fossmark project

The waterway system of Fossmark project initially consisted of headrace tunnel, unlined pressure shaft, unlined pressure tunnel and steel-lined penstock tunnel connecting powerhouse located at the surface. The main rock type in the project is granitic gneiss. According to Garshol (1988), the rock mass of the project area consists of two distinct joint sets. The first joint set (J1) represents the zones of weakness and has strike of about NE–SW, dipping 20°–70° towards SE. Another joint set (J2) is striking NS and steeply dipping towards west. In Fig. 12, some of the joints are marked along the shaft and tunnel.

Garshol (1988) described the failure of unlined tunnel and shaft in detail. The failure was encountered both during excavation and test water filling. Water inflow into the tunnel was measured as 0.4 L/(s m) while excavating steel-lined and unlined pressure tunnels. Out of 15 marked joints along the unlined tunnel, nine joints were found out to be filled with silt and clay and the rest were observed without infilling material. The joint aperture is 0–5 cm wide and infilling thickness is from 1 cm to 2 cm. There are also some zones of weakness along the tunnel. Record indicates that two distinct zones of weakness were encountered during excavation of the shaft. The zones of weakness consisted of open joints from where water was lost while drilling. The marked joints and zones of weakness along the tunnel and shaft were considered as potential path for the leakage from unlined pressure shaft and tunnel.

The first test water filling was carried out up to 357 masl and gate was closed, since heavy leakage was noticed in the topography at the level of about 300 masl. After draining the water from the waterway system, inspection was carried out in the pressure tunnel, and it was observed that three joints were hydraulically deformed (failure locations are shown in Fig. 13). The infilling material of two joints was completely washed away and came down to the tunnel. Post injection grouting and shotcreting were carried out as a remedial measure. Thereafter, the second water filling was carried out up to the maximum level of 410 masl. The inspection after water drainage showed that one joint that followed from pressure tunnel to the shaft at 40 m from the shaft bottom was

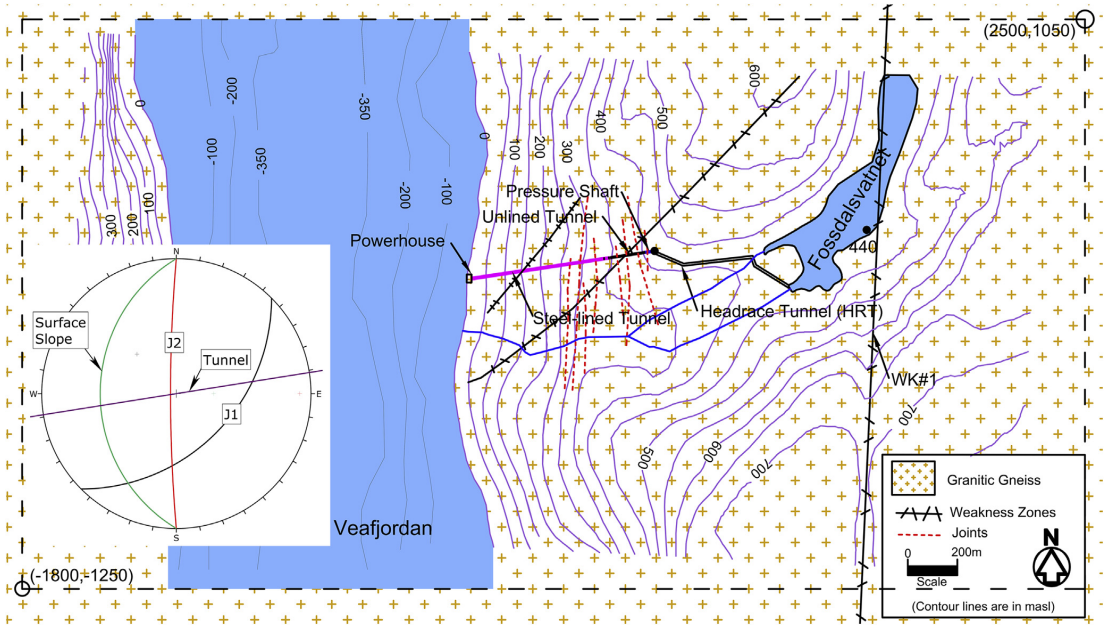

Fig. 12. Fossmark project area with various rock types, zones of weakness, and joints (stereographic projection).

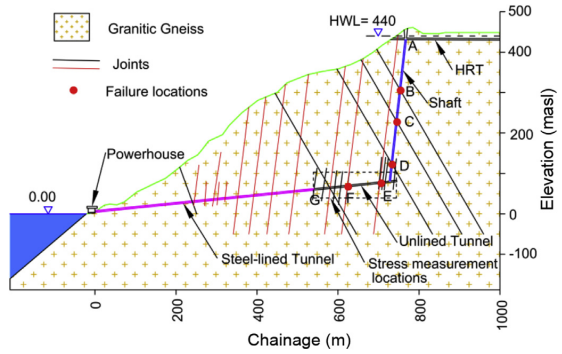

Fig. 13. Section through pressure shaft and tunnel of Fossmark project.

moved by 2–3 mm. In addition, several cubic meter rock fragments fell down at the bottom of the shaft. The inspection in the shaft was also carried out and it was observed that the rock fragments from the zones of weakness fell down. It was concluded that there existed cross communication between the joints in and nearby the shaft area. As a remedial measure, a comprehensive post grouting and shotcrete at the failure location in the shaft were applied.

During the last test water filling, which started with 2.75 m^3/min of water discharge, hydraulic splitting occurred at water level of 368 masl and water level in the shaft decreased even though the filling discharge was increased. The water level became stable at 330 masl with about 10 m^3/min of filling water discharge. At this water level, the overall leakage was estimated to be about 150 L/s (9 m^3/min). It was finally decided to use steel lining in both pressure shaft and tunnel. In order to examine the failure situation in terms of stress, both 3D-overcoring and hydraulic fracturings were employed close to the failure location of the unlined tunnel to find out the in situ stress state (Hanssen, 1997).

4.5. Naddevik project

The Naddevik project, one of the most successful unlined shaft projects, is located in south of Sogn and Fjordane on the west coast of Norway. As shown in Fig. 14, the main rock types of Naddevik area are dark gneiss and granitic gneiss (NGU, 2017). Dark gneiss is the basement rock where powerhouse is located and above which granitic gneiss is overlying.

According to Vik and Tunbridge (1986), a total of four 3D-overcoring and seven hydraulic fracturing stress measurement tests were carried out at this project to finalize the shaft alignment. The stress measurement locations are shown in both plan (Fig. 14) and profile (Fig. 15) of the project. Hydraulic fracturing was used in locations 1, 2 and 3 whereas 3D-overcoring was carried out at locations 2, 3, 4 and 5.

4.6. Nye Tyin project

Nye Tyin project is the highest head unlined tunnel project so far built worldwide. The maximum static head at the unlined tunnel of the project reaches 1047 m. The total length of unlined high pressure tunnel is about 11.5 km (Fig. 15).

The engineering geological aspect of the project area is described in Hydro (1998). The main rock types in the project area are dark gneiss as the basement rock, granitic gneiss, meta-arkose (sandstone), mica schist and phyllite (Fig. 15). According to SINTEF (2002), in situ stresses were measured at six locations along the powerhouse access tunnel, as indicated in Fig. 15 (location 1 starting from chainage 1100 m along access tunnel to location 6 at the penstock cone area). Both hydraulic fracturing (locations 1, 2, 4, 5 and 6) and 3D-overcoring (1, 3 and 6) techniques were applied to obtain the overview of the in situ stress state.

5. Input parameters for numerical analysis

The numerical modeling program FLAC^{3D} (Itasca, 2017a) is used for stress state analysis and UDEC (Itasca, 2017b) is used for fluid

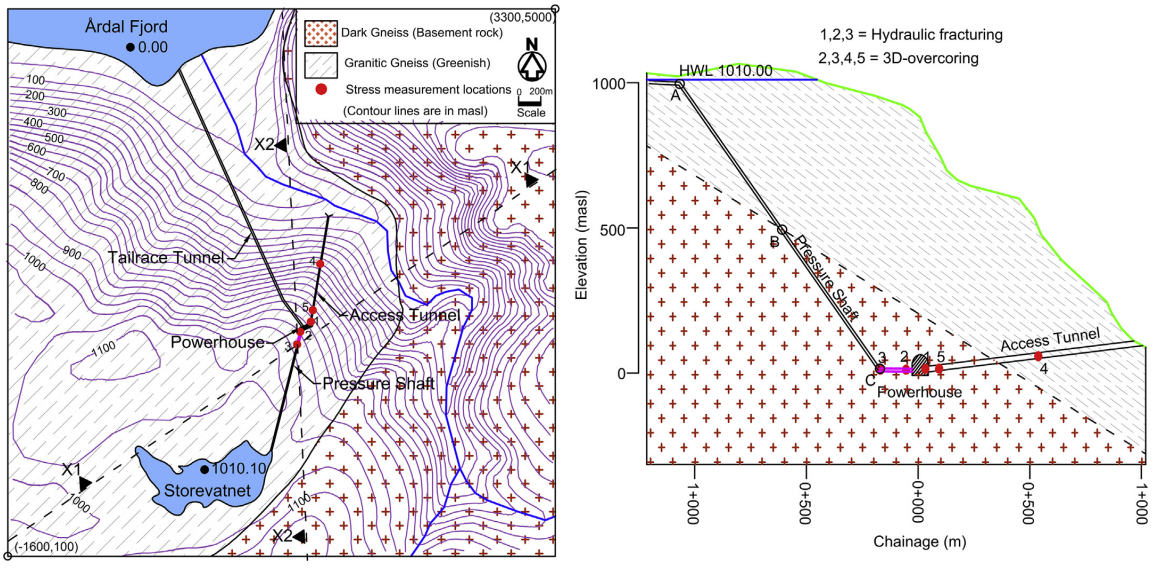

Fig. 14. Plan (left) and profile along the alignment (right) of Naddevik project.

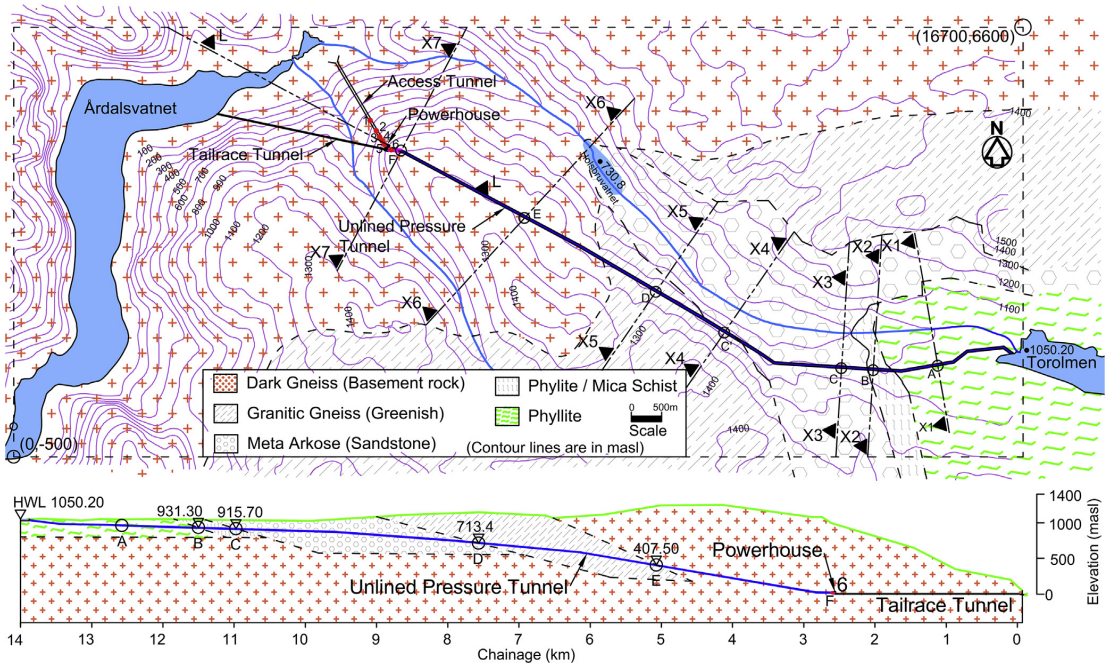

Fig. 15. Plan (upper) and profile (lower) along tunnel alignment of Nye Tyin project with stress measurement locations.

flow analysis in order to assess the occurrence of hydraulic jacking along the pre-existing joints. The input parameters required for the numerical analyses are quantified based on the detailed information collected from each project. The rock mass parameters, joint/interface parameters and in situ stress conditions are the most important input variables, which should be quantified for carrying out the numerical analyses.

5.1. Rock mass parameters

Rock mass parameters are required as input to define the quality of rock mass. Table 3 shows the mean values of rock mass parameters of different rock types. In Table 3, uniaxial compressive strength of intact rock (σ_{ci}), modulus of elasticity of intact rock (E_{ci}), Poisson's ratio (ν) and unit weight of the rock (γ) are the laboratory tested parameters of intact rock samples. Most of the laboratory tested values in Table 3 were collected from SINTEF (1998) excluding for unlined tunnels of Fossmark and Nye Tyin. The rock mass parameters of 'MS_weak' are assumed based on the description of rock mass conditions.

The bulk modulus (K) and shear modulus (G_{ci}) of intact rock in Table 3 are calculated using Eqs. (5) and (6), respectively, following Itasca (2017a):

$$K = \frac{E_{ci}}{3(1-2\nu)} \tag{5}$$

$$G_{ci} = \frac{E_{ci}}{2(1+\nu)} \tag{6}$$

The geological strength index (GSI) values are assumed 25 for zones of weakness and 90 for massive rock formations based on the engineering geological conditions of the particular case project. The disturbance factor (D) is assumed zero for the in situ condition (Hoek et al., 2002) and the material constant (m_i) is chosen from Hoek (2001) for the given rock types. The RocData software is used to estimate the rock mass deformation modulus (E_m). The rock mass shear modulus (G_m) is calculated using Eq. (6) where E_{ci} is replaced by E_m.

5.2. Joints/interface parameters

In the projects such as Byrte, Askara and Fossmark, fault/zones of weakness are modeled as plane of weakness in FLAC^{3D}. The planes are considered as the interface between two different rock formations and/or weakness/fault plane in the same or different rock formations. The joints are modeled in UDEC for fluid flow analysis and interfaces are modeled in FLAC^{3D} for stress state analysis. Joint parameters such as stiffness, aperture and permeability factor are important input parameters to UDEC model for fluid flow analysis and interface parameters such as stiffness and friction angle are important parameters to FLAC^{3D} (Itasca, 2017a, b).

5.2.1. Joint/interface stiffness

The joint stiffness is estimated by using the elastic properties of adjacent rock and rock mass. In this regard, Eqs. (7) and (8) are used to calculate joint normal and shear stiffnesses, respectively, as recommended by Itasca (2017a, b):

$$k_n = \frac{E_{ci}E_m}{s(E_{ci}-E_m)} \tag{7}$$

$$k_s = \frac{G_{ci}G_m}{s(G_{ci}-G_m)} \tag{8}$$

Table 3
Mechanical properties of different rock types of case projects.

Project	Rock type	σ_{ci} (MPa)	E_{ci} (GPa)	ν	G_{ci} (GPa)	K (GPa)	γ (kN/m^3)	GSI	D	m_i	E_m (GPa)	G_m (GPa)
Herlandsfoss	Mica schist[a]	56.1	31.1	0.14	13.6	14.5	27.7	60	0	12	16.2	7.1
	Hornblende schist[a]	80.4	61.2	0.23	24.8	37.9	30.5	75	0	26	49.9	20.3
	MS_Weak	16	20	0.14	8.8	9.3	27.7	25	0	12	1.2	0.5
Byrte	Granitic gneiss[a]	94.9	22.5	0.11	10.2	9.5	26.4	75	0	28	18.4	8.3
	Basalt[a]	186.8	69.5	0.31	26.6	59.7	27.7	75	0	25	56.7	21.7
Askara	Massive sandstone[a]	144.7	30.9	0.26	21.6	12.2	27.1	90	0	17	29.6	11.7
	Fractured sandstone[a]	144.7	30.9	0.26	21.6	12.2	27.1	70	0	15	22.6	9
Fossmark	Granitic gneiss[b]	188.8	43.5	0.13	19.3	19.3	26.4	80	0	32	38.3	17
Naddevik	Dark gneiss[a]	109.3	41.9	0.12	18.7	18.3	28.4					
	Granitic gneiss[a]	94.9	22.5	0.11	10.2	9.5	26.4					
Nye Tyin	Dark gneiss[c]	109.3	41.9	0.12	18.7	18.3	28.4					
	Granitic gneiss[a]	94.9	22.5	0.11	10.2	9.5	26.4					
	Meta arkose[d]	120.4	60.1	0.25	24.1	39.6	26.8					
	Phyllite[a]	40.5	39.8	0.25	15.9	26.3	27.5					

[a] SINTEF (1998).
[b] Hanssen (1997).
[c] SINTEF (2002).
[d] Laboratory tested value by authors.

where k_n is the joint normal stiffness, k_s is the joint shear stiffness, and s is the joint spacing. The stiffnesses of the rock and rock mass are already defined and estimated. Furthermore, Rocscience (2017) mentioned that the stiffnesses of fault or zones of weakness can be estimated from the properties of infilling material and thickness of the zone:

$$k_n = \frac{E_0}{t} \tag{9}$$

$$k_s = \frac{G_0}{t} \tag{10}$$

where E_0 and G_0 are the Young's modulus and shear modulus of infilling material, respectively, and t is the thickness of weakness/fault zone. The shear modulus of infilling material is calculated using Eq. (6) where E_{ci} is replaced by E_0 and ν is replaced by the Poisson's ratio of infilling material (ν_0).

5.2.2. Friction angle

Friction angle of the interface is also an important parameter to be estimated. Usually, it ranges from 15° to 30° in case of fault/zones of weakness (Barton, 1973). Friction angle of 25° is taken as the most likely value in the model.

5.2.3. Joint aperture and joint permeability factor

Itasca (2017b) gave the relationship for flow rate through the joints. The flow through joints depends upon contact hydraulic aperture (a) and joint permeability factor (k_j). The theoretical value of joint permeability factor is calculated by

$$k_j = \frac{1}{12\mu} \tag{11}$$

where μ is the dynamic viscosity of the water, which is equal to 1.306×10^{-3} Pa s at 10 °C (Kestin et al., 1978). The average temperature of water of about 10 °C is assumed for water tunnels of the case projects.

On the other hand, the contact hydraulic aperture is calculated by

$$a = a_0 + u_n \tag{12}$$

where a_0 is the joint aperture at zero normal stress, and u_n is the joint normal displacement (positive denoting opening). In UDEC model, a minimum value of aperture, a_{res}, is assumed for the aperture below which mechanical closure does not affect the contact permeability. Similarly, a maximum value, a_{max}, is also assumed as five times the a_{res}. The values for a_0, a_{res} and a_{max} are estimated based on the detailed joint information given for each project. Table 4 shows the estimated values of different joint/interface parameters.

5.3. Stress

Stress is another key input parameter in order to define the initial and boundary conditions in numerical models. Stress along Z-axis is mainly due to the vertical overburden of the rock mass. Part of the horizontal stress is due to vertical overburden, which is related to the Poisson's ratio.

In FLAC^{3D}, Y-axis is aligned to the north direction. The normal stresses along X- and Y-axis and corresponding shear stresses are calculated by resolving the maximum horizontal stress (σ_{Hmax}) and minimum horizontal stress (σ_{hmin}), as shown in Fig. 16.

The total stresses along Y- and X-axis are calculated by using Eqs. (13) and (14), respectively. Since the maximum horizontal stress makes an angle (θ) with Y-axis, there will be shear stresses in YZ and XZ faces as shown in Fig. 16 (the box shown in the figure has thickness along Z-axis). The shear stresses will have the same magnitude in both faces and are estimated by using Eq. (15). The shear stresses shown in Fig. 16 are negative.

$$\sigma_{yy} = \sigma_{Hmax} \cos^2\theta + \sigma_{hmin} \sin^2\theta \tag{13}$$

$$\sigma_{xx} = \sigma_{Hmax} \sin^2\theta + \sigma_{hmin} \cos^2\theta \tag{14}$$

$$\sigma_{xy} = \sigma_{yx} = \frac{\sigma_{Hmax} - \sigma_{hmin}}{2} \sin(2\theta) \tag{15}$$

Since there was no stress measurement in Herlandsfoss, Byrte and Askara projects, measured stress data from nearby locations (as shown in Fig. 2) are taken as the reference values. The principal horizontal stresses at the measured locations are resolved along X- and Y-axis. Then the horizontal stress due to vertical overburden is subtracted from each resolved stress, which gives the stress due to tectonics along X- and Y-axis, respectively. These tectonic stresses along X- and Y-axis are transferred to initialize the horizontal stresses in 3D model of each project area. On the other hand, the

Table 4
Input parameters for joints and interfaces.

Project	Joints/zone of weakness	E_{ci} (GPa)	G_{ci} (GPa)	E_m (GPa)	G_m (GPa)	E_0 (GPa)	ν_0	G_0 (GPa)	s or t (m)	k_n (GPa)	k_s (GPa)	a_0 (mm)	a_{res} (mm)	Remarks
Herlandsfoss	Jf	20	8.8	1.2	0.5				5.6	0.23	0.095	1	0.5	Joint
	2	20	8.8	1.2	0.5				11.2	0.11	0.047	3	1	Joint
	3	20	8.8	1.2	0.5				11.2	0.11	0.047	3	1	Joint
	4	20	8.8	1.2	0.5				11.2	0.11	0.047	3	1	Joint
	5	61.2	24.8	49.9	20.3				18.1	15	6.2	0.1	0.05	Joint
	6	61.2	24.8	49.9	20.3				18.1	15	6.2	0.1	0.05	Joint
Byrte	Joint#a1	22.5	10.2	18.4	8.3				30	3.4	1.5	3	1	Joint
	Joint#a2	22.5	10.2	18.4	8.3				20	5	2.2	3	1	Joint
	Joint#a3	22.5	10.2	18.4	8.3				10	10	4.5	3	1	Joint
	Joint#b	22.5	10.2	18.4	8.3				35	2.9	1.3	10	5	Joint
	WK#1					0.4	0.1	0.2	3	0.13	0.061	10	5	Zone of weakness
	WK#2					0.4	0.1	0.2	3	0.13	0.061			Zone of weakness
	Byrte_Fault					0.4	0.1	0.2	20	0.02	0.0091	3	1	Fault
Askara	Jb	30.9	12.2	22.6	9				100	0.85	0.34	5	1	Sliding zone/Joint
	J1	30.9	12.2	22.6	9				10	8.5	3.4	5	1	Joint
Fossmark	WK#1					0.4	0.1	0.2	20	0.04	0.018			Zone of weakness
	J1					0.4	0.1	0.2	0.5	0.8	0.36	5	1	Joints/zones of weakness
	J2	43.5	19.3	38.3	17				20	16	7.1	5	1	Joint

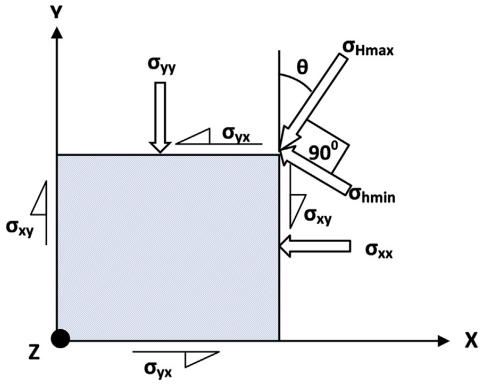

Fig. 16. Resolving horizontal stresses in X and Y directions.

shear stresses remain unchanged. The input stresses to FLAC^{3D} model of three projects are shown in Table 5.

For other three projects, i.e. Fossmark, Naddevik and Nye Tyin, the magnitude and orientation of maximum and minimum horizontal stresses are iterated in FLAC^{3D} to match the principal stresses measured by 3D-overcoring technique at respective locations. The orientation of maximum horizontal stress is also compared with the regional tectonic stress regime. In addition, the minor principal stress measured by hydraulic fracturing is also compared with the model result. The measured stress values, which are used for validation purpose, are given in Table 6.

6. Numerical analysis

As explained earlier, the minor principal stress is the key parameter for the design of unlined pressure shafts and tunnels. FLAC^{3D} model is used to analyze the stress state (especially the minor principal stress) for all six projects, i.e. Herlandsfoss, Byrte, Askara, Fossmark, Naddevik and Nye Tyin. In addition, hydraulic jacking and leakage assessment on the failed cases of pressure tunnels and shafts of Herlandsfoss, Byrte, Askara and Fossmark projects are carried out using UDEC model.

6.1. Stress state analysis

The stress state analysis is carried out in order to quantify the minor principal stress at the location of unlined shaft and tunnel. In FLAC^{3D}, a 3D geometry of the selected area for each project is created incorporating the surface topography, as shown in Fig. 17. After the geometry is defined, 3D tetrahedral volume grids of different sizes are created. The sizes of the grids are finer nearby the location of tunnel and shaft. In addition to the 3D geometry and grids, the model is supplemented with the defined interfaces in Byrte, Askara and Fossmark projects according to Figs. 8, 10 and 12, respectively. The mechanical properties of each rock type (Table 3) are assigned in the model. The mechanical properties of interfaces (Table 4) are also assigned in the model for Byrte, Askora and Fossmark projects where hydraulic jacking occurs. First, the model is run to initialize the gravity-induced vertical and horizontal stresses. Once the model is converged to the equilibrium within prescribed limit of unbalanced force, the total stresses including tectonic stresses are initialized and the model has been run once again until the second equilibrium state is reached. After that, the model is considered to be ready for in situ stress evaluation.

In Herlandsfoss project, the failed location having highly schistose mica schist band near the boundary with hornblende schist is considered to be very weak rock mass (MS_Weak), as indicated in Fig. 17a. Fig. 18 shows the minor principal stress along the tunnel alignment at Herlandsfoss project. As seen in Fig. 18, there is de-stressing in the in MS_Weak zone in comparison to the pressure tunnel area consisting of relatively good quality mica schist (MS) and hornblende schist (HS). Fig. 18b shows the influence of stiffness of weak mica schist (MS-Weak), which indicates that the lower the stiffness of the rock material is, the higher the de-stressing will be.

In Byrte project, the zones of weakness are also modeled as interfaces (Fig. 17b). The influence of zones of weakness on the stress state is clearly seen in Fig. 19a. An analysis is carried out to see whether failure is initiated at point C (Fig. 19) once the maximum water level reaches about 725 masl with the hydrostatic head of 195 m. Since a hydraulic jacking occurs at point C, it is logical to assume that the minor principal stress at this point is close to the hydrostatic pressure created by the maximum water level of 725 masl. It is observed in FLAC^{3D} model that the stress state at the rock mass 'G_Gneiss2' seems sensitive to the change in stiffness of the zones of weakness and the Byrte fault. Hence, the elastic modulus (E_0) of the rock material in the zone of weakness (the

Table 5
Calculation of input stresses to FLAC^{3D} model.

Project	γ (kN/m^3)	ν	Stress measurement					Input stresses (only tectonic) (MPa)		
			Location	h (m)	σ_{Hmax} (MPa)	σ_{Hmin} (MPa)	σ_{Hmax} direction (°)	σ_{xx}	σ_{yy}	σ_{xy}
Herlandsfoss	29.1	0.2	L-1	75	7	3	N35°E	3.8	5.1	1.88
Byrte	26.4	0.11	L-2	400	22.7	5.5	N90°E	21.4	4.2	0
Askora	27.1	0.26	L-3	20	17	10	N90°E	16.8	9.8	0

Table 6
Measured stresses at different locations of Fossmark, Naddevik and Nye Tyin projects.

Project	Location	h (m)	Major principal stress, σ_1			Intermediate principal stress, σ_2			Minor principal stress, σ_3			Remarks
			Mean (MPa)	SD (MPa)	Trend (°)/Plunge (°)	Mean (MPa)	SD (MPa)	Trend (°)/Plunge (°)	Mean (MPa)	SD (MPa)	Trend (°)/Plunge (°)	
Fossmark[a]	Unlined	275	7.1	3.4	350/35	5.5	1.5	198/52	0.6	4.4	089/13	OC
	tunnel	275							2.7	0.8		HF
Naddevik[b]	1	880							18			HF
	2	900	26.3		282/52	18.9		140/45	12.4		032/25	OC
	2	900							12.7			HF
	3	930	25		076/40	19.6		232/60	16.8		340/22	OC
	3	930							14.2			HF
	4	450	16.1		180/55	12.3		280/18	4.9		027/50	OC
	5	750	20.9		304/65	14.6		144/30	12.2		047/15	OC
Nye Tyin[c]	1	700	15.2	1.88	031/26	9.2	1	292/17	5.2	2	173/58	OC
	1								11.2	1.7		HS
	2								17.1	3.7		HS
	3	950	31.2	2.1	349/03	25.8	2.7	087/66	19.9	1.5	258/24	OC
	4								12.4	2.2		HS
	5								17	6.6		HS
	6	1000	49.5	4.6	013/13	21.1	2.1	262/58	15.9	4.4	110/29	OC
	6								26	4.1		HS

OC = 3D-overcoring; HF = Hydraulic fracturing; HS = Hydraulic splitting; SD = Standard deviation.
[a] Hanssen (1997).
[b] Vik and Tunbridge (1986).
[c] SINTEF (2002).

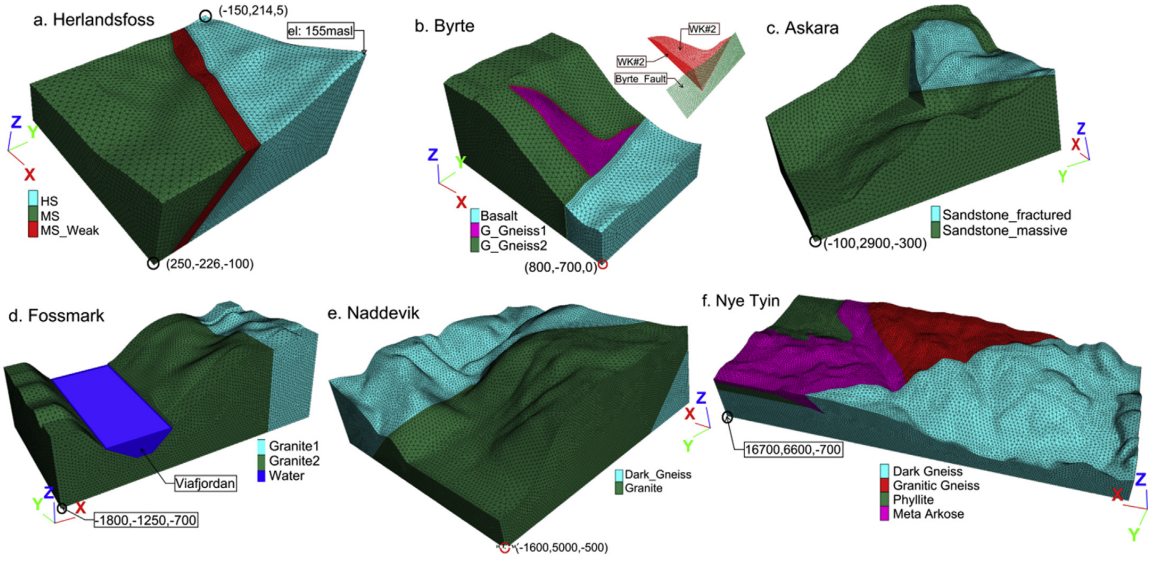

Fig. 17. 3D geometry of different project areas (HS: Hornblende schist; MS: Mica schist; G_Gneiss1 & G_Gneiss2: Granitic gneiss).

same is assumed for both WK#1 and WK#2 and for Byrte fault) is varied between 0.2 GPa and 1 GPa to assess the sensitivity and the corresponding minor principal stress at point C is identified (Fig. 19b). As seen in the figure, the minor principal stress becomes equal to the water pressure at point C with E_0 value of about 0.4 GPa. Hence, this value of E_0 is used to evaluate the final stress state along Byrte pressure shaft and tunnel system (Fig. 19c).

In Askora project, the surface topography has slopes in both north and west directions at the location of unlined tunnel. In addition to the rock mass, the crushed zone is also modeled in

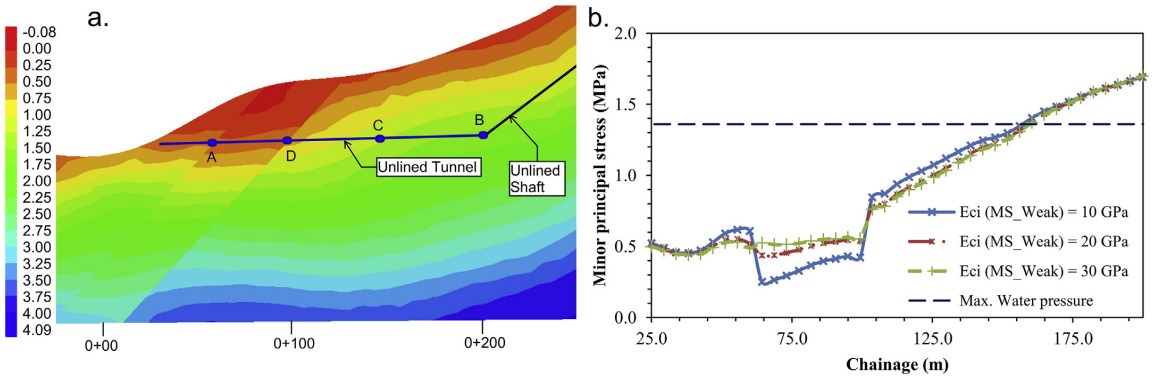

Fig. 18. (a) Minor principal stress (MPa) along the tunnel alignment (E_{ci} of MS_Weak is 20 GPa); (b) Minor principal stress at different E_{ci} values in Herlandsfoss project.

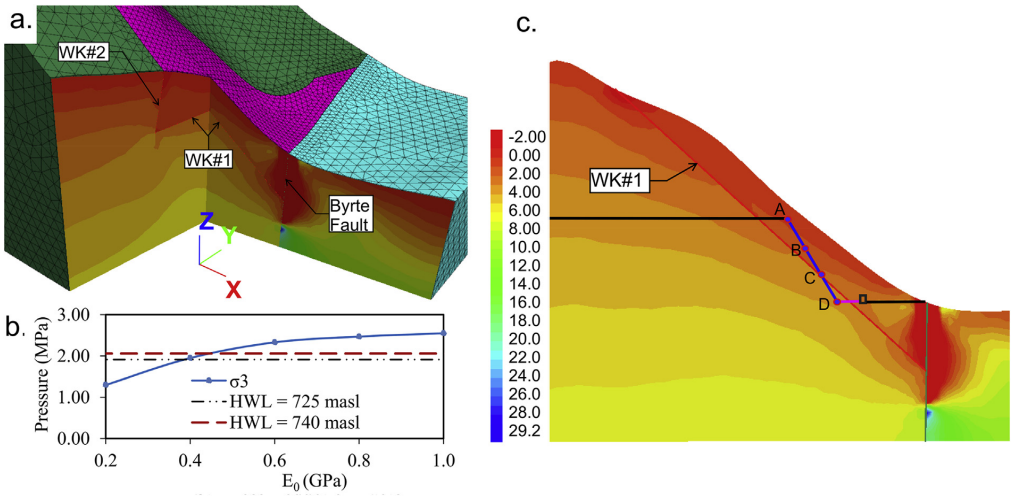

Fig. 19. (a) Influence of zones of weakness on stress state; (b) Minor principal stress at point *C* at different values of E_0; (c) Minor principal stress (MPa) along tunnel and shaft alignment of Byrte project.

FLAC^{3D} (Fig. 17c). The influences of both the slopes and the crushed zone on the stress state of the area are shown in Fig. 20a and b, respectively. The magnitude of the minor principal stress along the tunnel and shaft alignment shown in Fig. 20b is further used for the evaluation of stress requirement for the unlined tunnel at locations *A*, *B* and *C*.

In case of Fossmark project, the stiffness of the zone of weakness is assumed, as indicated in Table 4. The magnitude and orientation of the maximum and minimum horizontal stresses are assumed based on the stress regime of nearby area and the model is run for each stress input in order to match the measured stress. It is found that the maximum horizontal stress of about 9 MPa (only tectonic stress) with orientation of about N15°E and the minimum horizontal stress of about 5 MPa (only tectonic) gives good match with the measured stress at Fossmark project (Table 6).

Fig. 21 shows the magnitude of the minor principal stress along the shaft and tunnel alignment of Fossmark project. The model is run for two different conditions. At first, the model is run with the zone of weakness and the corresponding stresses are converged to measured stresses. The minor principal stress indicated in Fig. 21a is accounted as the final result for the analysis of stress state along the shaft and tunnel alignment of Fossmark project. The model is once again run without incorporating zone of weakness (Fig. 21b) to observe the influence of the zone of weakness on the stress regime. Fig. 21a and b clearly indicates that there is a considerable influence of zone of weakness on the stress state.

In Naddevik project, the 3D stresses measured at different locations are used to compare the result from FLAC^{3D}. The locations 2 and 3 are chosen to be decisive for the comparison, because there is less influence by the valley slope on the stress development since they are located in the innermost locations from the slope topography. In FLAC^{3D}, magnitude of the principal stresses at these locations is converged to the corresponding measured values when the maximum horizontal stress (only tectonic) of 21 MPa is applied along N125°E. The corresponding minimum horizontal stress is 13 MPa. The model is then considered to be ready for the final stress

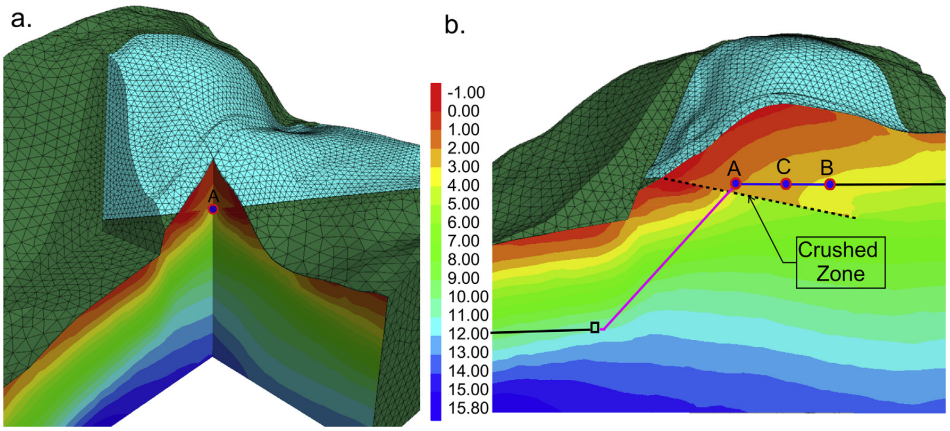

Fig. 20. (a) 3D influence of valley side slopes and sliding zone on stress state; (b) Minor principal stress (MPa) along tunnel and shaft alignment of Askora project.

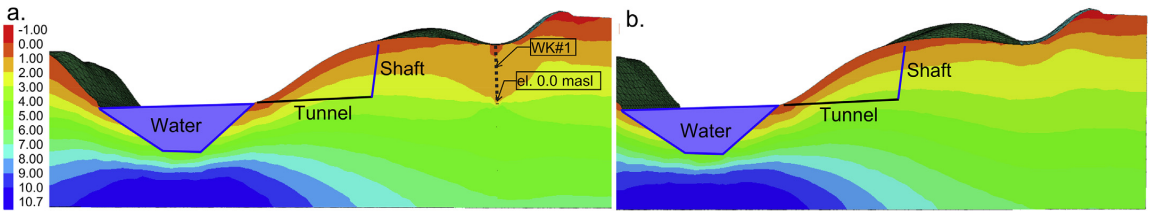

Fig. 21. Minor principal stress (MPa) along tunnel and shaft alignment of Fossmark project (a) with zone of weakness and (b) without zone of weakness.

state evaluation. Fig. 22a shows the final result of magnitude of the minor principal stress along the alignment of Naddevik project, and Fig. 22b shows the comparison between the model result and the minor principal stress measured at different locations.

In Nye Tyin project, the result obtained from FLAC^{3D} is compared with the measured stress magnitudes at different locations, and location 3 is found to be representative with respect to the orientation of the maximum horizontal stress as explained by Fejerskov et al. (2000). Fig. 23a shows the final result of magnitude of the minor principal stress along the tunnel alignment of Nye Tyin project. Fig. 23b shows the comparison between the minor principal stress obtained from the model and measured at different locations.

6.2. Fluid flow analysis

The fluid flow analysis through the joints is carried out in order to evaluate the possibility of hydraulic jacking and leakage. In this regard, 2D geometries along the pressure tunnel/shaft alignment of Herlandsfoss, Byrte, Askara and Fossmark are created in UDEC program and the coordinates of the geometries are in accordance with Figs. 7, 9, 11 and 13, respectively. The rock mass and representative joint systems are also modeled in the geometry (Fig. 24). The assigned properties of rock mass and joints shown in Tables 3 and 4, respectively, are used as input variables. The boundary stress along *X*-axis is assigned based on the values from FLAC^{3D}, whereas the stress along *Y*-axis is generated by gravity itself and the bottom

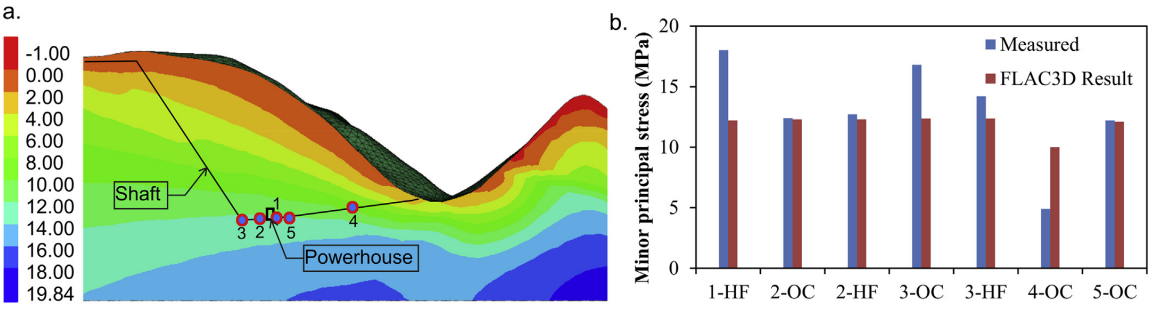

Fig. 22. (a) Minor principal stress (MPa) along shaft alignment, and (b) Comparison between measured values and FLAC^{3D} result at stress measurement locations of Naddevik project.

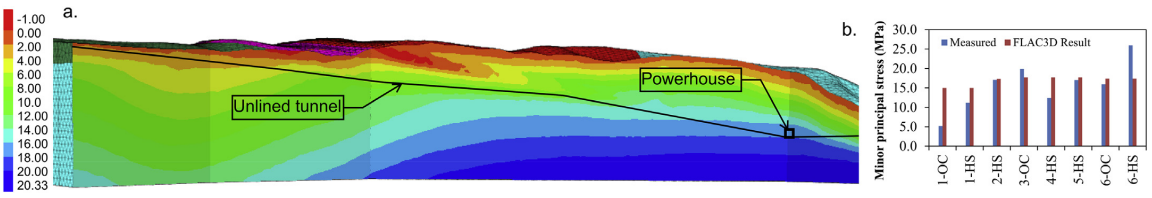

Fig. 23. (a) Minor principal stress (MPa) along tunnel alignment, and (b) Comparison between measured values and FLAC^{3D} result at stress measurement locations of Nye Tyin project.

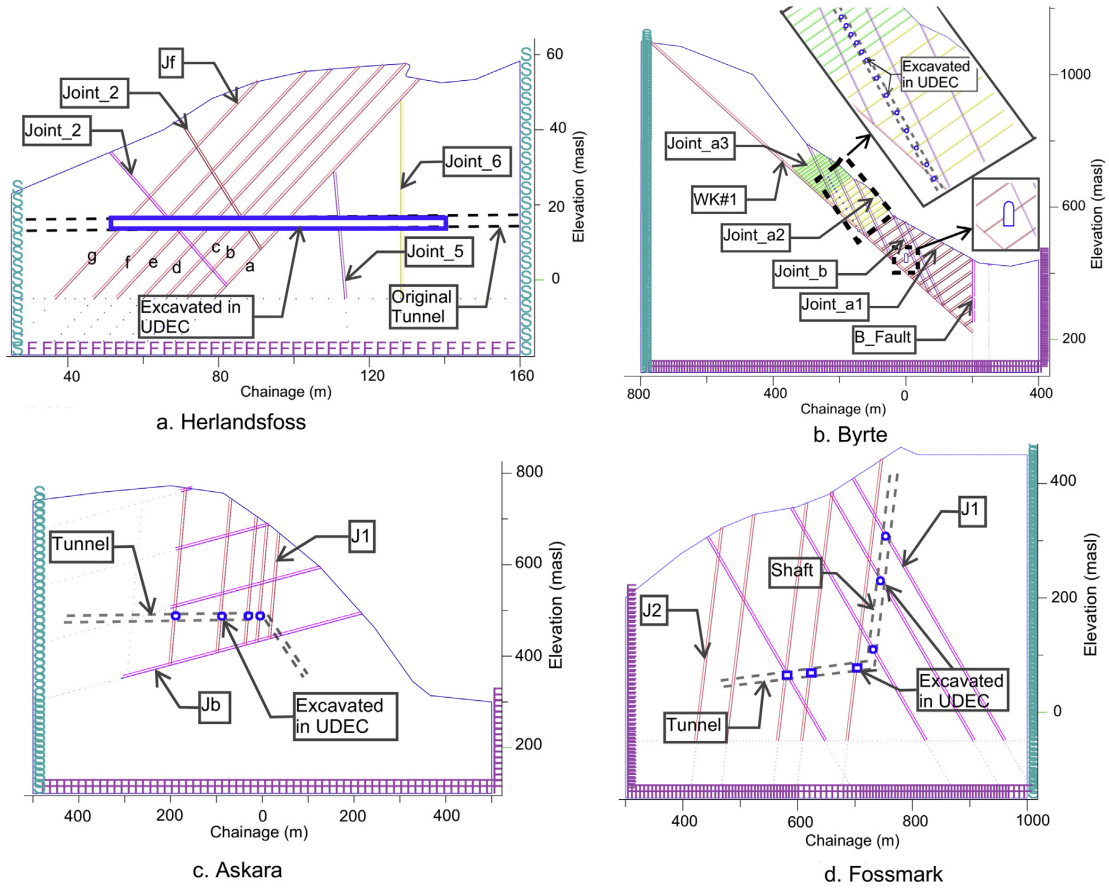

Fig. 24. 2D geometry in UDEC with rock types and representative joints of the selected projects.

of the model is fixed against displacement. All the boundaries except the top are made impermeable against fluid flow. The model is run for incompressible fluid flow through the joints.

The UDEC model is run until it comes to the mechanical equilibrium after the geometry has been created and boundary conditions have been applied. The tunnel/shaft is excavated at the selected locations only as shown in Fig. 24. The excavation locations are selected keeping in mind that all the representative joints along the alignment can be assigned with designed water flow without violating the model equilibrium. If the whole tunnel/shaft is excavated in UDEC, it is difficult to generate the required amount of fluid pressure especially in case of inclined or vertical alignment. Fluid flow at the excavated locations (Fig. 24) is then assigned and the maximum pressure is limited to the maximum hydrostatic head at the respective locations. The model is once again run until the total fluid flow time is reached. Domain pore pressure developed after the end of total fluid flow time is shown in Fig. 25. Furthermore, as shown in Fig. 25, different locations are selected to track the pore pressure built-up along the joints. The locations are chosen nearby the tunnel/shaft and at the surface topography in order to assess potential hydraulic jacking and their potential leakage.

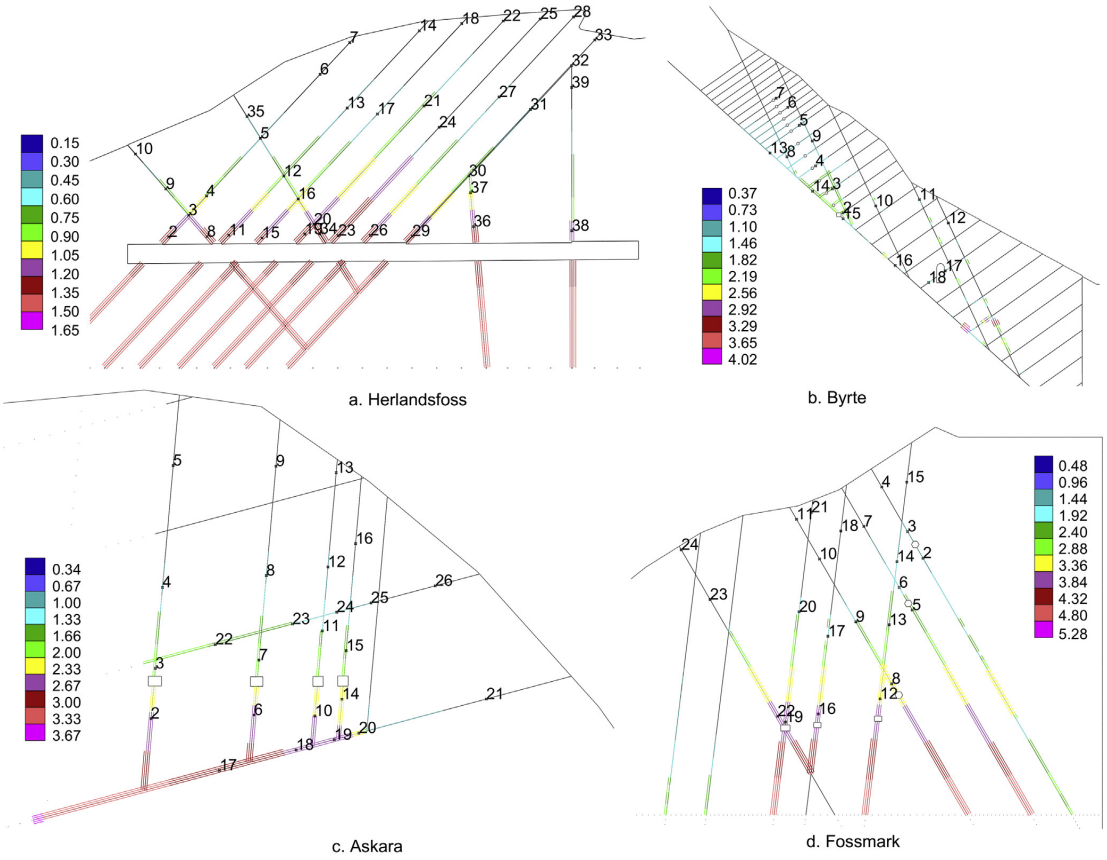

Fig. 25. Domain pore pressure (MPa) and tracking locations.

7. Analysis results

In the following, the results of the analysis are summarized. The results include assessment on the overall engineering geological conditions of the failed cases, the minor principal stress state at different locations of unlined tunnels and shafts, and assessment of hydraulic jacking and leakage through the pre-existing joints.

7.1. Engineering geological assessment

Engineering geological assessment and comparison of the failed cases are made based on geological formations, rock types, jointing conditions, faulting, severity of leakage and failure condition experienced by each case. Even though all seven failure cases, which experienced partial collapse after first water filling, are situated in different geological formations, there exists commonness regarding jointing conditions. The geological formations, rock types, jointing and infilling conditions, and nearby faults are highlighted in Table 7.

As seen in Table 7, all the cases have two major joint sets with one of the joint set steeply dipping and unfavorably orientated. In addition, the joints are filled with silt and clay mineral coating, which could be washed away. Open and permeable joints formed leakage paths, making it easy for the pressure built-up, and increased hydraulic jacking potential. The nearby faults facilitate this process further. Therefore, the real challenge for the successful unlined pressure tunnels and shafts is to avoid potential hydraulic jacking, which leads to excessive leakage and potential tunnel collapse.

7.2. Minor principal stress

The minor principal stresses obtained from FLAC^{3D} model at different locations of all selected projects are shown in Fig. 26. The factor of safety (FoS_3) is calculated by dividing the minor principal stress by water pressure (Fig. 26). FoS_3 is more than one in most of the locations except the locations Hf-A, Hf-D, Br-C, As-A, Fo-B, Fo-C, Fo-D, Fo-E, Fo-F and Fo-G. The figure also shows the factors of safety calculated using Norwegian design criterion discussed previously (FoS_1 and FoS_2). In general, there is an agreement between different factors of safety in terms of whether they are more or less than one excluding Hf-C and Br-D where FoS_1 and FoS_2 are less than one and FoS_3 is more than one. It is highlighted here that no failure is experienced in these locations. In the locations such as As-A, Fo-B, Fo-C, Fo-D, Fo-E and Fo-F (except Fo-G), the results of FoS_3 agree with the actual incident that had occurred during test water filling and initial phase of the project operation.

In the locations such as Br-A and Br-B, the calculated factor of safety using all three approaches is higher than one. However, this does not agree with the actual conditions because failure occurred

Table 7
Summary of the geology, rock types, jointing, joint filling conditions, faulting, leakage and failure description.

Project	Geology and rock types	Jointing	Joint infilling	Fault and zones of weakness	Leakage (L/s)	Specific leakage (L/(min m))	Failure condition
Herlandsfoss	Cambro Silurian hornblende schist and mica schist	Two joint sets: intersecting joints consisting foliation joint and cross joints	Mica schist is highly schistose and rich in chlorite and muscovite at the failure location	Failure occurred through the band of highly schistose rock mass representing a zone of weakness	300	419	Hydraulic jacking and lifting of rock mass occurred
Skar	Precambrian granitic gneiss	Foliation joints and random joints in all directions	Schistosity formation along the foliation joint and occasional hornblende mineral coating	No nearby fault exists	100	10	Hydraulic jacking occurred
Svelgen	Devonian sandstone	Gently dipping bedding joints and cross joints dipping almost perpendicular to the tunnel alignment intersect	Altered joints either open or filled with silt and clay	No nearby fault exists	70	3	Minor leakage and no hydraulic splitting
Byrte	Precambrian granitic gneiss	Several systems of joints with some steeply dipping joints	Joints are silt and clay filled	Long persisting clay filled zone of weakness almost parallel to the valley side slope. Byrte fault is located at about 200 m downstream from powerhouse	1000	194	Hydraulic jacking occurred through zone of weakness and movement of rock mass outside of the zones of weakness
Askara	Devonian sandstone	Two distinct joint sets consisting of foliation and steeply dipping cross joints	Cross joints have opening of 5–20 mm and are filled with silt and clay	A crushed zone separates fractured rock mass with massive one	1000	185	Hydraulic jacking occurred and a joint at the end of unlined tunnel was opened by about 3–4 cm and extended up to the ground surface
Bjerka	Cambro-Silurian granitic gneiss	Two joint sets: widely spaced foliation joints and steeply dipping cross joints	The cross joints that are perpendicular to the tunnel alignment have 1–10 mm opening and filled with silt and clay	No fault zone	1200	900	Hydraulic jacking occurred in a joint that opened approximately 2 cm in walls and 5.3 cm in the floor at the end of unlined tunnel
Fossmark	Precambrian granitic gneiss	Two distinct joint sets: Steeply dipping joint set striking parallel to valley side and other joint set representing the zones of weakness	Some joints along pressure tunnel are filled with silt and clay and some are without filling. The joints have opening from 0 to 5 cm and infilling from 1 cm to 2 cm	Zones of weakness in shaft and tunnel area dipping towards the mountain. A distinct zone of weakness is found across the reservoir lake striking parallel to the fjord valley	150	12	Hydraulic jacking occurred in three joints along the pressure tunnel. The infilling of two joints was completely washed away into the tunnel. Rock mass failed in two zones of weakness in the shaft

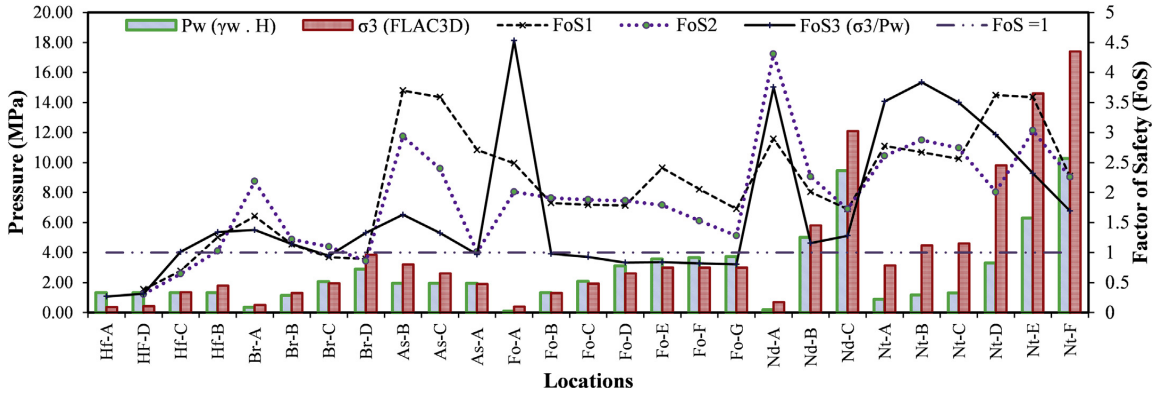

Fig. 26. Minor principal stress (σ_3) from FLAC^{3D} model, water pressure (P_w), and factor of safety at different locations of the projects.

in these locations during test water filling. The reason behind the failure may have been attributed to the situation that the failure initiated from the lower part of shaft, which initiated deformation along the joints that are subparallel to the shaft alignment and extended to the surface. Further, the fluid flow analysis would be helpful to assess hydraulic jacking and leakage in such condition. On the other hand, the minor principal stresses along the unlined shaft and tunnel of Naddevik and Nye Tyin projects satisfy the required factor of safety.

7.3. Hydraulic jacking and leakage assessment

An assessment of occurrence of hydraulic jacking and leakage is carried out in all four projects (Herlandsfoss, Byrte, Askara and Fossmark). Fig. 27 shows the pore pressure built-up at different locations of Herlandsfoss project over the specified fluid flow time in the UDEC at different joints (joints a, c, e, g, 2, 4, 5 and 6). There is rise in the pressure built-up at the beginning of fluid flow time in all the locations. After a while, the pressure reached to the maximum hydrostatic head in the locations nearby tunnel (locations 2, 8, 15, 23, 26, 29 and 34) and remained constant until the total flow time. However, in most of the other locations, the pressure drops when it reaches the corresponding hydrostatic head or sometimes even before. This condition shows the sign of hydraulic jacking of joints at these locations. More interestingly, there is pressure built-up and eventually hydraulic jacking in the locations nearby the surface topography, which indicates the possibility of leakage through the joints all the way to the surface.

In Byrte project, there is pressure built-up in almost all the locations (Fig. 28). The pressure starts to rise after certain fluid flow time and reaches its maximum in the locations nearby the shaft (locations 2, 3, 4, 5, 6 and 7) and indication of hydraulic jacking can be seen in locations 2, 3, 5 and 6. The pressure starts to rise up in the location nearby the powerhouse (location 18) along joint a1. This pressure built-up and hydraulic jacking at location 18 clearly indicate water leakage into the powerhouse cavern experienced during operation. Similarly, the locations along joint b also experienced pressure built-up and hydraulic jacking. The pressure built-up at locations nearby the surface topography (locations 11 and 12) clearly indicates the possibility for water leakage at surface. There is also pressure built-up and hydraulic jacking at locations along the zone of weakness (locations 13, 14, 15 and 16), as indicated in Fig. 28d.

Fig. 29 shows the domain pressure at different locations of Askara project. There is pressure built-up in almost all the locations except locations 5, 9 and 13 that are located well above the

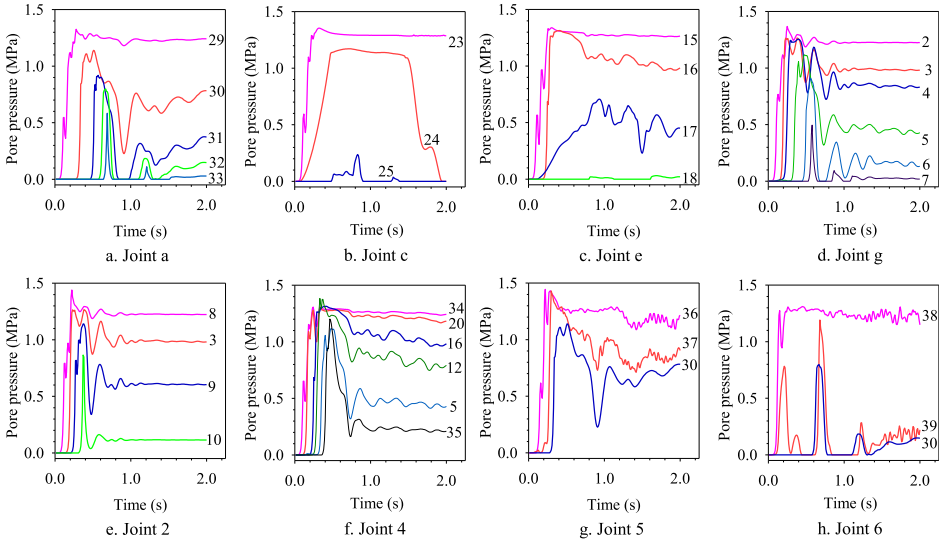

Fig. 27. Domain pore pressure vs. fluid flow time along different joints of Herlandsfoss project.

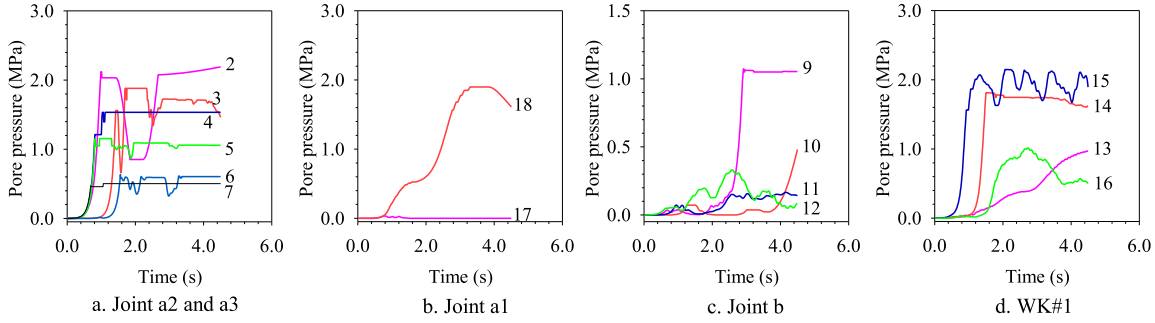

Fig. 28. Domain pore pressure vs. fluid flow time along different joints of Byrte project.

maximum water level. The hydraulic jacking observed in locations 16, 21 and 26 clearly indicates the leakage through the corresponding joints. Fig. 29 also shows that the hydraulic jacking occurs in locations 11, 12, 18, 19, 20, 23, 24 and 25. However, the extent of jacking is different from location to location.

In Fossmark project, the locations are chosen along both joints J1 and J2. There is pressure built-up in almost all the locations considered (Fig. 30). The pressure increases after the certain fluid flow time in all the locations and eventually reaches its maximum in the locations nearby shaft and tunnel. There is clear indication of hydraulic jacking at location 7, which is near the surface topography. The pressure vs. flow time diagram does not clearly indicate the hydraulic jacking of joints at the locations nearby shaft and tunnel. However, the pressure built-up at these locations confirms that the fluid flows through the pre-existing permeable joints.

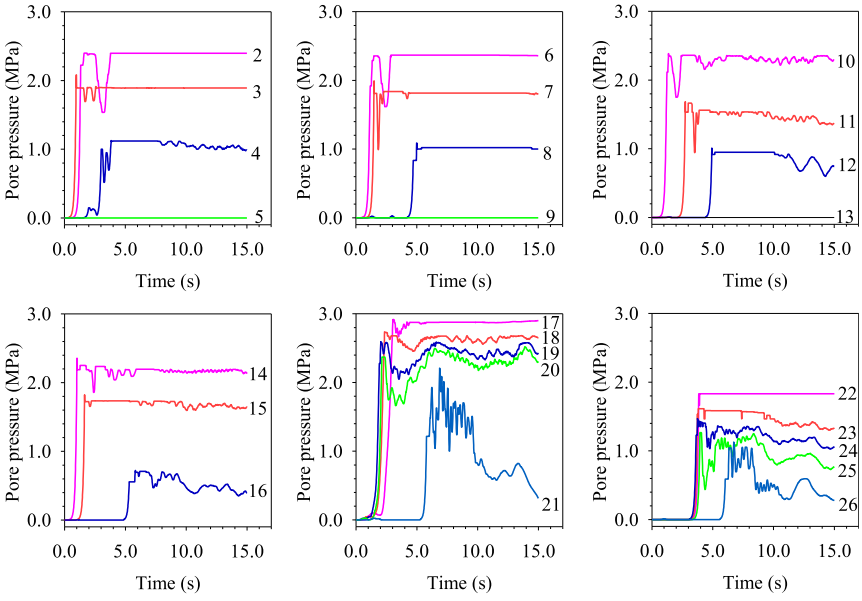

Fig. 29. Domain pore pressure vs. fluid flow time at different locations of Askara project.

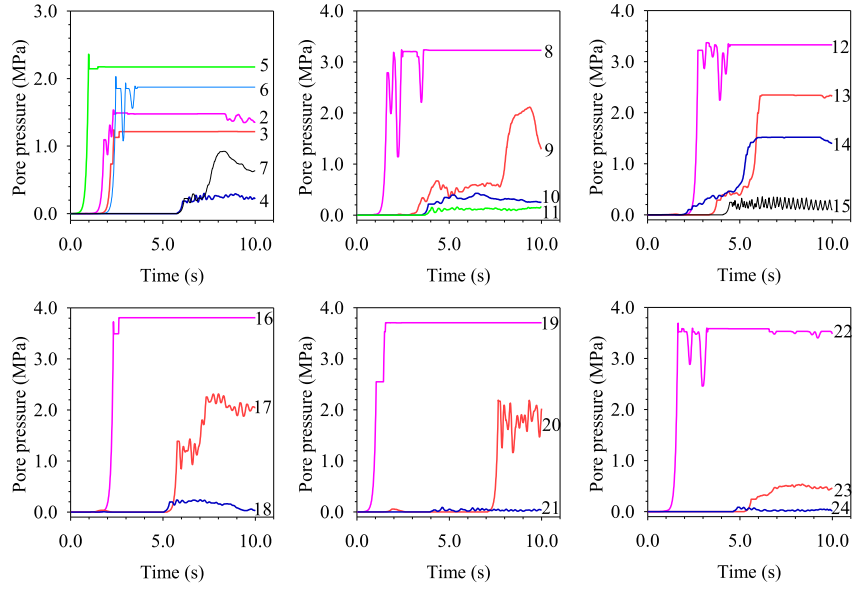

Fig. 30. Domain pore pressure vs. fluid flow time at different locations of Fossmark project.

8. Discussions

This section compares and highlights the reasons for the failure cases and the cases with success in the use of unlined pressure shafts and tunnels. The comparison is mainly made with the main focus on the engineering geological conditions of the cases, in situ stress state, fluid flow and groundwater conditions. These reasons will be the basis to enrich and develop the concept of favorable and unfavorable ground conditions for the applicability of the Norwegian confinement criteria in order to locate unlined pressure shafts and tunnels under constant hydrostatic head.

8.1. The cases of failure

It is highlighted here that at Herlandsfoss project, hornblende schist has very tight foliation joints almost parallel to the valley slope and consists of very few cross joints. The condition was favorable for unlined shaft and tunnel and there was no leakage occurring even though the maximum static water head is far above the potential groundwater table (GWT), as shown in Fig. 31a. On the other hand, excessive water leakage occurred in the outer part of horizontal high-pressure tunnel passing through weak mica schist. This is mainly due to the fact that the highly schistose foliation joints and prevailing cross joints were easy for the water at high pressure to make them open by hydraulic jacking. The joints along this stretch of pressure tunnel were filled with silt and clay and were easy for hydraulic jacking to occur. Further, the stress situation in hornblende schist at the tunnel level is relatively favorable because the location is at the level of valley bottom and the rock mass is strong enough to store the stress without failure. Opposite is the case with weak mica schist, since it is exposed more towards the valley side and hence stress anisotropy is more pronounced and de-stressing in Fig. 31a is very logical. Hence, the main causes for the failure in this case were relatively low rock cover (overburden) and weak and highly schistose rock mass.

In Byrte project, GWT is influenced by steep topography and major zone of weakness that almost follows the topographic slope (Fig. 31b). It is obvious that the hydraulic jacking and leakage occur at this inclined unlined pressure shaft since the de-stressing in the rock mass lying above pre-existing zone of weakness and GWT shall follow the zone, which is almost parallel to the topography and is at the near proximity of the surface. The major causes of the failure at this project were steep topography, presence of weakness and fault zones, and unfavorable jointing conditions.

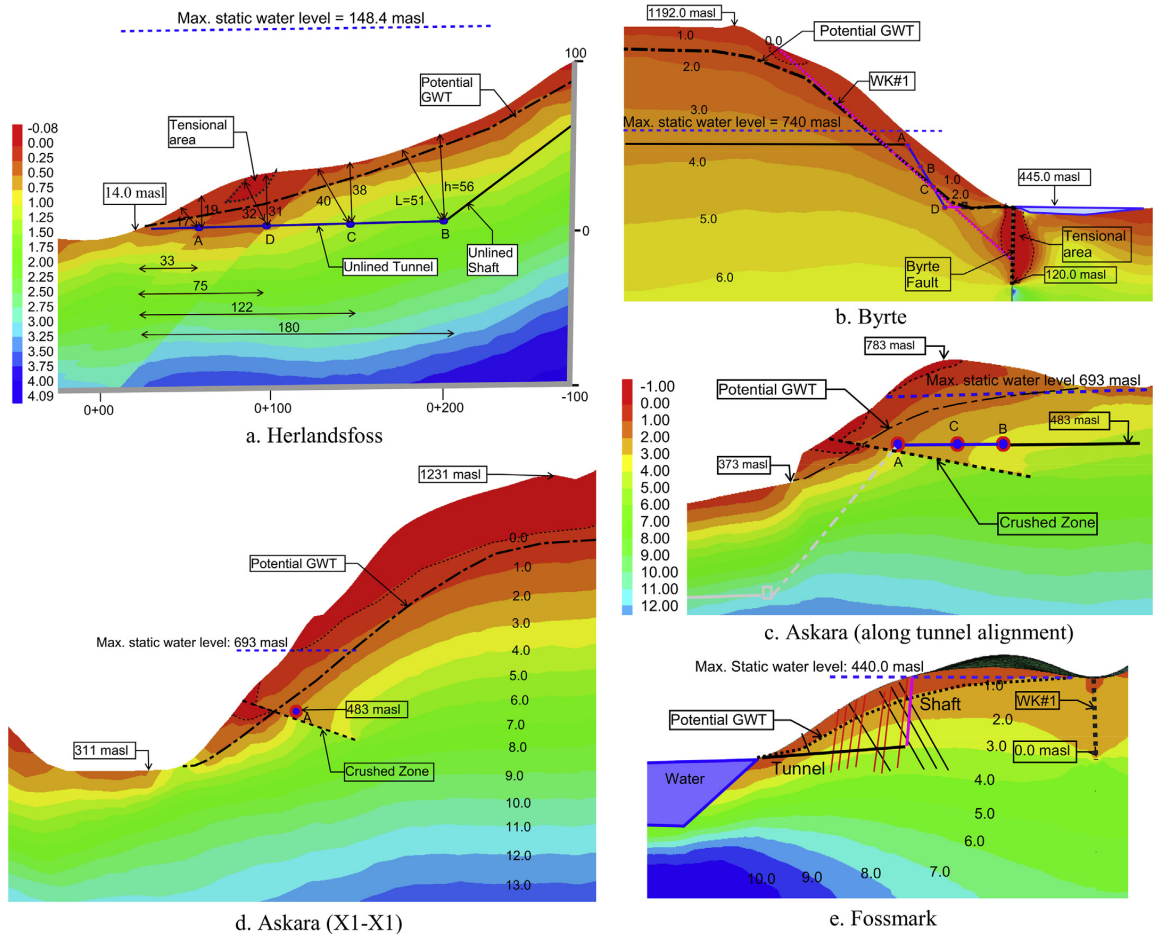

Fig. 31. Unlined shafts and tunnels with respect to groundwater table (GWT), minor principal stress (MPa), maximum static water level, zones of weakness, and joints.

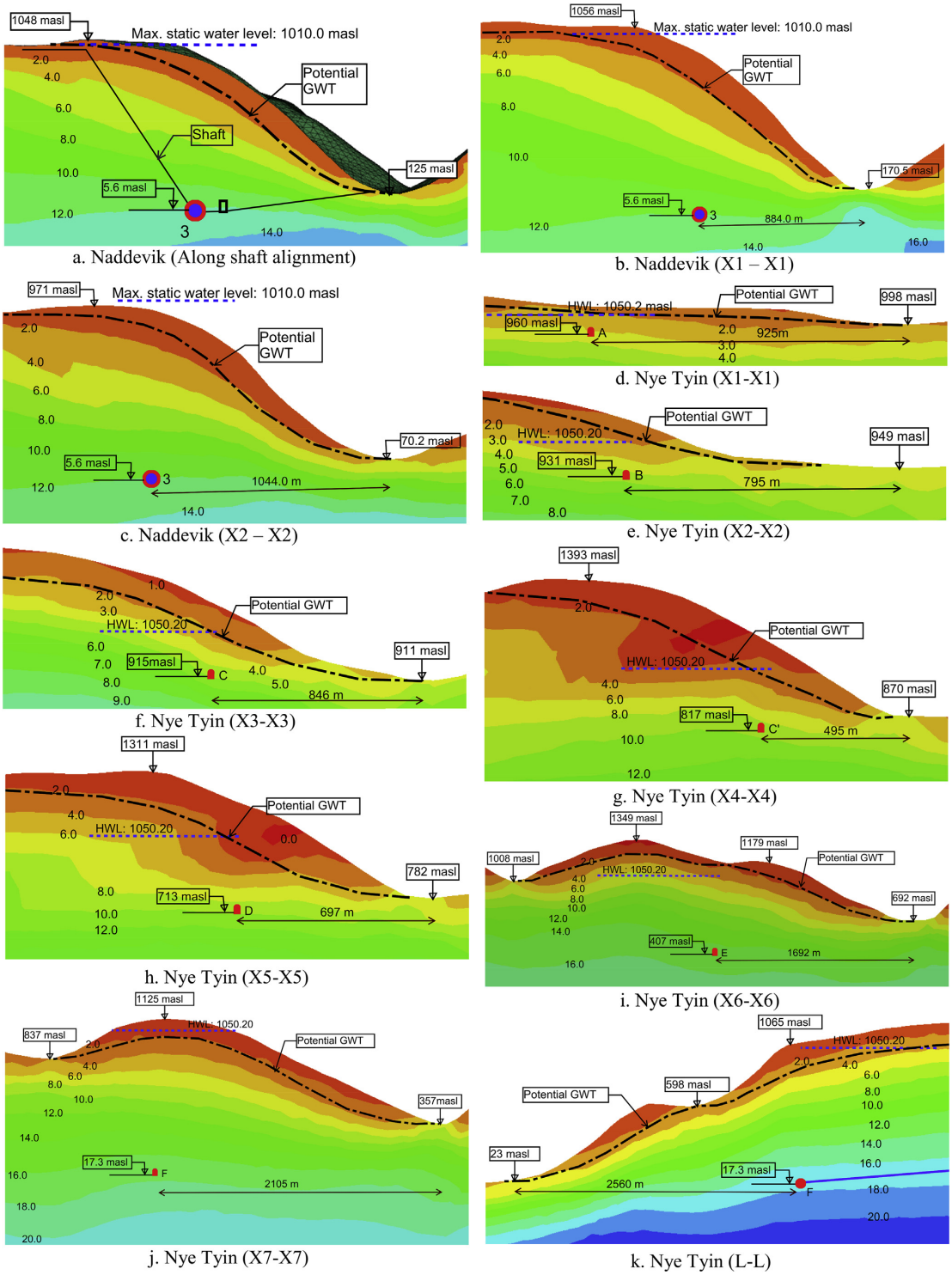

Fig. 32. Locations of unlined high-pressure shaft and tunnel along different sections of Naddevik and Nye Tyin projects (minor principal stress in MPa).

Table 8
Both favorable and unfavorable ground conditions for the applicability of Norwegian confinement criteria.

Category	Favorable conditions	Unfavorable conditions
Topography	Relatively gentle valley slope topography	Deep, steep and complex valley slope topography
Rock mass and jointing	Homogeneous and strong rock mass formations with no or single joint set having tight joint wall, wide spacing and anti-dip against valley slope	Weak rock mass with high degree of schistosity; Highly porous rock mass of volcanic and sedimentary origin; Jointed rock mass having more than two systematic and long persisting joint sets with one or more joint sets dipping steeply towards valley slope; Pre-existing open joints or the joints filled with sand and silt, which could easily be washed away; and sub-horizontal joints at low overburden area
Faults and weak/crushed zones	No nearby major faults and zones of weakness	Nearby fault and zones of weakness that are parallel or cross-cutting to the valley slope
In situ stress state	The minimum principal stress always higher than the static water head	De-stressed area and location not far away from steep valley slope topography; Not sufficiently far away from the locally overstressed areas
Hydrogeology	Hydrostatic water line below natural groundwater table or tunnel aligned deep into the rock mass and far away from the steep valley slope restricting flow paths to reach valley slope topography	Hydro-static line above the groundwater table and relatively near from the valley side slope; and Highly permeable and communicating joint sets

At the Askara project, the joints are steeply dipping and cross-cut each other at the fractured sandstone above the crushed zone (Fig. 31c and d). The crushed zone has considerable impact on the rock mass overlying above, which results in de-stressing in the fractured sandstone formation. The main failure phenomenon at this project is hence leakage through pre-existing joints, which have very low normal stress acting perpendicular to the dip. In addition, the failure location *A* is very near to the potential GWT. In summary, the failure in this case was mainly due to the presence of unfavorable topography, fractured rock mass with unfavorable jointing conditions, and crushed zone cross-cutting the shaft alignment.

At the Fossmark project, zone of weakness and steep topography with deep fjord valley influenced the stress state at the unlined pressure shaft and tunnel. Due to de-stressing, which leads to hydraulic jacking through pre-existing two cross-cutting joint systems, as shown in Fig. 31e, aggravated water leakage from the shaft and tunnel might occur. Hence, in this project, steep topography, deep fjord valley, zone of weakness parallel to the fjord valley and unfavorable jointing conditions were the main causes of the failure.

8.2. The cases of success

Different sections of both Naddevik and Nye Tyin projects are presented in Fig. 32 in order to build the concept of the successful placement of unlined high-pressure shafts and tunnels.

At the Naddevik project (Fig. 32a–c), the shaft bottom is located well below the valley bottom and the whole shaft alignment is considerably far away from the valley slope topography, leading to the increment in the stress confinement. In addition, there are no nearby pronounced faults and zones of weakness presented along the alignment and nearby area. Similarly, the rock formations mainly consist of Scandinavian hard rock composed of massive dark gneiss and granitic gneiss. There is almost no influence induced by the GWT, which should presumably follow the surface topography.

The pressure tunnel system of Nye Tyin project, on the other hand, passes through different rock formations consisting of relatively weak and micro-folded phyllite, mica schist and strong dark gneiss. The alignment of the pressure tunnel system at this project is located in such a way that the minor principal stress is considerably higher than the static head acting over it (Fig. 32d–k). However, favorability condition varies from location to location along this pressure tunnel system. One should note here that the pressure tunnel follows the alignment in such a way that the tunnel is always below the lowest point of the valley bottom and is considerably far away from it. Even at the tunnel segment where relatively weak phyllite and mica schist exist (Fig. 32d–f), the overburden cover exceeds 89 m and side cover is quite significant (85 m) in the relatively flat valley, which produces favorable in situ stress state. Similarly, the GWT is always above the hydro-static line, which hinders water to leak. On the other hand, one should note that the locations *C′* and *D* are somewhat critical since the tunnel is relatively closer to the valley side and valley slope is relatively steeper compared to the other part of the tunnel alignment (Fig. 32g and h). Still, as indicated in Fig. 32, the stress condition is quite favorable and the GWT is well above the maximum static water level.

8.3. Summary of discussions

It is important to summarize the common points and differences of the successful and failure cases. In doing so, both successful and failure cases are compared in terms of detail engineering geological assessment, stress state analysis, fluid flow analysis, potential groundwater conditions and Norwegian confinement criteria. The detailed analysis allowed us to suggest both favorable and unfavorable ground conditions for the applicability of the Norwegian confinement criteria and unlined high-pressure shafts/tunnel concepts beyond the Scandinavia. The different factors are summarized under each category of ground condition consisting of topography, rock mass, jointing and presence of faults and weak/crushed zones, in situ stress state and hydrogeology (Table 8).

9. Conclusions

Among more than 4000 km-long unlined tunnels and shafts so far built in Norway, the successful history is over 99% excluding few failure cases. The selected four failure cases were studied in detail considering engineering geological conditions, in situ stress state, hydraulic jacking and leakage potential. In addition, two successful cases of significance regarding the use of unlined high-pressure tunnel and shaft were also reviewed and analyzed. It is noteworthy to mention that along the analyzing process of this research, the news of operational failure came out from a newly constructed unlined high-pressure tunnel in Norway, indicating that the design of unlined pressure shafts and tunnels is very challenging. Aligning and placing the unlined pressure shafts and tunnels at a favorable conditions meeting all geological, geotectonic and hydrogeological aspects are complicated. Therefore, the

Norwegian design criteria for confinement cannot be directly copied to other geological and geotectonic environments. However, the authors are confident that the detailed review, analysis and assessment presented in this paper will certainly help users of unlined high-pressure shafts and tunnels concept to locate the alignment correctly with favorable ground conditions. It is highlighted that the confinement criteria must be supplemented with the detailed engineering geological assessment, stress state analysis, fluid flow analysis and hydrogeological analysis to make this concept a success outside the Scandinavia. It is emphasized here that no matter what the design methodology is used, the ultimate challenge in the design of unlined pressure tunnel/shaft is to ascertain the risk of hydraulic jacking/splitting, potential leakage and both short- and long-term stability of the tunnel itself.

Conflicts of interest

The authors wish to confirm that there are no known conflicts of interest associated with this publication and there has been no significant financial support for this work that could have influenced its outcome.

References

Barton N, Vik G, Johansen PM, Makurat A. Rock mechanics investigations for unlined pressure tunnels and air cushion surge chambers. In: Proceedings of the international conference on hydropower; 1987. p. 1–16.

Barton N. A review of the shear strength of filled discontinuities in rock. Oslo, Norway: Norwegian Geotechnical Institute (NGI); 1973.

Benson R. Design of unlined and lined pressure tunnels. Tunnelling and Underground Space Technology 1989;4(2):155–70.

Bergh-Christensen J, Dannevig NT. Engineering geological evaluations of the unlined pressure shaft at the Mauranger hydropower plant. Technical report. Oslo, Norway: Geoteam A/S; 1971.

Bergh-Christensen J, Kjolberg RS. Investigations for a 1000 m head unlined pressure shaft at the Nyset/Steggje project, Norway. In: Proceedings of the ISRM international symposium. ISRM; 1982. p. 537–43.

Bergh-Christensen J. Design of unlined pressure shaft at Mauranger Power Plant, Norway. In: Proceedings of the International Society for Rock Mechanics (ISRM) international symposium. ISRM; 1982. p. 531–6.

Bergh-Christensen J. Failure of unlined pressure tunnel at Åskåra Power Plant. In: Proceedings of the rock mechanics day; 1975. p. 15.1–8 (in Norwegian).

Bergh-Christensen J. Rock stress measurements for the design of a 965 metre head unlined pressure shaft. In: Proceedings of the ISRM international symposium. ISRM; 1986. p. 583–90.

Brekke TL, Ripley BD. Design guidelines for pressure tunnels and shafts. Technical report No. EPRI-AP-5273. Department of Civil Engineering, California University at Berkeley; 1987.

Broch E, Christensen J. Investigations of unlined pressure shafts. Trondheim, Norway: Norwegian Institute of Technology; 1961.

Broch E, Eslava LF, Marulanda A. Design of high pressure tunnels for the Guavio Hydroelectric Project, Colombia. In: Proceedings of the international conference on underground hydropower plants; 1987. p. 87–99.

Broch E. The development of unlined pressure shafts and tunnels in Norway. In: Proceedings of the ISRM international symposium. ISRM; 1982. p. 545–54.

Broch E. Underground hydropower projects - lessons learned in home country and from projects abroad. Norwegian Tunneling Society; 2013. p. 11–9.

Broch E. Unlined high pressure tunnels in areas of complex topography. International Water Power and Dam Construction 1984;36(11):21–3.

Buen B, Palmstrom A. Design and supervision of unlined hydro power shafts and tunnels with head up to 590 meters. In: Proceedings of the international ISRM international symposium. ISRM; 1982. p. 567–74.

Buen B. Documentation of unlined water conduits in Norway. Oslo, Norway: FHS; 1984. p. 75–85.

Edvardsson S, Broch E. Underground powerhouses and high pressure tunnels. Hyderopower development, vol. 14. Trondheim, Norway: Division of Hydraulic Engineering, Norwegian Institute of Technology; 2002.

Esteves C, Plasencia N, Pinto P, Marques T. First filling of hydraulic tunnels of Venda Nova III hydropower scheme. In: Proceedings of the world tunnel congress; 2017.

Fejerskov M, Lindholm C, Myrvang A, Bungum H. Crustal stress in and around Norway: a compilation of in situ stress observations. London, UK: Geological Society; 2000. p. 441–50.

Fejerskov M, Lindholm C. Crustal stress in and around Norway: an evaluation of stress-generating mechanisms. London, UK: Geological Society; 2000. p. 451–67.

Fejerskov M. Determination of in-situ stresses related to petroleum activities on the Norwegian continental shelf [Ph.D. Thesis]. Department of Geology and Mineral Resources Engineering, Norwegian University of Science and Technology; 1996.

Garshol K. Fossmark hydropower scheme, leakages from the unlined pressure shaft. In: Proceedings of rock blasting technology, rock mechanics and geotechnics; 1988. p. 25.1–25.11.

Geological Survey of Norway (NGU). National bedrock database. 2017. http://geo.ngu.no/kart/berggrunn_mobil/?lang =eng.

Hanssen TH. Investigations of some rock stress measuring techniques and the stress field in Norway [Ph.D. Thesis]. Department of Geology and Mineral Resources Engineering, Norwegian University of Science and Technology; 1997.

Hartmaier HH, Doe TW, Dixon G. Evaluation of hydrojacking tests for an unlined pressure tunnel. Tunnelling and Underground Space Technology 1998;13(4):393–401.

Hoek E, Carranza-Torres C, Corkum B. Hoek-Brown failure criterion - 2002 edition. In: Proceedings of NARMS-Tac; 2002. p. 267–73.

Hoek E. Rock mass properties for underground mines. In: Underground mining methods: engineering fundamentals and international case studies. Society for Mining, Metallurgy, and Exploration; 2001. p. 467–74.

Hydro. The new Tyin power system. Engineering geological report. Norsk Hydro ASA; 1998. Project No. ED1546.

Itasca. FLAC^{3D} 5.0 user's manual: interfaces. Itasca; 2017a.

Itasca. UDEC 5.0 user's manual: fluid flow in joints. Itasca; 2017b.

Johansen T. Norwegian tunneling. Oslo, Norway: FHS; 1984.

Kestin J, Sokolov M, Wakeham WA. Viscosity of liquid water in the range − 8 °C to 150 °C. Journal of Physical and Chemical Reference Data 1978;7(3):941–8.

Lamas LN, Leitao NS, Esteves C, Plasencia N. First infilling of the Venda Nova II unlined high-pressure tunnel: observed behaviour and numerical modelling. Rock Mechanics and Rock Engineering 2014;47(3):885–904.

Liu K. Stress calculation of unlined pressure tunnel surrounding rock in hydraulic engineering. In: Instrumentation and measurement, sensor network and automation (IMSNA). Institute of Electrical and Electronics Engineers; 2013. p. 57–60.

Marwa EM. Geotechnical considerations in an unlined high pressure tunnel at Lower Kihansi in Tanzania. Bulletin of Engineering Geology and the Environment 2004;63(1):51–5.

Ming L, Brown ET. Designing unlined pressure tunnels in jointed rock. International Water Power and Dam Construction 1988;40(11):37–41.

Myrset O, Lien R. High pressure tunnel systems at Sima power plant. In: Proceedings of the ISRM international symposium. ISRM; 1982.

Myrvang A. Personal communication with Arne Myrvang on 15th February 2017. 2017.

NGI. Overview of Norwegian unlined tunnels and shafts with water pressure over 100 m and some others with lower pressures. Oslo, Norway: NGI; 1972.

Nilsen B, Thidemann A. Rock engineering. Trondheim, Norway: Division of Hydraulic Engineering, Norwegian Institute of Technology; 1993.

Norconsult. Alto Maipo hydropower. 2017. https://www.norconsult.com/references/energy/alto-maipo-hydropower.

Norges Vassdrags og Elektrisitetsvesen (NVE). Byrte power plant: failure in pressure shaft. NVE; 1970.

Palmstrom A, Broch E. The design of unlined hydropower tunnels and shafts: 100 years of Norwegian experience. International Journal on Hydropower and Dams 2017;(3):1–9.

Palmstrom A. Norwegian design and construction of unlined pressure shafts and tunnels. In: Proceedings of the international conference on hydropower in Oslo, Norway; 1987. p. 87–111.

Panthi KK, Basnet CB. Design review of the headrace system for the Upper Tamakoshi project, Nepal. International Journal on Hydropower and Dams 2017;1:60–7.

Panthi KK, Basnet CB. Review on the major failure cases of unlined pressure shafts/tunnels of Norwegian hydropower projects. Journal of Water, Energy and Environment 2016;18:6–15.

Panthi KK. Norwegian design principle for high pressure tunnels and shafts: its applicability in the Himalaya. Journal of Water, Energy and Environment 2014;14:36–40.

Rocscience. Estimating joint stiffness. 2017. https://www.rocscience.com/help/phase2/webhelp9/theory/Estimating_Joint_Stiffness.htm.

Selmer-Olsen R. Experience gained from unlined high pressure tunnels and shafts in hydroelectric power stations in Norway. Norwegian Soil and Rock Engineering Association; 1985.

Selmer-Olsen R. Experience with unlined pressure shafts in Norway. In: Proceedings of the international symposium on large permanent underground opening; 1969.

Selmer-Olsen R. Underground openings filled with high-pressure water or air. Bulletin of the International Association of Engineering Geology 1974;9(1):91–5.

SINTEF. Rock mechanical properties. SINTEF Building and Infrastructure; 1998. Report No. STF22 A98034.

SINTEF. Rock stress measurements at the Nye Tyin hydropower project. SINTEF Building and Infrastructure; 2002.

Valstad T. Unlined water tunnels and shafts: water leakage from headrace tunnel of Bjerka power plant. Oslo, Norway: NGI; 1981 (in Norwegian).

Vik G, Tunbridge L. Hydraulic fracturing - a simple tool for controlling the safety of unlined high pressure shafts and headrace tunnels. In: Proceedings of the ISRM international symposium. ISRM; 1986.

Vogt JHL. Pressure tunnels and geology. Technical Report No. 93. Oslo, Norway: NGU; 1922.

Chhatra Bahadur Basnet is conducting his PhD research at the Department of Geoscience and Petroleum, Norwegian University of Science and Technology (NTNU), Norway. His current research work is related to unlined pressure tunnels in hydropower projects. He holds MSc degree in Hydropower Development from NTNU. He has more than six years of working experience in planning, design, and construction supervision of numbers of hydropower projects in Nepal.

Krishna Kanta Panthi is an Associate Professor in Geological Engineering at the Department of Geoscience and Petroleum, Norwegian University of Science and Technology (NTNU) since 2008. He holds the degrees of PhD in Rock Engineering, MSc in Hydropower Engineering and MSc in Tunneling. He has approximately 25 years of experience in design, construction management and research of tunneling, hydropower, slope stability and mining projects. He is the author of many scientific papers published in renowned international journals.

Paper III

Title:

Design review of the headrace system for the Upper Tamakoshi project, Nepal

Authors:

Panthi, Krishna Kanta

Basnet, Chhatra Bahadur

Published in:

The International Journal on Hydropower and Dams (2017)

Volume 24 (1), pages 60-67

NB: Word version for the manuscript is included due to reduced quality of scan version of the published manuscript.

Design review of the headrace system for the Upper Tamakoshi project, Nepal

K.K. Panthi and C.B. Basnet
Norwegian University of Science and Technology (NTNU), Norway

Abstract

One way to reduce the cost of construction of hydroelectric projects with underground waterway systems is to allow the rock mass to act as natural concrete and to adopt unlined/shotcrete-lined pressure tunnels to the extent that the rock mass permits. This article reviews engineering geological design aspects and design changes adopted for the headrace system of Upper Tamakoshi hydro project in Nepal, as more studies were done to increase knowledge of the geological characteristics of the rock mass and in situ stresses in the project area.

Introduction

The use of unlined pressure shafts and tunnels at hydropower schemes is quite common around the world, especially in Norway [Broch, 2016[1]]. The principle behind the unlined concept is that the rock mass itself works as a structural member to counteract the pressure exerted by the hydrostatic head. Success with the use of unlined pressure tunnels and shafts in Scandinavia relates mainly to both the favorable geological conditions and the stable geotectonic environment. The Himalayan geology and geotectonic environment are quite different, and the rock mass in the region is of both weak and strong quality, and is influenced by the active tectonic movements (earthquake events) prevailing in the Himalayas [Panthi, 2014[2]]. In general, flexible rock support systems, consisting of rockbolts and shotcrete linings, are used in most of the tunnels constructed today, to provide safe working conditions at the tunnel face during the excavation work, and often also to provide permanent support. However, shotcrete is a permeable material, and cannot be considered as a structural member to act against water pressure. Therefore shotcrete-lined water tunnels must be considered as unlined pressure tunnels.

Panthi [2006[3]] and Panthi and Nilsen [2007[4]] highlight the relatively high degree of geological uncertainty in the design, during the feasibility stage, of hydro projects involving many underground elements such as tunnels, caverns and shafts. This is because of the limited amount of geological information which is generally available at the pre-construction phase from geological investigations. The level of confidence regarding knowledge of rock quality is enhanced as the design and implementation process advances.

This was the case through the design process of the underground structures for the Upper Tamakoshi hydroelectric project (UTHP), which is the highest head project under construction in Nepal since 2011. The project went through various stages of design, and changes were made from time to time based on the results of more detailed and thorough geological investigation obtained during the detailed design phase, and as underground excavation proceeded [Norconsult, 2005[5]; Norconsult and Lahmeyer, 2008[6]; Norconsult and Lahmeyer, 2013[7]; Norconsult and Lahmeyer, 2014[8]; Reimer and Bock, 2013[9]].

1 Himalayan geology and tectonics

The collision of the Indian and Asian continental plates is supposed to have occurred in past 100 millenia and is responsible for the uplift of the Himalayan and Tibetan plateau. This event is thought

to be responsible for geological, geochemical and climatological consequences of global extent [Rowley, 1996[10]]. After the collision, the rigid and strong granulitic lower crust of the Indian plate was underthrust beneath the Himalaya to an unknown distance further north into the warm Tibetan lower crust, which is indicated by a question mark in Fig. 1 [Jackson *et al*., 2008[11]]. Because of this collision and underthrust process, the upper part of the Indian crust near the plate boundary was squeezed and became short and thick as a result of the push from the Tibetan upper crust, which must have been stronger. A number of rupture zones were then formed in the Himalayas, such as the Main Frontal Thrust (MFT), Main Boundary Thrust (MBT) and Main Central Thrust (MCT), as shown on the left in Fig. 1.

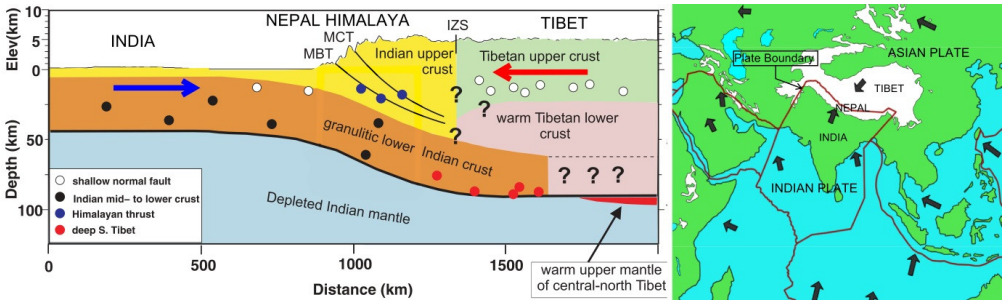

Fig. 1. Schematic cross-section through the Himalayan region, showing structures and the earthquake distribution (black, white, blue and red dots) in the left part of the Figure, updated from Jackson et al. [2008[11]]; and on the right, the location of the Indian and Asian plate (Tibet) with the Nepal Himalaya [Strobel, 2016[27]].

The strain energy stored in the earth's crust is released as a result of differential movement in the interfaces/thrusts. The release of this energy causes periodic strong, medium and small-scale earthquakes in the region. An example of these strong, medium and small earthquake events in tectonically active areas of the Himalayas was the series of earthquakes (more than 500 with Richter magnitudes of more than 4.0) which occurred after the M 7.8 Gorkha earthquake of 25 April 2015. The coloured dots in Fig. 1 indicate the epicentres of strong earthquakes in the Himalayan region, which have occurred at various locations and time periods in the past. In general, the earthquakes occurred at depths of about 15 km in shallow-dipping thrusts, as shown by the blue dots in Fig. 1, and they were devastating as they were so near to the surface. The Himalayan region has been experiencing a large number of strong to medium strong earthquakes with epicentre depths of less than 15 km. More importantly, the Himalayan seismic belt is mostly confined within the MFT, MCT and MBT, and the most dominant mode of energy release in this region occurs through the rupture along these active major thrust faults [Shanker et al., 2011[12] Chamlagain, 2009[13]; Lavé and Avouac, 2000[14]; Nakata, 1989[15]].

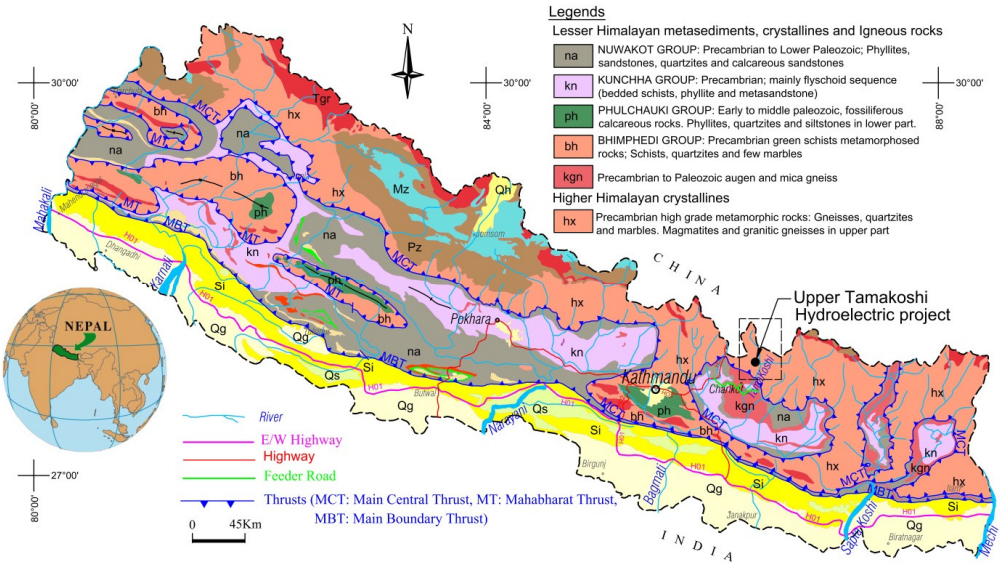

Fig. 2. Geological map of the Nepalese Himalayan region showing the project location (developed from DGM [1994[28]].

A considerable amount of energy is accumulated as a result of the persistent compression caused by the collision of the two plates and this energy is released through frequent earthquakes in the Himalayas, and the stresses locked within the rock mass are released through thrust faults and large-scale discontinuities such as zones of weakness, lineaments and fractures. The general trend of the stress orientation is NE-SW in the western region of the Himalayas, and tends more to N-S in the eastern region [Panthi, 2012[16]]. This general trend appears to be in the direction of tectonic plate movement as shown in Fig. 1 (right section of figure).

The whole Himalayan range is mainly composed of Indian upper crust and some part of the Tibetan upper crust. Fig. 2 shows the geological map of the Nepalese Himalayas with major geological formations and thrusts. Tectonically, the Himalayan region of Nepal can be divided into five major zones from south to north, each characterized by its own lithology, tectonics, structure and geologic history [Upreti, 1999[17]]. The southernmost zone is Terai, and the northernmost is the Tibetan-Tethys zone whereas the Siwalik, Lesser Himalayan and Higher Himalayan zones are in between these former zones from the south towards the north, respectively.

2 Upper Tamakoshi project

The Upper Tamakoshi hydroelectric project (UTHP) is under construction in the Dolakha district of Nepal, which is northeast of Kathmandu valley (Fig. 2). It will have a gross head of 822 m and an installed capacity of 456 MW. It is the highest head hydro project so far constructed in Nepal and will generate approximately 2300 GWh/year.

Construction started at the beginning of 2011 with a scheduled completion date of late 2016. However, construction activities were in halted by the M 7.8 Gorkha earthquake of 25 April 2015. The earthquake caused many rock slides along the Tamakoshi valley, and as a result the access road to the project was severely damaged. However, there was no serious damage to the underground structures of the project. After most of the damaged road had been repaired, excluding the part to Lamabagar (the

headworks site) which was still blocked by a large-scale rock slide, work on the project was recently able to resume at the sites of the powerhouse, vertical shafts and headrace tunnel, from the downstream end. Tunnel excavation from the headworks site will resume after completion of the 300 m-long road tunnel which will bypass the rock slide. The Gorkha earthquake has considerably delayed the completion date of the project, which is now likely to be 2018.

The UTHP aims to exploit water from the Tamakoshi River with the construction a concrete gravity dam located at Lamabagar. The river water will be conveyed from the intake via a surface settling basin, an unlined/shotcrete lined headrace tunnel and two vertical penstock shafts to the underground powerhouse cavern, which is located at Gonger. The water will then be discharged into the Tamakoshi River through the tailrace tunnel. In the first stage, the project will use water from the Tamakoshi River only, and in the second stage, water from Rolwaling Khola will be added, through the intake at Lamabager. After completion of the second stage, the total installed capacity will be 456 MW, with a design discharge of 66 m3/s and a 822 m gross static head [Reimer and Bock, 2013[9]]. The total annual energy production from the plant will be around 2300 GWh.

2.1 Project geology in the regional and local perspective

The project is located in the Higher Himalayan Tectonic Zone of the eastern Nepal Himalayas (see Fig. 2), which is characterized mainly by high grade Precambrian metamorphic rocks, consisting mostly of gneiss, granitic gneiss, schist, amphibolite, migmatite and quartzite. Schelling [1992[18]] prepared the geological map of the eastern Nepalese Himalayas, including the middle and lower reaches of the Tamakoshi River valley, but the project area is located in the upper reach of the valley. Although he did not include this area in his study, important information was provided which improved the understanding of geology in the eastern region of Nepal. Similarly, Ishida [1969[19]] mapped thrust faults between almost every tectonic unit of the lower and middle Tamakoshi valley; each of these faults is considered to have been originally north-dipping, and to have accommodated top-to-the-south displacement [Larson, 2012[20]]. The project location is in the Higher Himalayan Zone, and is above the MCT, so the characteristics of the rocks from a similar area in this zone help to provide an idea about the characteristics of the rocks in the project area.

Larson [2012[20]] mapped the upper reach of the Tamakoshi valley, including the Rolwaling and Khare valleys, which had not been included in previous studies by other authors. However, his study builds on the previous work by Schelling [1992[18]] and Ishida and Ohta [1973[21]]. Fig. 3 is a geological map covering the Upper Tamakoshi project area, which was developed based on the map prepared by Larson [2012[20]]. All the rocks in this area have been metamorphosed and the metamorphic grade increases northwards, which corresponds to other similar regions such as the Everest region and the Kathmandu nappe. In particular, Lesser Himalayan meta-sediments such as graphitic schist and biotite, and garnet-bearing schist are at the foothill of the MCT, and kyanite-bearing magmatitic paragneiss is in the project area above the MCT, followed by quartzite in the vicinity of the MCT in the form of a hanging wall (Fig. 3).

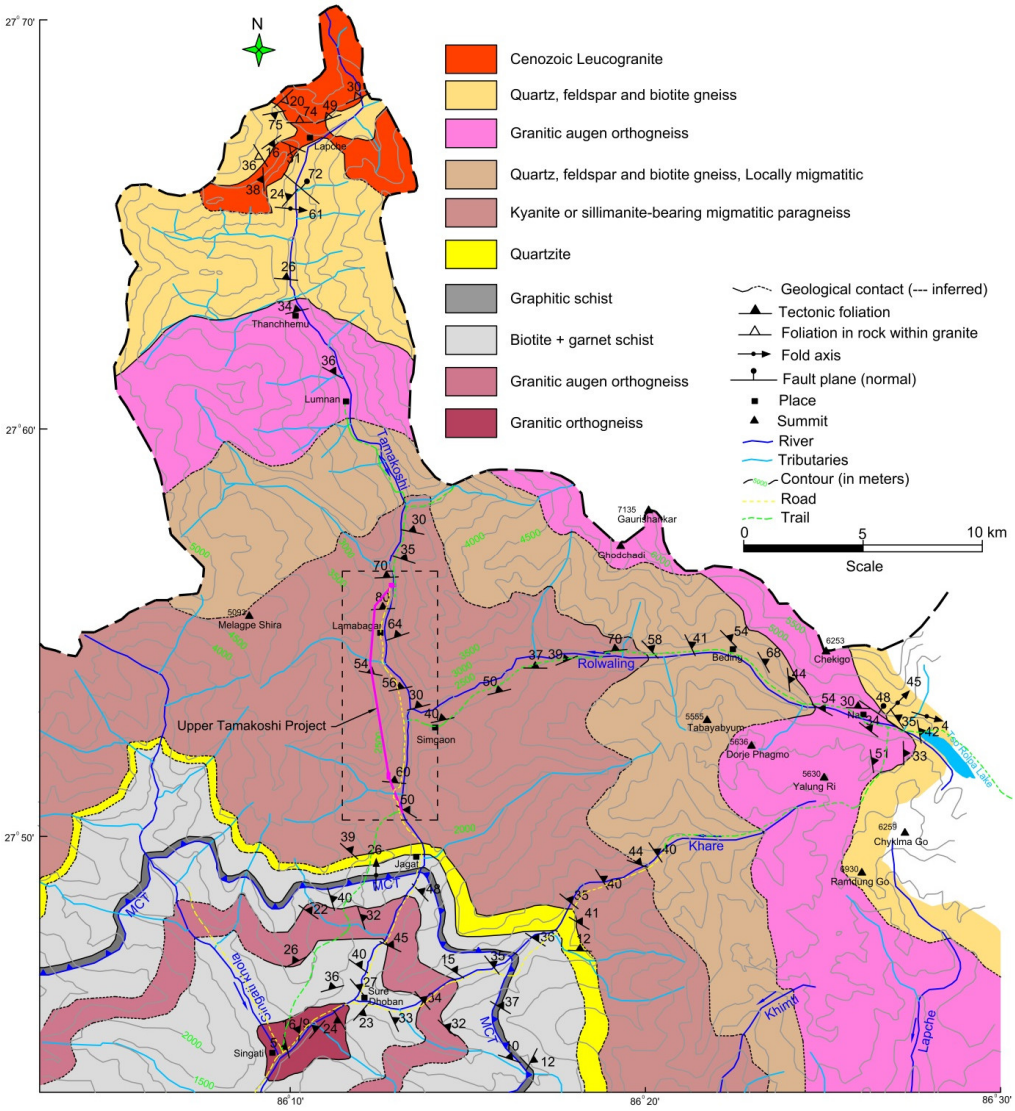

Fig. 3. Geological map of the Upper Tamakoshi area, enhanced from Larson [2012[20]].

The detailed geological mapping of the project area during the feasibility study concluded that the rock types in the project area can be characterized as micaceous schist and banded gneiss, with abundant mica contents [Norconsult, 2005[5]]. These rock types are comparable with those mentioned by various authors including Larson, except that the mica content is not clearly defined in their studies. According to Norconsult [2005[5]], cores from different drill holes indicate 20-40 per cent of mica and 40-72 per cent of quartz and feldspar, with quartz dominating. The general strikes of the foliation joints are WNW to NNW, with dip angles of 35^0-75^0 NE. A detailed geological map of the project area is shown in Fig. 4, which represents updated information collected since the feasibility study in 2005.

2.2 Review of the headrace tunnel alignment

The pressurized headrace tunnel begins from the downstream end of the settling basins at Lamabagar and ends at the top of the penstock shaft, which connects to the powerhouse cavern. The main focus in this paper is on the design of the headrace tunnel. Since the pre-feasibility study in 2001 there have been several changes in the headrace tunnel alignment, as indicated in Fig. 4. Until the second phase of the feasibility study in 2005, the project was designed with a low pressure horse-shoe shaped headrace tunnel (almost horizontal) up to the top of the upper shaft, as shown in Figs. 4 and 5 [Norconsult, 2005[5]]. This design option is referred to as FS-2005 in this paper, and is shown in blue in the Figures. For this option, the maximum water head at the end of headrace tunnel is about 38 m, and 10 cm-thick shotcrete was recommended for the wall and roof of the tunnel, except in some of the stretches where a concrete lining (30 cm thick) was considered to be necessary. Invert concrete with a minimum thickness of 20 cm was also proposed throughout the headrace tunnel.

In the FS-2005 option, an upper vertical shaft from T5 to T6 (see Fig. 5) was designed with a circular concrete lining. From T6, there is a 432 m-long horizontal pressure tunnel running towards the penstock (with a circular steel lining) transition up to T7, which was designed with shotcrete and concrete linings in accordance with the requirement for the support up to the penstock bellmouth. The position of the penstock transition (T7) was proposed to be fixed based on the in-situ stress measurement during construction [Norconsult, 2005[5]] to avoid hydraulic splitting in the rock mass around the shotcreted and concrete-lined part of the headrace tunnel. It should be noted that the shotcreted and concrete-lined part of this pressure tunnel is functionally unlined because the static water head will vary between 380 m at T6 and 424 m at T7.

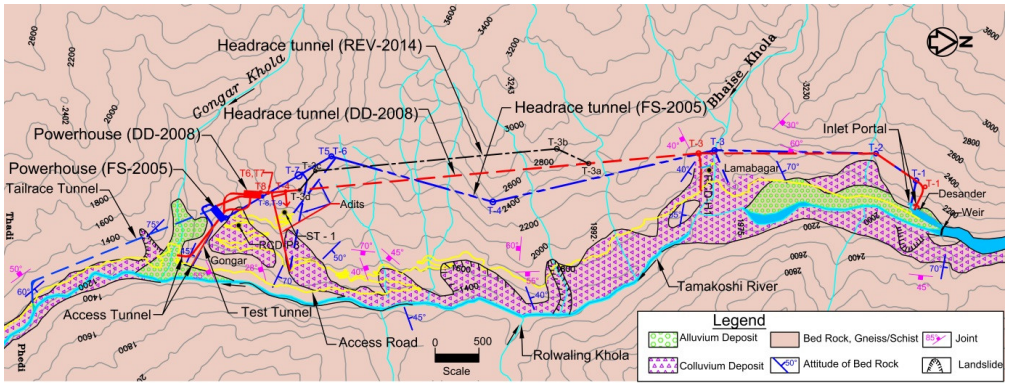

Fig. 4. Geological map of the Upper Tamakoshi project, showing the various project options.

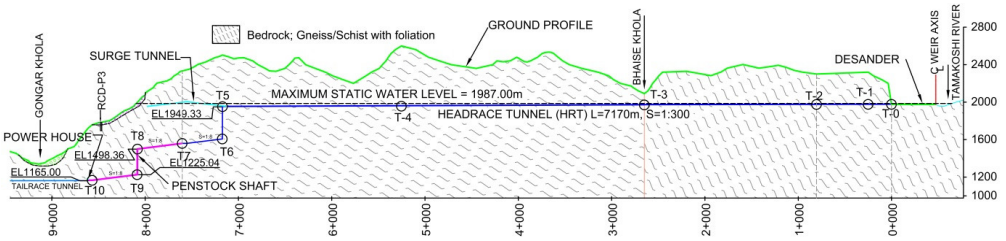

Fig. 5. Geological and tunnel alignment profile of FS-2005.

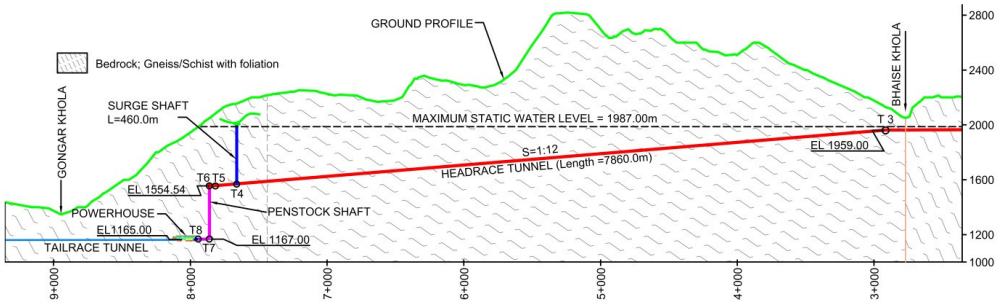

Fig. 6: Geological and tunnel alignment profile of DD-2008.

During the detailed design in 2008, the alignment of the headrace tunnel and shaft was changed from that proposed in 2005 (see Figs. 4 and 5). The second option is referred to as DD-2008 (see Figs. 4 and 6). The changes made were based on data from more detailed engineering geological investigations and information available from the construction of a 500 m-long test tunnel, and 500 m-deep core drilling done at ST-1 (the locations are shown in Fig. 4). The in-situ rock stresses were also measured using the 3D over-coring technique at three locations along the test tunnel [SINTEF, 2008[22]].

For the headrace tunnel, it was planned to have only a shotcrete lining up to T5, as indicated in Fig. 6, where the maximum static water head will reach about 430 m. Provision was only made for concrete lining at the tunnel stretches where weakness and fault zones would be encountered. After 265 m of headrace tunnel excavation from T5 upstream (towards T3), a 30m wide crushed zone with completely fragmented and weathered rock mass was encountered. Also, the tunnel passes a 70 m-wide crushed zone about 650 m downstream from T3 (towards T5). After reaching a point about 450 m upstream from T5, it was realized that the tunnel alignment is not suitable for a shotcrete lined/unlined pressure tunnel in view of the need to deal with the hydrostatic head of 430 m. It is likely that more crushed zones will be encountered in the remaining alignment, and a high pressure unlined or shotcrete lined headrace tunnel could require a considerable extra length of steel penstock lining. As a result of this situation, rock stress was measured [SINTEF, 2013[23]] using hydraulic fracturing at two locations; at about 70 m and 250 m upstream from T5, respectively. The tests revealed minor principle stress lower than hydrostatic head at both locations, which did not satisfy the design criteria for an unlined high pressure tunnel with a static head of 430 m. After this, in 2014, the alignment between T5 and T3 was reviewed for different possible options. This latest alignment is referred to as REV-2014, and is illustrated in Figs. 4 and 7. This arrangement consists of a 7.9 km headrace tunnel, a 150 m-deep surge shaft, a 307 m-deep upper vertical penstock shaft, a 100 m-long horizontal penstock shaft, a 398 m-deep vertical penstock shaft, a 1.5 km-long access tunnel, a 2.9 km-long tailrace tunnel, a 142 m-long underground powerhouse cavern (13 m wide and 25 m high) and an underground transformer cavern located parallel to the powerhouse cavern.

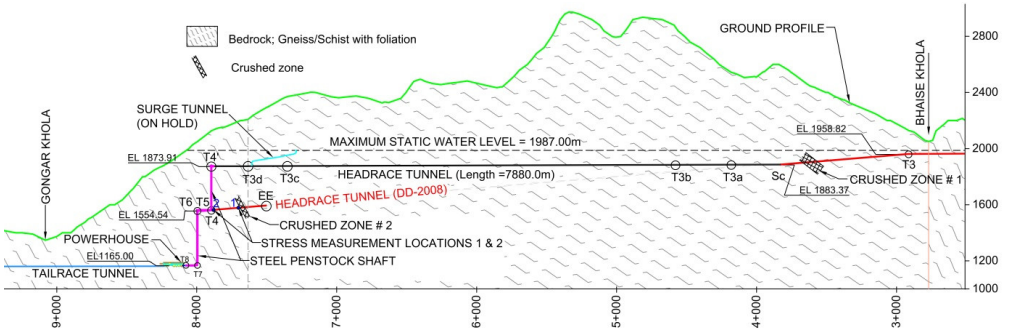

Fig. 7. Geological and tunnel alignment profile of REV-2014.

In this new arrangement, a shotcrete lined/unlined medium pressure headrace tunnel (for 113 m of hydrostatic head at the end of headrace tunnel) is proposed (see Fig. 7). For this static pressure, a reinforced concrete lining can be designed in case crushed zones are encountered along the headrace tunnel after excavation, and this will give much more flexibility for the future decision.

2.3 Design issues of a pressurized unlined headrace tunnel

The Norwegian design criteria for overburden and distance from the valley slope for unlined pressure tunnels and shafts as explained by Broch [1982[24]] have been used for all three design options for the UTHP. The results show a factor of safety of more than 2. It is important to note here that even with the fulfillment of overburden and valley distance criteria; there have been a few cases in Norway where initial leakage and hydraulic splitting problems were faced. Panthi and Basnet [2016[25]] highlighted that it is equally important to assess other aspects of engineering geology, such as rock types, jointing frequency and joint infilling conditions, faults and weakness zones and degree of weathering, as well as the in-situ stress condition, to ensure a safe design. Whatever the design approach, the unlined pressure tunnel should provide long-term stability, safety against hydraulic splitting in the rock mass, and ensure that any water leakage from the tunnel is within a permissible limit. With this in mind, the geotectonic environment in the project area where all underground structures are being located has been assessed.

2.4 Mechanical properties of the rock

The rock mass at the periphery of an unlined/shotcrete lined pressure tunnel should be competent and strong enough to bear the in-situ stress without its properties being altered. The rock mass works in the same way as natural concrete in an unlined pressure tunnel, so the hydrostatic pressure exerted by the water should not split the rock mass. The bedrock in the UTHP area is predominantly banded gneiss, with occasional intercalation of bands of micaceous schist, and it is medium strong to strong. Table 1 gives the physical and mechanical properties of the rock samples tested from the test tunnel and ST-1.

Table 1: Physical and mechanical properties of gneiss/schist of UTHP

	UCS MPa	Young's modulus GPa	Poissons ratio ν	Density kg/m^3	Sound velocity m/sec	Angle of failure degree
Loading normal to the foliation						
Min	37.7	19.6	0.10	2700	2193	18
Max	112.0	49.8	0.30	2798	4084	25
Mean	61.7	30.2	0.20	2745	2893	22
SD	18.3	7.8	0.06	26	570	3
Loading parallel to the foliation						
Min	15.0	23.0	0.10		4183	17
Max	74.0	48.2	0.34		4558	17
Mean	32.7	32.0	0.22		4358	17
SD	17.2	7.7	0.09		130	0

As can be seen in this Table, the rock has a certain degree of strength anisotropy, which is a typical property of the foliated rocks. In addition to the strength, other properties, such as Young's modulus of elasticity, sound velocity and Poisson's ratio, also show some anisotropy.

2.5 Joints and their characteristics

The rock mass in the project area is blocky to locally fractured in nature, and is more fractured towards the outlet of the pressure tunnel (at the downstream end) compared with the inlet site (upstream). It is massive to highly jointed, and has three main joint sets including foliation (Jf, J1 and J2 shown in Fig. 8) and joint spacing is mostly greater 0.3 m along the headrace tunnel alignment. The surface mapping shows that none of these main joint sets is parallel to the valley side slope. However, ex-foliation joints (J3 in Fig. 8, left), which were mapped along the surface topography, are more or less parallel to the valley slope, and these were not noticed along the excavated headrace tunnel. The exfoliation joints dip steeply towards valley side. According to Selmer-Olsen [1969[26]], if the joints are parallel to valley slope and steeply dipping, there is a chance of an increase in cleft water pressure during operation of pressure tunnel, which may lead to the movement of rock mass near the surface [Selmer-Olsen, 1969[26]]. There is also a chance of the development of a leakage path if the main joint sets are interlinked with the exfoliation joints.

Fig. 8 (right) shows the joint orientation in the tunnel section from T6 to EE (see also Fig. 7). There is a crushed zone in this stretch, and it has an orientation more or less the same as that of the foliation joint. As in the surface mapping, three joint sets have also been mapped inside the tunnel however; J2 differed in its orientation (both strike and dip).

The tunnel mapping revealed the characteristics of some dominant joint sets. The aperture in the joints varies between 5 and 15 mm and exceeds 5 cm at the crushed zones. Some of these joints are filled with silt and clay. However, where inflow was registered at some locations, no washout materials were observed through the joints. The joints seem quite regular and occasionally occur at spacing of more than every 10 m. The joint walls are slightly altered and weathered except in the zones of weakness. However, the rock mass observed in the headrace tunnel downstream from T3 is mostly massive, and joint sets other than foliation joints are widely spaced and even quite rare, except in those areas where small bands of fractured zones were encountered at the beginning. The foliation seems to be tight and intact. This indicates that it is likely that most of the headrace tunnel can be kept unlined or only shotcreted provided no hydraulic splitting occurs.

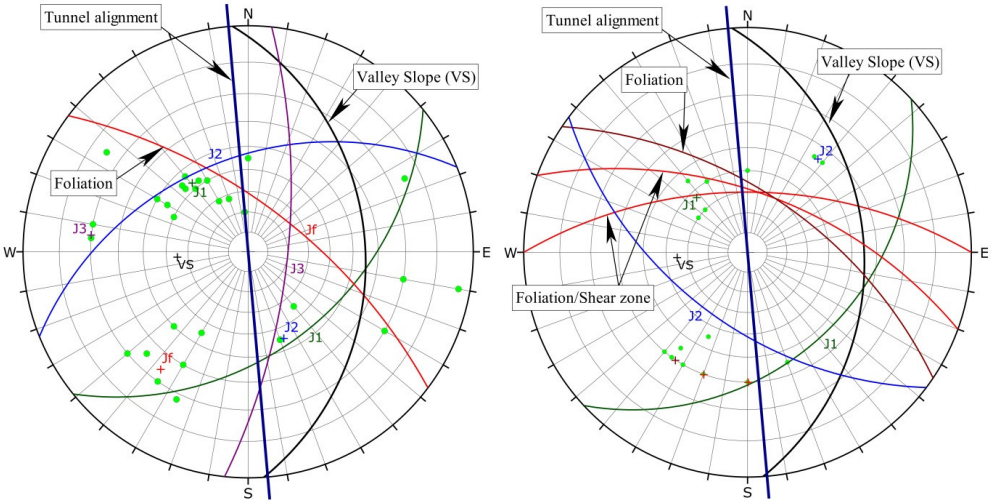

Fig. 8. Equal area lower hemisphere stereographic projection of the jointing system. On the left, results from surface mapping at the shaft area; and, on the right, results from tunnel mapping from T6 to EE in Fig. 7.

2.6 Weathering

The rock mass on the surface is slightly to moderately weathered. The weathering depth was marked during the core drilling in the headrace tunnel and shaft area at the time of the feasibility study in 2005. In a drill hole near Bhaise Khola (RCD-H1), gravel and boulders of banded gneiss were found to be present continuously down to a depth of about 48 m from the surface, which means the bedrock level is at about EL. 1959. Similarly, the weathering depth in another drill hole (RCD-P3) near the shaft area was found to be about 25 m from the surface, whereas it is 43 m in RCD-P2 on the right bank of the Gongar Khola. No significant weathering can be seen in the portal area of the powerhouse access tunnel. Later, in 2008, another hole (ST-1) was drilled near the shaft area, and the bedrock was found to be about 14 m from the surface. The materials found above the bedrock were classified as silt to gravel to boulder sized rock fragments. In general, the weathering depth in the project area varies from 10 to 50 m up in the hills, and in the depressions and tributaries, but there are some overhanging cliffs on the banks of Tamakoshi River, where fresh rock mass is exposed to the surface topography.

2.7 Folding and faulting (shearing)

The project is located in the 'Higher Himalayan' rock formation, and very close to MCT (3 to 12 km). The Tamakoshi River itself is thought to run above some major lineaments crossing the MCT. In addition to this, some of the tributaries to this river, such as the Rolwalling Khola, Bhaise Khola, Gongar Khola and Khare Khola (shown in Figs. 3 and 4) represent prominent lineaments.

During the feasibility study in 2005, no major lineaments were observed along the tunnel alignment, but some moderate and minor lineaments were encountered, mostly coinciding with the joint system of the rock mass. Later, during excavation work, the crushed zones 1 and 2 (shown in Fig. 7) were found and these are referred to as zones of weakness along the tunnel alignment. Similar weakness zones may occur in the remaining unexcavated part of headrace tunnel. It is believed that these zones will definitely have an influence on rock stresses in the area.

2.8 In-situ rock stresses

The magnitude and orientation of the rock stress were measured using the 3D over-coring technique inside the test tunnel in 2008. The stress was measured in three locations along the tunnel alignment and the result is given in Table 2. The principle stresses (σ_1, σ_2 and σ_3) were measured and the vertical (σ_v) and horizontal stresses ($\sigma_{h,max}$ and $\sigma_{h,min}$) were calculated from these stresses [SINTEF, 2008[22]]. The result shows that there is considerable stress anisotropy.

The general trend in the maximum horizontal stress ($\sigma_{h,max}$) is attributed to the direction of the tectonic stress in the region, but it differs from location to location. This may be caused by the presence of some local discontinuities. However, the trend (in the location at chainage 280 m) is comparable with the general trend of tectonic stress in the Himalaya, as explained by Panthi [2014[2]].

Table 2: Result of stress measurement by 3D overcoring in Test Tunnel (SINTEF, 2008)

Stresses	Chainage 500m, h=408m			Chainage 400m, h=364m			Chainage 280m, h=330m		
	MPa	Trend	Plunge	MPa	Trend	Plunge	MPa	Trend	Plunge
σ_1	18.4±2.9	N120.5^{0}E	27.9^0	17.4±2.2	N204.6^{0}E	30.3^0	21.6±3.8	N21.1^{0}E	10.4^0
σ_2	12.4±4.7	N239.5^{0}E	42.5^0	10.8±1.7	N100.2^{0}E	23^0	12.6±2.8	N116.5^{0}E	27.2^0
σ_3	7.1±1.8	N9.0^{0}E	34.7^0	1.1±2.7	N339.4^{0}E	50.4^0	6.4±4.8	N272.2^{0}E	60.6^0
σ_v	12		90^0	6.7		90^0	8.2		90^0
$\sigma_{h,max}$	16.8	N111.3^{0}E	0	14.5	N43.7^{0}E	0	21.2	N18.5^{0}E	0
$\sigma_{h\,min}$	9.1	N21.3^{0}E	0	8.1	N133.7^{0}E	0	11.2	N108.5^{0}E	0
Note: h = vertical rock cover									

The results from the over-coring process can be used as input for the topographical model at the location of the unlined pressure tunnel to determine the minimum principle stress. However, it is equally important to measure the stress at the location of tunnel. For this, minimum principle stress was measured by SINTEF in 2013 using the hydraulic fracturing technique at two locations, as shown in Fig. 7. The result shows that the average minimum principal stress component σ_3 is 3.2 MPa at location 1 and 5.4 MPa at location 2, with some critical values as low as 1.9 MPa and 1.2 MPa, respectively. It was quite surprising to have such low values of minor principal stress at a location where the vertical rock cover is approximately 550 m. However, it should be noted that periodic major earthquakes in the Himalayan region greatly influence the magnitude of in-situ stress in the rock mass. The energy released through the rock mass destresses areas close to the major tectonic thrust faults having a weaker rock mass, whereas a stronger rock mass will store the energy in the form of in-situ stress.

The lower values at the headrace tunnel could be attributed to the effect of nearby zones of weakness; since location 1 is only about 45 m from the crushed zone 2 towards T5 (see Fig. 7). The critical values at both locations and even the average value at location 1 are less than the future hydrostatic water pressure at these locations. This required a design modification of the unlined pressure tunnel as shown in Fig. 7.

2.9 Groundwater table and water inflow during excavation

The groundwater table will help to define potential areas from which leakage from an unlined pressure tunnel could occur if the rock mass is jointed and joint systems are interconnected. RCD-P3 is indicated with a groundwater level at 20.6 m, whereas RCD-H1 is reported with groundwater at a vertical depth from the surface of 53 m. Both of these measurements were taken during the dry season.

Based on the Lugeon permeability test carried out in 2005 in various holes, the permeability of the rock mass was classified as low to moderate in the relatively strong rock mass and higher in the zones of weakness. The typical Lugeon values measured were 1.0 to 2.0 in the surge shaft area and at the end of the headrace tunnel.

The extent of water leakage into the tunnel during excavation will give an indication of potential leakage from the pressure tunnel. This will also help to identify the potential water bearing joints, which could work as a reverse pathway when there is high water pressure in the tunnel. The inflow was registered as 1-12 l/min per metre of tunnel in the stretch from T6 to EE, and the maximum was measured close to weakness zone 1. Norconsult and Lahmeyer [2013[7]] mentioned that leakage was higher immediately after excavation, and it reduced after several days, indicating locally isolated water pockets in the rock mass. Overall, the amount of inflow and observations of open joints indicated that the rock mass is quite permeable in areas where fracture zones (weak zones) are located.

3 Conclusions

Along with the use of the prevailing design criteria, it is equally important to define the geotectonic environment to ensure the safe design of unlined pressure tunnels and shafts. In the case of Upper Tamakoshi, even though the Norwegian design criteria for overburden and valley side distance had been fulfilled, the minimum principle stress was found to be inadequate with regard to the originally proposed unlined pressure tunnel with a hydrostatic head of about 430 m.

The low stress values in the locations studied could be attributed to the effect of shear zones nearby. Such zones occur frequently at the downstream section of the headrace tunnel. The over-coring results at the test tunnel also show a large local variation in the magnitude and direction of in-situ stresses. The variation might be more pronounced near the slope topography since the rock mass is influenced by weathering, fracturing and shearing caused by strong earthquakes, such as the Gorkha earthquake of 2015. In conclusion, the stress distribution at the UTHP seems quite complex, and it is recommended to carry out hydraulic splitting tests covering the headrace tunnel areas where hydrostatic heads will exceed 50 m.

Acknowledgement

The authors are grateful to the project management team of the Upper Tamakoshi hydroelectric project for providing project data and information, and for giving permission to carry out research on this project, which will be a milestone in the use of the unlined pressure tunnel concept in the Himalayan region. The paper represents part of an academic research study, and the results presented in the paper will not be used as base material for the settlement of contractual issues of the project.

References

1. **Broch, E.,** "Planning and utilisation of rock caverns and tunnels in Norway", *Tunnelling and Underground Space Technology*, Vol. 55; 2016.
2. **Panthi, K.K.,** "Norwegian Design Principle for High Pressure Tunnels and Shafts: Its Applicability in the Himalayas", *Hydro Nepal: Journal of Water, Energy and Environment*, Vol. 14, 2014.
3. **Panthi, K.K.,** "Analysis of engineering geological uncertainties related to tunnelling in Himalayan rock mass conditions", PhD Thesis, NTNU, Trondheim, Norway; 2006.

4. Panthi K.K. and Nilsen, B., "Predicted versus actual rock mass conditions: a review of four tunnel projects in Nepal Himalaya", *Tunnelling and Underground Space Technology*, Vol. 22, No 2; 2007.
5. **Norconsult,** "Feasibility study report of Upper Tamakoshi Hydroelectric Project", for the Nepal Electricity Authority, Nepal; 2005.
6. **Norconsult and Lahmeyer,** "Detailed design report of Upper Tamakoshi Hydroelectric Project", Nepal Electricity Authority, Nepal; 2008.
7. **Norconsult, and Lahmeyer,** "Headrace tunnel and shafts: Design modification, Upper Tamakoshi Hydroelectric Project", for the Nepal Electricity Authority, Nepal; 2013.
8. **Norconsult and Lahmeyer,** "Final drawings for the headrace tunnel and shafts, Upper Tamakoshi Hydroelectric Project", for the Nepal Electricity Authority, Nepal; 2014.
9. **Reimer, W. and Bock, H.,** "Report on the October 2013 project mission, Upper Tamakoshi Hydroelectric Project", for the Nepal Electricity Authority, Nepal; 2013.
10. **Rowley, D.B.,** "Age of initiation of collision between India and Asia: A review of stratigraphic data", *Earth and Planetary Science Letters*, Vol. 145; 1996.
11. **Jackson, J., McKenzie, D.,** Priestley, K. and Emmerson, B., "New views on the structure and rheology of the lithosphere", *Journal of the Geological Society*, Vol. 165, No. 2; 2008.
12. **Shanker, D., Paudyal, H. and Singh, H.,** "Discourse on seismotectonics of Nepal Himalaya and vicinity: appraisal to earthquake hazard", *Geosciences*, No. 1; 2011.
13. **Chamlagain, D.,** "Earthquake scenario and recent efforts toward earthquake risk reduction in Nepal", *Journal of South Asia Disaster Studies*, Vol. 2, No. 1, 2009.
14. **Lavé, J. and Avouac, J-P.,** "Active folding of fluvial terraces across the Siwaliks Hills, Himalayas of central Nepal", *Journal of Geophysical Research: Solid Earth* (1978–2012), Vol. 105; 2000.
15. **Nakata, T.,** "Active faults of the Himalaya of India and Nepal", Special Paper of the *Geological Society of America*, USA; 1989.
16. **Panthi, K.K.,** "Evaluation of rock bursting phenomena in a tunnel in the Himalayas", *Bulletin of Engineering Geology and the Environment*, Vol. 71, No. 4; 2012.
17. **Upreti, B.,** "An overview of the stratigraphy and tectonics of the Nepal Himalaya", *Journal of Asian Earth Sciences*, Vol.17, No. 5; 1999.
18. **Schelling, D.,** "The tectonostratigraphy and structure of the eastern Nepal Himalaya", *Tectonics*, Vol. 11, No. 5; 1992.
19. **Ishida, T.,** "Petrography and structure of the area between the Dudh Kosi and the Tamba Kosi, east Nepal", *Journal of the Geological Society of Japan*, Vol. 75, No. 3; 1969.
20. **Larson, K.P.,** "The geology of the Tama Kosi and Rolwaling Valley region, east-central Nepal", *Geosphere*, Vol. 8, No. 2; 2012.
21. **Ishida, T. and Ohta, Y.,** "Ramechhap-okhaldhunga region", Himalayan Committee of Hokkaido University (Hashimota, S., Supervisor), in: Geology of the Nepal Himalayas, Hokkaido University, Japan; 1973.
22. **SINTEF,** "Rock stress measurement at the Upper Tamakoshi Hydroelectric project", Report SBF IN F08112; 2008.
23. **SINTEF,** "Rock stress measurement by hydraulic fracturing at Upper Tamakoshi Hydroelectric project, Nepal", Report SBF IN F08112; 2013.
24. **Broch, E.,** "The development of unlined pressure shafts and tunnels in Norway", ISRM International Symposium. International Society for Rock Mechanics; 1982.
25. **Panthi, K.K. and Basnet, C.B.,** "Review on the Major Failure Cases of Unlined Pressure Shafts/Tunnels of Norwegian Hydropower Projects", *Hydro Nepal: Journal of Water, Energy and Environment*, Vol. 18, 2016.

26. **Selmer-Olsen, R.,** "Experience with unlined pressure shafts in Norway", Proceedings, International Symposium on Large Permanent Underground Openings, Oslo, Norway; 1969.
27. **Strobel, N.,** www.astronomynotes.com/solarsys/s8c.; 2016.
28. **DGM,** "Geological Map of Nepal (scale 1:1,000,000)", Department of Geology and Mines, Nepal; 1994.

K.K. Panthi

C.B. Basnet

Dr. K.K. Panthi has been an Associate Professor in Geological Engineering at the Department of Geology and Mineral Resources Engineering, Norwegian University of Science and Technology (NTNU) since 2008. He holds a PhD in Rock Engineering, an MSc in Hydropower Engineering and an MSc in Tunneling. He has approximately 25 years of experience in design, construction management and research of tunneling, hydropower, slope stability and mining projects. He is the author of many scientific papers published in renowned international journals.

Chhatra Bahadur Basnet has an MSc in Civil Engineering and is currently conducting PhD research at the Department of Geology and Mineral Resources Engineering, Norwegian University of Science and Technology (NTNU), Norway. His current research work is related to unlined pressure tunnels for hydroelectric projects. He has more than six years of working experience in the planning, design, and construction supervision of hydropower projects in Nepal.

Norwegian University of Science and Technology (NTNU), Høgskoleringen 1, 7491 Trondheim, Norway.

Paper IV

Title:

Evaluation on the minimum principal stress state and potential hydraulic jacking from the shotcrete lined pressure tunnel – A case from Nepal

Authors:

Basnet, Chhatra Bahadur

Panthi, Krishna Kanta

Submitted to and under review in:

Rock Mechanics and Rock Engineering (submitted on 26th July, 2018)

Is not included due to copyright

Paper V

Title:

Detailed assessment on the use of unlined or shotcrete lined pressure tunnel in the Himalayan rock mass conditions: A case study from Nepal

Authors:

Basnet, Chhatra Bahadur

Panthi, Krishna Kanta

Submitted to and under review in:

Bulletin of Engineering Geology and the Environment (submitted on 12th August, 2018)

Is not included due to copyright

Paper VI

Title:

Hydraulic jacking and leakage assessment in an unlined or shotcrete lined pressure tunnel - A case study from the Nepal Himalaya

Authors:

Basnet, Chhatra Bahadur

Panthi, Krishna Kanta

To be submitted, not yet decided on which journal

Is not included due to copyright

Paper VII

Title:

State-of-the-art design guidelines in the use of unlined pressure tunnels / shafts for hydropower scheme.

Authors:

Panthi, Krishna Kanta

Basnet, Chhatra Bahadur

Published in:

The proceeding of 10th Asian Rock Mechanics Symposium (ARMS10), the ISRM International Symposium, Singapore, 2018

Is not included due to copyright

Appendix

Lists of other publications during PhD study

Panthi, K.K. and **Basnet, C.B**., 2018b. A dynamic stress state analysis at the pressure tunnel of Upper Tamakoshi HPP, Nepal. *Third International Conference on Rock Dynamics and Applications (RocDyn-3)*.

Basnet, C.B. and Panthi, K.K., 2017. Topographic Effect in the Selection of Unlined Pressure Tunnels/Shafts-A Review of a case from Nepal Himalaya. *In Proceedings of the ITA World Tunnel Congress 2017. NFF-Norwegian Tunnelling Society*.

Basnet, C.B. and Panthi, K.K., 2017. 3D in-Situ Stress Model of Upper Tamakoshi Hydroelectric Project Area. *Hydro Nepal: Journal of Water, Energy and Environme*nt, 21: 34-41.

Panthi, K.K. and **Basnet, C.B**., 2016. Review on the Major Failure Cases of Unlined Pressure Shafts/Tunnels of Norwegian Hydropower Projects. *Hydro Nepal: Journal of Water, Energy and Environment*, 18: 6-15.

Basnet, C.B. and Panthi, K.K., 2016. Unlined/Shotcrete Lined Pressure Tunnel Passing Through Himalayan Rock Mass – Design Review of Upper Tamakoshi Headrace Tunnel, Nepal. *9th Asian Rock Mechanics Symposium (ARMS9*).